2017

Product Qualification And Performance Assessment Of HSRM Prestressed Concrete Railroad Ties Through Laboratory Testing

Ali Haider Abdulqader
University of South Carolina

PRODUCT QUALIFICATION AND PERFORMANCE ASSESSMENT OF HSRM PRESTRESSED CONCRETE RAILROAD TIES THROUGH LABORATORY TESTING

by

ALI HAIDER ABDULQADER

Bachelor of Science
Al-Mustansiriya University, 2007

Submitted in Partial Fulfillment of the Requirements

For the Degree of Master of Science in

Civil Engineering

College of Engineering and Computing

University of South Carolina

2017

Accepted by:

Dimitris Rizos, Director of Thesis

Robert Mullen, Reader

Michael Sutton, Reader

Juan Caicedo, Reader

Cheryl L. Addy, Vice Provost and Dean of the Graduate School

ACKNOWLEDGEMENTS

This work has been funded by the Federal Railroad Administration (FRA) under contract DTFR5314C00023. The opinions, findings, and conclusions expressed in this work are those of the authors and not necessarily those of the FRA.

ABSTRACT

This study focuses on the performance assessment of prestressed concrete railroad ties made of a newly developed High Strength Reduce Modulus (HSRM) concrete. The HSRM material has been developed by researchers at the University of South Carolina laboratories. The HSRM material was originally considered as a high-performance concrete for highway bridge girders, but it was rejected because it shows very low modulus of elasticity. A current project at USC proposed to use this HSRM material in prestressed concrete railroad ties. The experimental tests during the material development phase of the project showed that the HSRM-HPC has a reduced Modulus of elasticity as much as 50 % compared to conventional high strength concrete. The hypothesis is that a more resilient concrete tie will better distribute the loads and delay the initiation of cracking. This work discusses the qualification of the new HSRM concrete tie according to the guidelines of the American Railway and Maintenance of Way Association (AREMA) requirements and assesses its performance by comparing its performance to the equivalent Standard prestressed concrete ties currently in use in order to validate the hypothesis. To this end, a number of prototype HSRM ties and Standard concrete ties have been fabricated at a major US concrete tie manufacturer and tested in the structures laboratories at the University of South Carolina. Conventional instrumentation, as well as state of the art laboratory instrumentation based on vision system, is employed in these studies. Experimental investigations have shown that the newly developed of HSRM ties not only satisfy the requirements of the design guidelines but also have shown superior

structural performance to the Standard ties under static and cyclic load tests. The higher flexibility of the HSRM ties leads to normalized stress fields, reduced stress amplitudes in critical areas, and better post cracking performance and ultimate strength as compared to the Standard ties.

TABLE OF CONTENTS

LIST OF TABLES

LIST OF FIGURES

CHAPTER 1

INTRODUCTION

A railroad tie is a main part of the railway system structure. Ties transfer and distribute train axle loads from the rails to the underlying ballast supporting system [1]. Railroad ties play an important function in supporting the rail, maintaining the track gage, isolating the two parallel rails and work as an anchorage stand for the fastening system [2]. The use of concrete ties is increasing in North America as they have become an economical alternative to the commercial wood ties as the concrete ties provide a significant performance improvement [3].

To offset the higher initial costs, concrete ties should have longer service life and require less maintenance. High-Performance Concrete (HPC) with early strength development is the material of choice in the fabrication of prestressed concrete railroad ties with a design life of over 50 years [4]. HPC prestressed ties have a number of strong environmental and economic benefits, as well as improved performance characteristics. However, it has been reported that concrete ties do not reach their design life due to a number of unresolved performance issues [5].

Zeman (2009) has shown that the most critical issues in crosstie performance are the rail seat deterioration (RSD), shoulder/fastener wear or fatigue, derailment damage, and cracking from center binding, cracking from dynamic loads and tamping damage. One of the main causes of derailments is RSD, and the primary causes appear to be high

stresses at the rail seat, a loosened fastening system, the presence of moisture, and the presence of abrasive fines [5].

Cracking from the center binding and dynamic loads are due to the development of high tensile stresses. Therefore, the development of high amplitude stresses and the corresponding stress distribution within the tie appear to be common underlying causes of the most critical issues that affect the tie performance. In turn, the high stresses and stress distribution are directly related to a combination of the strength and the stiffness of the crosstie. Typically, a high strength but relatively flexible load-bearing element results to more regularized (smoother) stress field gradients with reduced amplitudes that should alleviate the issues associated with high stresses in concrete ties. However, for a given concrete tie geometry, the strength and stiffness depending on the strength and elastic modulus of the materials. The higher strength of HPC is directly correlated to higher values of the Elastic Modulus increasing, thus, an increase in brittleness and the rigidity of the material. As a consequence, the combination of increased strength, rigidity and brittleness may lead to premature cracking and deterioration of the concrete ties [4][5][6].

High-performance concrete is concrete with higher structural capacity and improved durability as compared to conventional Portland cement concrete. HPC is now being used for bridges to prevent corrosion reinforcement and to protect the construction from chemical and physical attack [7]. The HPC used in this work was originally considered as a high-performance concrete for highway bridge girders, but it was rejected because it's exhibited very low elastic modulus as determined in an experimental study. The elastic modulus was shown to be reduced by as much as 50 % compared to typical

high performance concretes of the same strength. The lower elastic modulus is attributed to the types of aggregates used that are classified as weathered granites.

A research project at the University of South Carolina has proposed the use this reduced modulus concrete, hereafter designated as High Strength Reduced Modulus (HSRM) concrete, in the fabrication of concrete ties. The use of this HSRM concrete in the fabrication of rail ties combine the advantages of the high strength of HPC while preserving the structural performance advantages of the more flexible structural material, like timber, or composite ties, since the HSRP-HPC elastic modulus is similar to regular strength concrete. The use of HSRM concrete directly addresses critical issues related to rail seat deterioration, (RSD) cracking from center binding, and cracking from dynamic loads.

Thesis Objectives

This research investigates the using HSRM in concrete ties. To this end, prototype HSRM ties have been fabricated and qualified following the AREMA guidelines. Subsequently, the performance of this new product is investigated and benchmarked against the commercial ties of the same design that use the Standard concrete mix. The end goal of this project is to produce the HSRM tie design which will be capable of withstanding the anticipated loads of heavy haul railways in North America while maintaining current tie geometry.

Thesis Organization

The following chapters present background information, the adopted research methodology. In particular, Chapter 2 provides an overview of prestressed concrete railroad ties and the process used for their design with a concentration on the use and

design of ties for heavy haul applications. Chapter 3 introduces the geometry and materials used in the concrete ties. Chapter 4 provides the laboratory procedures, the setup of the various tests and the convention deformation and load measurement instrumentations as well as the Digital Image correlation technology used in this work. Chapter 5 shows the design qualification tests per AREMA. Chapter 6 discusses the performance of tie under static and cycling loads. Chapter 7 presents an alternate four-point bending test proposed in this work for the center binding assessment. Chapter 9 presents the conclusions of this work.

CHAPTER 2

LITERATURE REVIEW

Railroad track structure is a complex system of components that are designed to provide a smooth running surface for rail traffic. As traffic conditions have been changing and new technologies have been developing, it became more necessary to reconsider the track structure and its components in the system context [5]. The major component of the railway tracks is the railway tie which is playing a significant role in distributing the load from the rails to the ballast bed [8].

Since the 1960s, the railway industry in the United States began to use concrete for producing railway ties with the purpose of developing safer and more durable railway structures with an estimated service life of 50 years. In South Korea started to replace the wood ties with prestressed concrete ties in 1958. Due to increasing loading demands, and interest in the development a high-speed train system, prestressed concrete ties have been studied in North America as well [9][10]. Most European and Asian railways also now use prestressed concrete ties and concrete crossing layouts due to the longer life and lower life-cycle cost of concrete ties compared to timber, which has become increasingly difficult and expensive to source in sufficient quantities and quality.

2.1 Design approach of prestressed concrete ties.

An allowable stress approach that depends on simple impact factors is often employed in the design of prestressed concrete ties and also the railway track. Tie designs are predicated on vertical loads applied from train wheels and ballast support. Together

with vertical loads, ties are subjected to lateral loads, especially, on curved track. The prestressed concrete ties generally depend on bearing of the ends against ballast, gravity, and friction between tie and ballast, to resist the lateral loads. Recently, to extend this resistance, haunches are placed on the sides of ties [11][12].

The design of the prestressed concrete ties is based on different design Standards, such as USA [4], Australia [13] and Europe [13]. Following the concrete tie testing procedures in the aforementioned Standards, the concrete ties were investigated for bending moments, estimation of the vertical design axle load, and computation of the permissible in the ties materials. Many tests have been done on prestressed concrete ties in order to achieve the performance exhibited with respect to materials and design. The interaction between the concrete and prestressing provides the necessary strength to resist the cyclic loading of the trains while concrete provides the protection and rigidity to hold the system together [11].

Shin (2016) has investigated the use of the granulated blast furnace slag (GGBFS) and the steel fibers in the prestressed concrete railway ties. The use of GGBFS is considered an eco-friendly material intended to reduce the CO_2 energy consumption and emission, also to improve the durability performance of the railway ties. The use of steel fibers improved the flexibility and the structure behaviors in terms of crack control and can improve the shear reinforcement. A series of laboratory tests have improved the use of steel fiber (56% GGBFS and 0.75% steel fibers). These mixes fulfilled the requirements of Korean Railway Standard and showed an improvement in flexural capacity and slightly better durability performance than other mixes [2].

Koh (2016) studied the structural performance of a newly developed eco-friendly prestressed concrete ties for railway tracks in South Korea. An eco-friendly concrete has been industrialized by researchers at the Korea Railroad Research Institute (KRRI) with the goals of decreasing carbon dioxide (CO2) emissions and discovering a replacement of natural sand for fine aggregate. Decreasing the cement content is very important to the issue of CO2 emission in the concrete industry. In South Korea, the lack of natural sand as a fine aggregate led researchers to investigate the use of two types of reprocessed industrial byproducts (slag) to control the environmental issues of railway prestressed concrete ties. Ground granulated blast furnace (GGBF) slag was used to replace 30% of Portland Type III cement, and electric arc furnace (EAF) oxidizing slag was used to replace fine natural aggregate. This new concrete exhibited high initial compressive strength with high early strength at the time of prestressing release (>5000psi) and high enough 28-day compressive strength (>7250 psi) [9].

Manda (2014) reported on an intensive study that investigates the vertical load path under static and dynamic loads in concrete ties and the fastening system. An extensive field test program was conducted to measure forces, strains, displacements and rail seat pressures. The objective of the field instrumentation was to quantify the response of the concrete tie and the fastening system and determine of system mechanics. A Track Loading Vehicle (TLV) was used to apply a load on the test section under static (zero speed) condition. The dynamic load was applied using passenger and freight cars of known weights.

The rail seat load was varied between 30-80% of the vertical load that applied by the track wheel. It was noticed that the vertical tie deflection significantly influenced the

rail seat load, so the high degree of variability in the fraction transferred as the tie deflections varied significantly. Lower rail seat loads were observed at ties with higher vertical deflection, and higher rail seat loads were noticed at ties with lower vertical deflection [14].

Sýkorová at al. (2012) have investigated the optimum design of the prestressed concrete ties by studying two different cases. The first case was related to the design of the tie to resist the Standard load 125 KN per rail seat. The second case deals with a tie that holds 400 KN per rail seat which represents the impact of the flat wheel. The resulting shape of the ties was obtained by the optimization of the shape of the Standard prestressed concrete mono-block sleeper. The prestressing force and the position of prestressing wires are then determined accordingly for the optimized shape of the tie. The prestressing forces resulted from a similar distribution of the prestressed strands. The arrangement of the prestressed wires reflects the increased loading conditions. The tie with a load of 125 KN on both rail seats is prestressed with ten wires that have a diameter of 6 mm. The tie designed for impact load of 400 KN on both rail seats is prestressed with 12 wires with a diameter of 8 mm. The 28-day compressive strength of concrete used in the analyzed tie must be greater than 50 MPa, which is a common value for prestressed concrete ties [15].

2.2 The behavior of prestressed concrete ties under static and dynamic loads.

Dynamic loading of the ties is produced by the rail-wheel interaction, and the dynamic impact depends largely on the condition of the rail and wheel surfaces. For perfect surface conditions, the impact load is small and dynamic effects are governed by the high number of load cycles. However, when irregularities in the rail surface and the

wheel are significant, the impact effects are high, but these loads are generally applied over a much smaller number of cycles [12].

Sakdirat at al. (2009 a) have investigated the energy absorption capacity of the prestressed concrete ties under static and dynamic loadings in addition to the residual moment capacity after the ultimate impact load. They concluded that the energy balance method can be used to indicate the ultimate impact behavior of the prestressed concrete ties. The amount of the energy absorption can clearly show the damage severity of the specimens that have been designed and tested based on Australian Standard: AS1085.14. The crack initiation was detected visually during all tests as well as through the load-deflection curves [16].

Sakdirat (2007a) have investigated the performance of the prestressed concrete ties under static and dynamic loading conditions according to Australian Standard. The ties were subjected to impact loading by using a drop hammer that has very large capacity in order to simulate the repeated impacts due to wheel flats or engine burns. The static results showed that the prestressed concrete tie has relatively low ductility; also, the results found that the modified compression field theory can be used to expect the static responses of the prestressed concrete rail road ties. The result showed 10% difference from the experimental results and also the energy absorption capacities of PC ties under loading conditions [17].

Sakdirat (2007 b) have reported on experimental and numerical studies of railway prestressed concrete ties under static and impact loads. They presented the results of the finite element analyses and discussed the impact and the static loads of the prestressed concrete tie. The results showed that the tensile strength based on 0.4 $\sqrt{fc'}$ is

inappropriate for the high strength concrete. Then the finite element model was extended by using finite element updating technique. The researchers found that the impact during the simulation can be used to predict the impact response of the prestressed concrete ties [18].

2.3 Bending moments.

The structural design of a concrete tie is based on locating the maximum allowable quasi-static bending moment. However, the most important parameter for designing the prestressed concrete ties is the dynamic amplification factor (DAF) for bending moment [12]. The ties' support conditions are the main reasons that affect the flexural behavior of the prestressed concrete tie. The current tie design guidelines make assumptions for these ties support conditions which lead to different recommendations for estimating the design bending moments [19]. This research study shows the high level of sensitivity of the center moment estimation as a function of the support conditions.

Kumaran (2013) have estimated the dynamic amplification factor (DAF) at mid-span and rail seat due to different excitation through Finite Element Simulations. The result shows DAFs for both positions increase with (1) increasing ballast elastic modulus, (2) increasing the subgrade stiffness, (3) decreasing rail pad stiffness and (4) loss of contact between the ballast and tie at the center. The results also indicate that the DAFs for deflection and ballast pressure on both positions (mid-span and rail seat) follow similar trends in the frequency domain. However, the magnitudes are higher [20][12].

The strains and its variation in prestressed concrete ties due to dynamic loads have been the topic of only a few studies. In-field measurements have been reported by Wolf (2015) to measure the surface strain by mounting strain gauges on the surface of the

prestressed concrete ties and used to calculate the bending moments for different support conditions. The data were taken from fourteen train passes corresponding to over 7500 axles loading. The statistical processing of measurements of the bending moments indicated that a large number of high bending moments were experienced by the concrete ties. Some minor cracks were observed at the center of most ties in the test section. Ballast support conditions were found to be the major source of the variation in the ties flexure [21]. Results show that the bending moments and the strain did not exceed the current industry Standard design limits. Wolf (2015) has also investigated the curling in concrete crossties due to temperature changing. Curling is a well-documented behavior in concrete pavements, girders, and slab-track. Wolf has documented curling in the concrete crossties using finite element modeling along with the data that was obtained in the laboratory and field experimentations. The results show a strong inverse relationship between temperature change and center negative bending moments [3].

CHAPTER 3

THE CONCRETE TIE

Railway prestressed concrete ties have been developed and used in railways for over 60 years. The current design approach is based on allowable stress design while the structural behavior or deformation is kept within the elastic range [22]. To achieve the performance showed by concrete ties, extensive amounts of engineering have been employed with realization to materials and design. The interaction between the concrete and the prestressed strands provides the required strength to resist the static and the dynamic load from the trains while concrete provides the rigidity to hold the system together [11].

Thirty-two HSRM (prototype) ties and eight Standards (baseline) ties have been fabricated at a major tie manufacturing plant and transported to the structures laboratories at University of South Carolina.

3.1 Tie Design Parameters

The geometry of the railroad ties in this work is shown Figure 3.1. These two figures show the prototype of the HSRM which had the same geometrical and sectional properties with the Standard ties. The overall length of the Prestressed Concrete tie of Standard production tie is 102 inches. The width of the tie is 8 inches at the bottom and 7 inches from the top surface. Prestressing is applied through eight 3/8 low relaxation steel strands placed in two rows. The total prestressing force is 110.4 kips after losses.

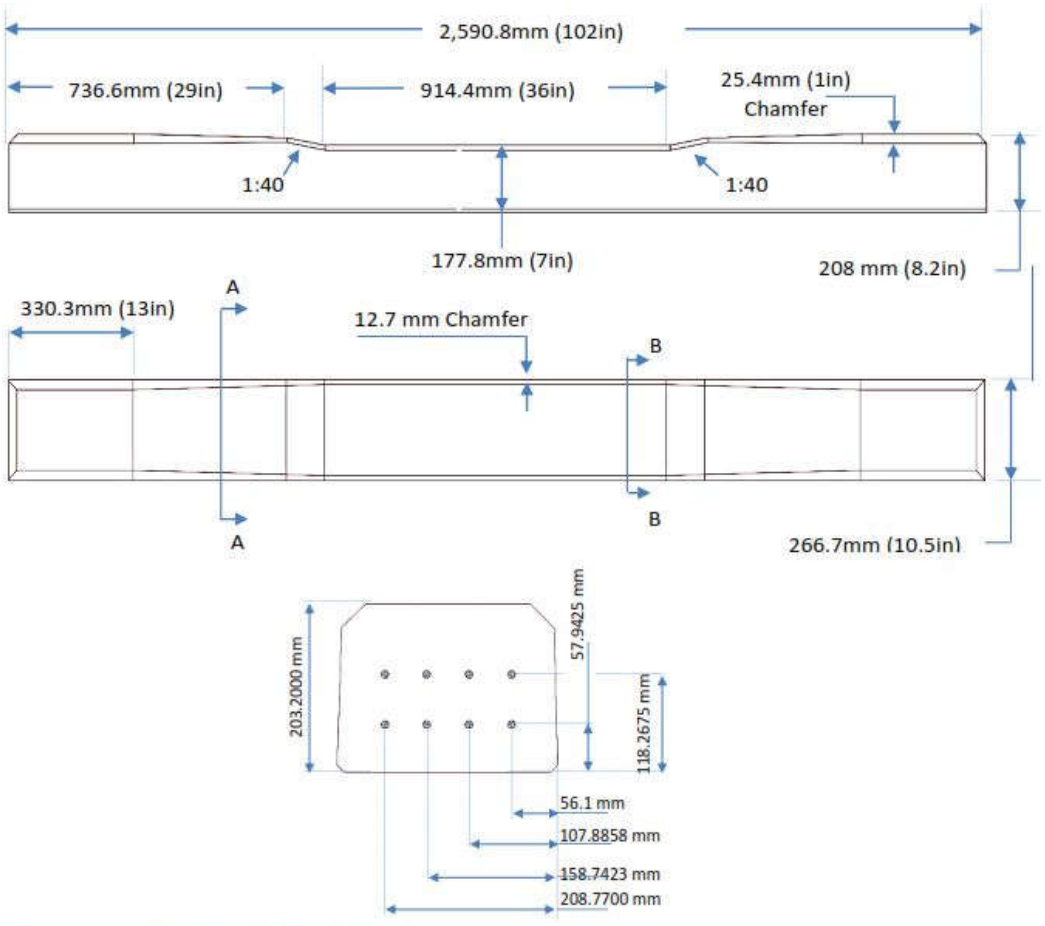

Figure 3.1 Tie Geometry

3.1.2 Flexural capacity by AREMA and manufacture.

The design capacity the Standard ties were provided by the tie manufacture table 3.1 illustrates the design moments, forces and the maximum stresses at top and bottom for the ties following AREMA guidelines for testing.

3.2 Tie Materials

The material properties of concrete and steel beyond question play a crucial role in the manufacture of a prestressed concrete tie. The strength and stiffness of the materials that comprise the ties dictate their capability and are also parts of the fabrication method. Therefore, an intensive understanding of their properties is needed.

Table 3.1 Load Design Parameters of Railroad Tie

	Rail Seat Center		Tie Center	
	Positive	Negative	Positive	Negative
Moment (in-Kip)	300	162	144	208
Force (Kips)	51.1	27.6	10.4	15.0
Stress Top (Ksi)	-3.79	0.69	-3.28	1.0
Stress Bottom (Ksi)	0.94	-3.31	0.15	-4.03

Standard to any prestressed concrete member is early high strength concrete and high tensile strength steel. Along with the concrete and prestressing steel, tie fasteners and pads are important to the concrete tie. However, it should be noted that the railroad operatives dictate the implementation of these connection devices and that their design should be outside of the scope of the tie producer duties. This presents a unique challenge because a component failure is often considered a tie failure.

3.2.1 Concrete

The use of high strength concrete is necessary for the production of concrete ties due to the use of prestressing. The minimum compressive strength of the concrete was 7,000 psi at 28 days. Reasons for high early strength concrete are the following:

• To professionally produce concrete ties or any prestressed member for that matter the prestressing force must be transferred to the tie at an early age. A compressive strength of 4,000 psi is normally considered acceptable for prestressing load transfer.

• High early strength concrete allows beds to be turned over more rapidly due to shorter release times.

Cement

Portland cement Type III, Low Alkali was used for manufacturing the railroad prestressed concrete ties HSRM and Standard. The Portland cement in the U.S. has been certified according to the American Society for Testing and Materials (ASTM) C150, which is a standard specification for Portland cement.

Aggregate

Four types of aggregate from four different sources were used in the mixtures' design as figure 3.2 shows. The first aggregate source is the limestone named as CA1; major tie producer manufacturer uses this limestone. The concrete that is made from the CA1 aggregate meets The American Railway Engineering and Maintenance -Of- Way Associated's guidelines, and is used as the baseline material for the HSRM performance studies. The other three types of aggregate are weathered granites identified as CA2, CA3, and CA4. In this work, all aggregates types were tested following ASTM tests (1) ASTM C127. Standard Test Method for Density, Relative Density (Specific Gravity), and Absorption of Coarse Aggregate (2) ASTM C131.Resistance to degradation of small-size coarse aggregate by abrasion and impact in the Los Angeles Machine. (3) ASTM C136. Sieve Analysis. Table 3.2 shows the tests that have been done in the aggregate, concrete, and mortar.

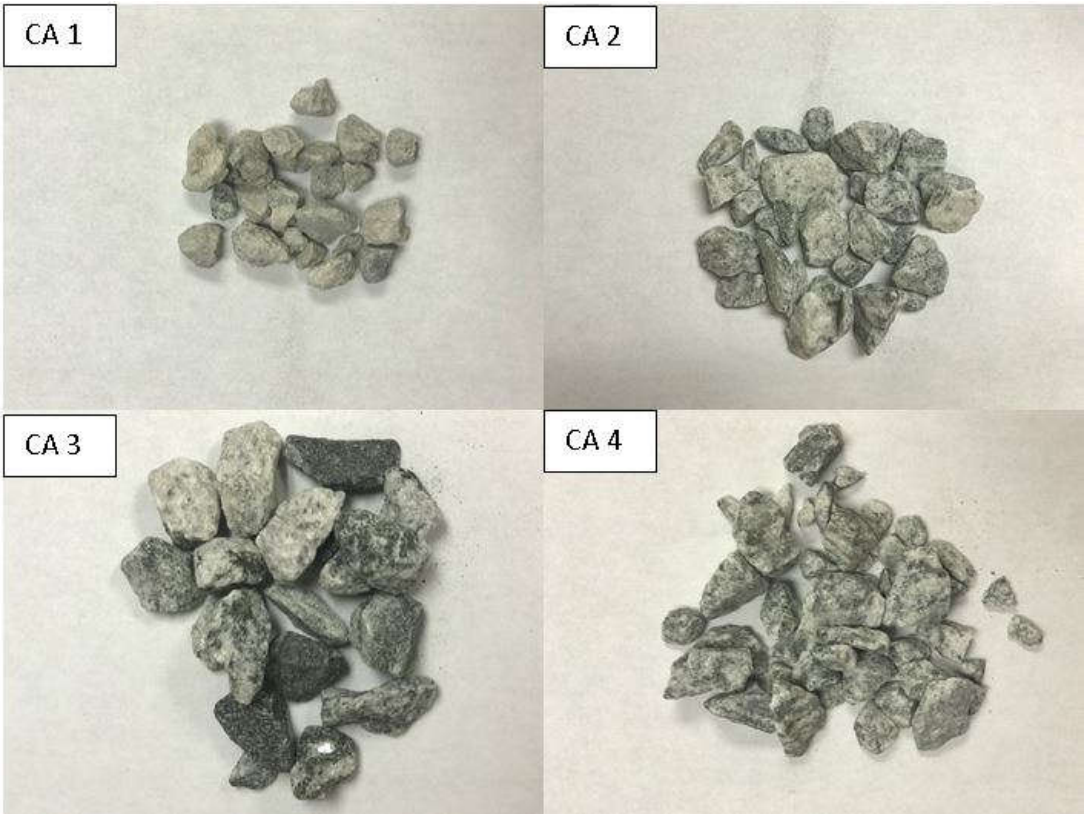

Figure 3.2 Aggregate Types

Admixture

The admixtures were used in this study in order to improve the workability and assist with the air content.

Concrete mix design

The tie manufacturer supplied all other materials in the mixture, including fine aggregate and cement. Four different mixtures have been produced using the four aggregate types (CA1, CA2, CA3, and CA4). Seven concrete batches were produced for each of the four mixtures, and each batch has been tested according to the American Society for Testing and Materials (ASTM) Standards, for the slump, air content, density, cement content, compressive strength, elastic modulus and abrasion resistance. Increase the compressive strength of the high-performance concrete leads to increase the modulus

of elasticity, as known. However, for the high-performance concrete that contains the weathered granite, the modulus of elasticity is lower than that with commercial high-performance concrete [23]. Table 3.3 shows the result for all tests that have been done on the aggregate and the concrete.

Table 3.2 ASTM Tests on rock, aggregate, mortar, and concrete

	Test	ASTM
Coarse Ag.	Los Angles Abrasion Test	C131
	Sieve Analysis (Particle Size Distribution)	C136
	Bulk Density and Voids	C29
	Density, Specific Gravity and Absorption	C127
Rock	Compressive Strength	D7012 - 14
	Modulus of Elasticity	D7012 - 14
Concrete	Slump	C143
	Density	C138
	Air Content by pressure method	C231
	Compressive Strength of Concrete	C39
	Flexural Strength of Concrete	C78
	Modulus of Elasticity of Concrete	C469
	Shrinkage	C157
Mortar	Compressive Strength	C 109- 13
	Tensile Strength	C 307-12
	Modulus of Elasticity	C 580-02
	Setting Time (Initial and Final)	C191 - 13

Table 3.3 Properties Comparison

Property		Aggregate			
		CA1	CA2	CA3	CA4
Aggregate	Voids	42.73	42.51	39.90	39.10
	Density (lb/ft^3)	161.65	164.50	165.00	167.50
	Relative Density	2.58	2.60	2.65	2.69
	LA Abrasion	27.5%	33.9%	44.3%	46.0%
Fresh concrete	Density (lb/ft^3)	152.90	153.73	154.14	158.55
	Yeild (Yd^3)	0.15	0.15	0.14	0.14
	Cement Content (lb/yd^3)	618.23	621.53	623.21	632.05
	Slump (in)	7.00	6.50	7.50	4.00
	Air Content (%)	5.0%	5.9%	4.8%	4.0%
Concrete	Compressive Strength (psi)	8.8E+03	8.8E+03	9.2E+03	8.7E+03
	Increase / Reduction %	0%	0%	4%	-1%
	Flexural Strength (psi)	0.13fc'	0.125fc'	0.12fc'	-
	Elastic Modulus (psi)	5.6E+06	3.6E+06	3.2E+06	2.8E+06
	Elastic Modulus Reduction %	0%	-37%	-43%	-50%
	Lapping Test Abrasion Rate (mm/min)	0.042	0.023	0.029	0.039

3.2.1 Standard Concrete

The Standard concrete, which is the base line for AREMA, has very high strength 7,000 psi at 28 days. The Standard tie concrete is made from limestone aggregate, and this is the only difference comparing with the HSRM prestressed concrete tie.

3.2.2 High Strength Reduced Modulus (HSRM) Concrete

The HSRM tie has the same mix design and structure of the Standard tie. The only difference is the aggregate type which is the weathered granite in the case of HSRM, and it also has a minimum high strength 7,000 psi at 28 days, but it showed very low modules of elasticity.

3.2.3 Strands

Pre-stressing is applied through eight 7-wire low relaxation steel strands that meet ASTM A886 Grade 270k specifications. The strand diameter is 9.525 mm (3/8in), and the elastic modulus is Es=29,000ksi [200GPa] per manufacturer's specifications. The strands are prestressed to 75% of ultimate capacity.

Figure 3.3 Prestressed concrete wire

3.3 Prototype fabrication and specimens

The ties in this study were fabricated at a plant facility of a major US tie manufacturer in September 2015. In the plant, the ties are cast in a pre-stressing bed made up of 37 steel form cavities placed in series. Each cavity holds eight ties side by side. Figure 3.4 shows a schematic of a segment of the prestressing bed. The strands run continuously through all cavities along the length of the bed while the cavities are separated by removable steel blades that complete the form enclosures. On one end of the bed, henceforth designated as the "live end," the strands are attached to a hydraulic system that applies the pretension. The strands are anchored on a bulkhead at the opposite end of the bed, henceforth designated as the "dead end." Before placement of

the concrete, each strand is pre-tensioned at 76.8kN (17.25 kips). After pre-tensioning has been completed, each bed is filled with concrete.

Thirty-two HSRM ties and eight Standard ties were cast at the plant and shipped to the Structural Testing Laboratory at USC approximately three months after fabrication. The HSRM ties were cast in cavities 2-5 of the prestressing bed, and the Standard ties were cast in cavities 6-9.

Figure 3.4 Ties Manufacture Plant

CHAPTER 4

LABORATORY SETUP AND INSTRUMENTATION

This chapter discusses the test setup and the instrumentation processing for all tests that have done at the University of South Carolina Laboratories Following The American Railway Engineering and Maintenance – of – Way Association guidelines. Also discusses the tests setup that not followed AREMA guidelines, and the using of the Digital Image Correlation technique to gain the full field measurements.

4.1 Test Setup

The railroad ties (HSRM and Standard) were investigated and tested in the laboratories at University of South Carolina. Qualification tests for the ties have been done following AREMA specification in chapter 30 [4]. Additional tests were conducted for the performance assessment of the new product. Although these tests required a different setup, as discussed in detail in the next chapter, the same equipment was used. The testing equipment consisted of a steel reaction frame consisting of four 16 ft long W12x87 columns two 7 feet long W18x119 beams and two 4 feet long W16x89 beams. In addition, 5 feet long W18x119 cross beam is attached to the long beams and carries the actuator. The actuator used in all tests is MTS brand, 110 kips with a 6 in. stroke. Two spreader beams of span 8 in. and 40 in, respectively, are attached to the actuator head to transfer the load to the test specimen as specified by the specific test configuration. The actuator is connected to a 40 GPM MTS hydraulic pump. The actuator is also equipped with a load cell and LVDT. All tests are carried out in load control mode.

Two concrete supports with 48 in. length, 30 in height, 12 in top width and 22 in bottom width. Figure 4.3 shows the dimensions of the concrete supports. Supports can be placed at a variable spacing to accommodate the test requirements.

4.2 Conventional Instrumentation

Conventional measurement devices are employed for all tests. Specifically, Linear Voltage Differential Transformers (LVDTs) are used to measure the deflections at discrete locations under the specimen (opposite side of the applied load) and to measure strand slippage. For deflection measurements, the LVDTs are attached to a single 2x4 wood tread at predetermined spacing as shown in figure 4.1 with their tips in contact with the side of the tie. For strand slippage measurements the LVDT is clamped to the specimen as shown in figure 5.22 and the tip is in contact with the exposed strand face. In all cases, the tips of the LVDTs are adhered to the specimen by a small amount of epoxy. Strain gages are also attached to the surface of the tie. These strain gauges were manufactured by Tokyo Sokki Kenkyujo Co, Ltd. (TML) and are specifically designed for use on concrete structural elements (Tokyo 2017). The gauge length is 1.18 in (30 mm), the gauge width is 0.1 in (2.3 mm), and the gauge resistance is 120 Ohms. The way that the strain gages were installed (1) Use a wire brush to remove surface irregularities (2) Brush all loose dust from the surface. (3) Apply Two-part 5 minutes time adhesive, applied in two coats: primer and secondary. Primer coat bonds with a concrete surface and provides a smooth surface for mounting strain gauge, secondary coat bonds strain gauge to primer coat. Strain gauges and the LVDTs were connected to Data acquisition system (VISHAY 7000) to get the displacement and the strain data.

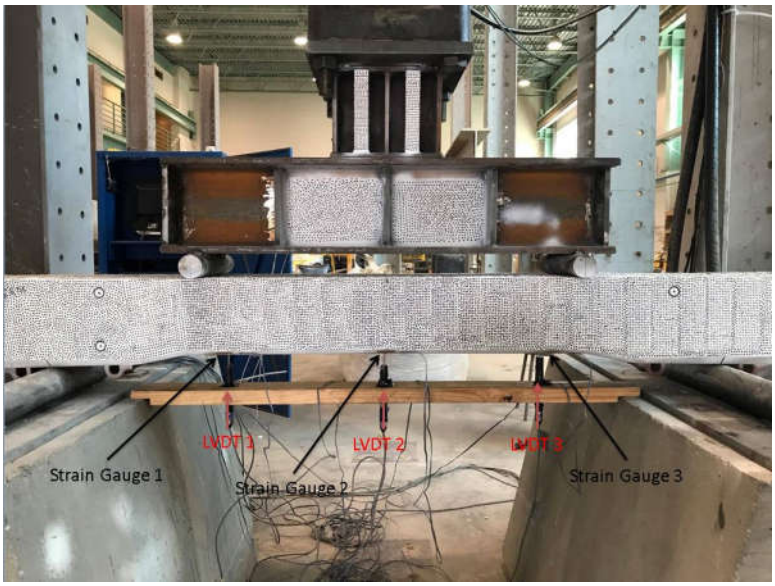

Figure 4.1 Test Setup Shows LVDT's and Strain gauges

Figure 4.2 Supports Dimensions

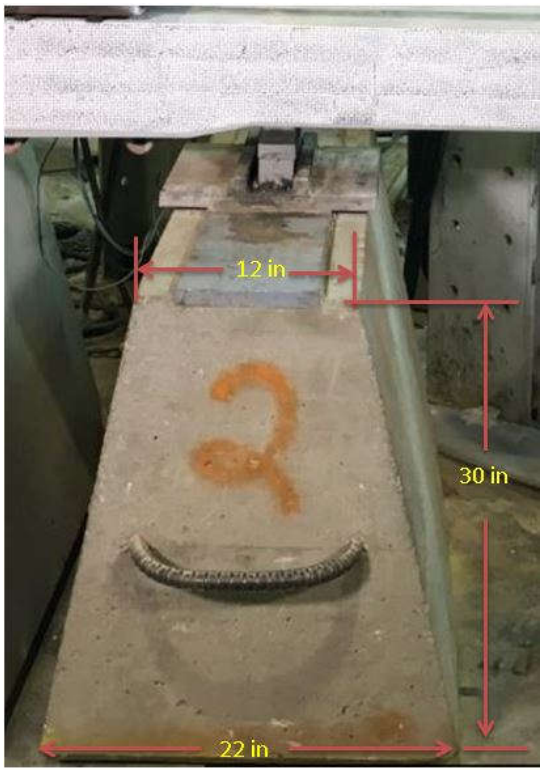

Figure 4.3 Support Geometry

4.3 Vision Based Full Field Measurements.

Digital image correlation (DIC) is a unique suite of non-contacting, vision-based full-field measurement methods developed in the USC laboratories over the past three decades [25][26]. The DIC methods can be used for large and extremely small specimens. The most effective method in the broadest range of applications employs stereo cameras. Once a pair of images is acquired, 3-D digital image correlation (3D-DIC) is performed on the image pair to extract the full 3-D displacement field for large or small specimens that may be curved or planar in shape. Measurements using both 2D-DIC and 3D-DIC have been successfully made for a wide range of materials, and loading and temperature conditions [27]. In addition to deformation measurements, the method

can be used to detect crack development and propagation and damage evolution. The following sections describe the Stereo Vision system used in this work in detail.

4.3.1 Imaging System and Components.

The proposed Stereo DIC system consists of a pair of cameras and lenses, low heat emission lighting, a computer for image acquisition, cables, calibration tablets, speckle application kits, and VIC-3D® software as shown in figure 4.4.

Figure 4.4 DIC System

Cameras and lenses

In these experiments, a matched pair of 9.1 Megapixel Point Grey cameras with 17 mm focal length lenses was used to capture overlapping images of the side surface of the tie. The camera-lenses combination and the distance of the cameras from the specimen were selected to obtain the desired field of view that ranges from 35-110 in. The cameras are mounted on a rigid aluminum bar and were spaced approximately 3ft-4in from each other, resulting in stereo angles between 15˚ - 25˚. Figure 4.5 shows the cameras and the lenses.

Figure 4.5 Cameras and lenses

Lighting

To obtain high contrast images, four Bi-color 500 Ultra Bright Dimmable LED Studio Light Panel - 9M-01LED009-500-07 were used to illuminate the surface with minimal heating of the surrounding air. Each bank of lights was mounted on portable supports placed on opposite sides of the specimen and tilted downward to illuminate the surface of the specimen. Figure 4.6 shows the lights. It is noted that the lights and cameras should not be located at the same level to avoid direct reflection.

Figure 4.6 Bi-color 500 Ultra Bright Dimmable LED Studio Light Panel

Calibration Tablet

Each test had a different calibration tablet depending on the field of view. The calibration tablet has to be at least one-third of the field of view. For example, in this study rigid rectangular sheets with a 9 x 12 grid of circular dots with a dot size of 0.51inch (13mm) and dot spacing of 1.38 inch (35mm) were used to get the calibration parameters.

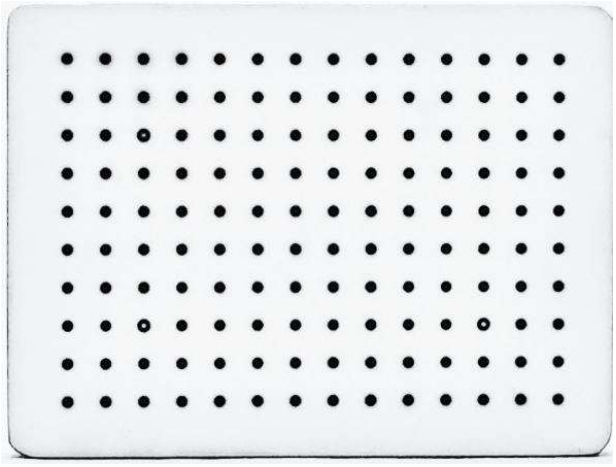

Figure 4.7 Calibration Tablet

Speckle Application Kit

The speckled pattern is applied on the specimen surface by a cylindrical roller stamp shown in figure 4.8. The stamp is manufactured with a raised, randomly distributed dot pattern of a diameter appropriate to create a speckle pattern on the surface of the prestressed concrete that is sampled by more than 3 pixels in each direction. The type of ink was using is Rust-Oleum 249127 Painter's Touch Multi-Purpose Spray Paint, 12-Ounce, Flat Black.

Figure 4.8 VIC Speckle Pattern Application Kit

VIC-3D / VIC Snap Software

Commercial software VIC-3D supplied by Correlated Solution Inc. is used for the image processing. The Vic software family is very easy to use and provides a user interface consistent with all the other commonly used software applications. This software includes powerful tools for visualization and interfaces well with other graphing and plotting software. VIC Snap which is also commercial software that uses to captures the images.

Application of speckle-pattern

Digital image correlation requires (a) a high contrast random pattern on the surface of the prestressed concrete beam and (b) an appropriate size for the pattern, so that oversampling of the pattern is performed during imaging. If both of these requirements are met, then accurate measurement of displacements and strains is achievable. As noted in a recent publication [28] the size of each feature in the random pattern should be sampled by at least 3 x 3 pixels to improve the accuracy of the required intensity interpolation and to minimize aliasing of the pattern. In our experiments, the Point Grey camera used a Sony ICX625 imaging sensor with a resolution of 2448 x 2048 pixels and a physical size of 3.45μm for each pixel. The approximate "digital magnification" for each camera in the stereo system is 0.029 in./pixel [0.72mm/pixel]. Since each pixel is 0.00345mm in size, the optical magnification of the imaging system is 1/2000, indicating high demagnification for this experiment. Therefore the minimum dimension of the feature size in the random pattern should be on the order of 0.087 in. [2.2 mm] (3 pixels x 0.020 in./pixel) To ensure adequate sampling for accurate measurements. The cylindrical roller stamp is manufactured with a raised, randomly distributed dot pattern of 0.118 in. [3mm] diameter to create a speckle pattern on the surface of the prestressed concrete that was sampled by more than 3 pixels in each direction. For making accurate measurements with a Stereo DIC system, a histogram should show relatively uniform contrast ranging from 20–220 gray levels, which is over 75% of the maximum available (256 gray levels) for the eight bit Point Gray cameras used in this study.

4.3.2 Image Acquisition

The imaging systems' cameras are activated at least one hour before acquiring the first set of images to ensure that they have reached steady-state. Once all initial preparation of the specimens for Stereo DIC measurements has been completed, the imaging system is calibrated using the calibration template. During calibration, the rigid grid specimen is translated and rotated into a broad range of positions within the field of view of the camera system. At each position and orientation, time-synchronized images of the grid are obtained with commercial software and hardware manufactured by Correlated Solutions [29]. In these studies, a total of 100 grid images are acquired by each camera, and a 2^{nd} order radial distortion correction algorithm is employed to minimize potential errors associated with lens distortions. Once successful calibration is complete, a total of 200 synchronized images (100 for each camera) of the unloaded specimen is obtained. This is SET-0 of the image acquisition, and the captured images are used as reference images in subsequent data processing. After the images have been obtained, the load is increased by a predetermined amount. Upon completion of the incremental loading, a total of 200 additional synchronized images (100 for each camera) are obtained by the imaging system. This is SET-n of the image acquisition, and the captured images are the images of the deformed ties also used in subsequent data processing. Figure 4.9 shows the deformation parameters of a facet after some steps in testing with regard to the original (reference) state. The 2-D coordinates of the same facet are determined using the points on the corner from both cameras to find a common 3-D coordinate [30].

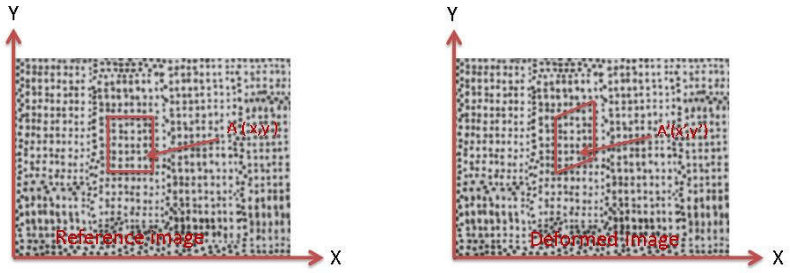

Figure 4.9 shows the deformation parameters of a facet after some steps in testing with regard to the original (reference) state

4.3.3 Image Analysis and Deformation Measurements

Once loading has reached its final level, or tie failure has occurred, and all images have been acquired, the experimental process is complete. Correlation of sets SET-0 and SET-n produces shapes and the full field deformations and strains produced by the loading at "step n".

Digital CCD cameras, including the Point Gray cameras used in this study, are known to have variability in each pixel's intensity that is Gaussian in distribution. The Point Gray cameras used in this work have a Standard deviation that is approximately 0.4% of the range or +/- 1 gray level out of 256. These small changes in the intensity pattern introduce errors in the image-based measurement of displacements and strains that can range up to +/- 0.02 pixels for low contrast images. Since the average compressive strain on the surface of the tie is expected to be below 200 $\mu\varepsilon$ at early loading stages, it is important to reduce the level of variability in the image-based measurements. One of the most important noise sources in imaging is variability in the pixel-level intensity data, which has been shown to be random Gaussian in form. Since the image noise is Gaussian in form, and then it is possible to use averaging of the data in each set of images SET-n to significantly reduce the effect of this noise source on the

measurements. In addition to averaging results from many images, the following steps are taken to limit the noise introduced in the Stereo DIC measurements by other experimental factors:

- Cameras are attached to a rigid aluminum extruded bar and then isolated from laboratory vibrations through use of rubberized compression mounts.
- The cameras are allowed to reach a steady state temperature before camera calibration. Our investigations have confirmed that various internal components of the camera will undergo transient changes during heat-up that induce errors in the recorded images.
- A 2^{nd} order radial lens distortion function is used in the camera calibration to more accurately account for image distortions that can occur when using a wide angle lens.

4.4 DIC System Verification

In order to verify the consistency among the measurements taken by the different instrumentation, a validation study is conducted. To this end, a four-point bending test of a Standard Concrete (Section 3.2.1) tie for center binding loading is considered. The specimen is loaded to 20 kips, and the load is applied in 2 kip increments. The load rate is set to 5 kips per minute, and the load is held for one minute at each increment. The test setup is shown in previous Figure 4.2. The instrumentation consists of:

(a) One strain gage installed at the mid-span and two strain gages installed at 15 in. On each side of the mid-span and at the tension side of the tie as shown in Figure 4.1

(b) One LVDT installed at the mid-span and two LVDT installed at 15 in. On each side of the mid-span at the tension side of the tie.

(c) Stereo-DIC imaging of the side of the tie to compute the deformation and strain fields during testing. At each load hold, 100 image pairs are acquired, and images were averaged to minimize the noise [31].

Figure 4.10 shows the longitudinal strain profile at mid-span of the prestressed concrete tie from DIC and the strain gage by taking a line on the mid-span and extrapolate the data to get the exact location of the strain gage strain.

Figure 4.12 shows the vertical displacement vs. loads for the DIC and the LVDTs at the mid-span and 15 in. sides. The results show almost the same values for all points. Excellent agreement among the different measurements is observed.

Figure 4.11 shows the comparison between the DIC measurements and the strain gage values for the whole test load at the same point with an error in DIC measurements between 20 – 40 micro strains.

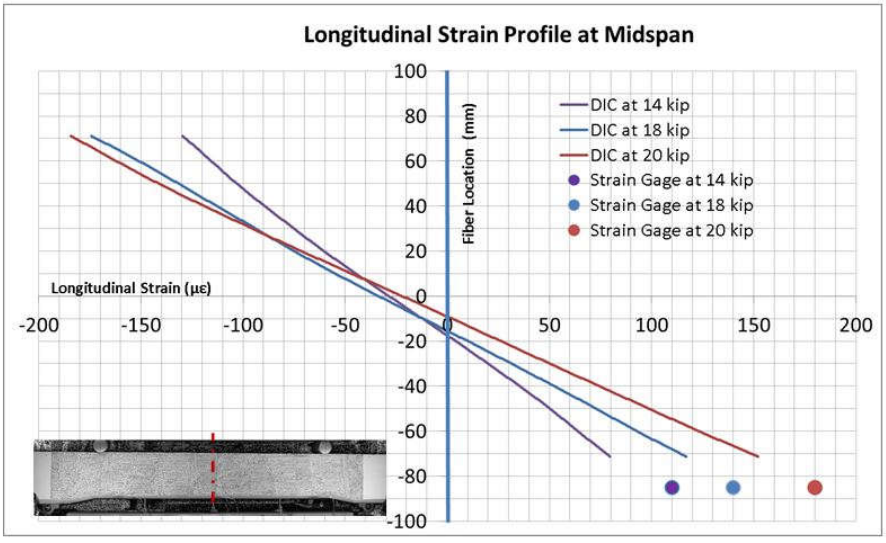

Figure 4.10 The Longitudinal Strain Profile at Mid-span of the Prestressed Concrete Tie from DIC and the Strain Gages

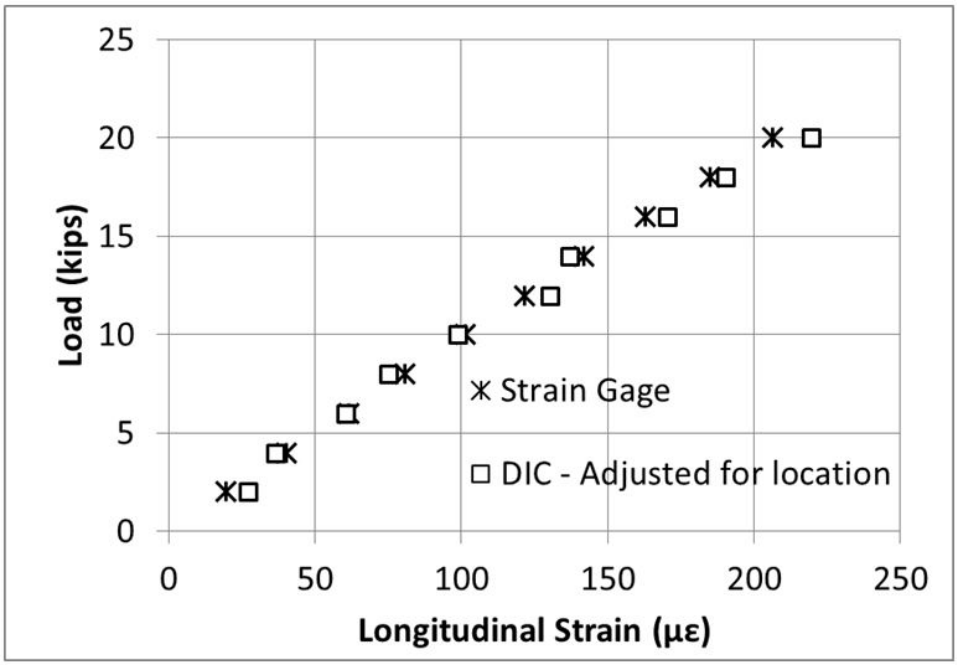

Figure 4.11 Validate the Strain gages with the DIC

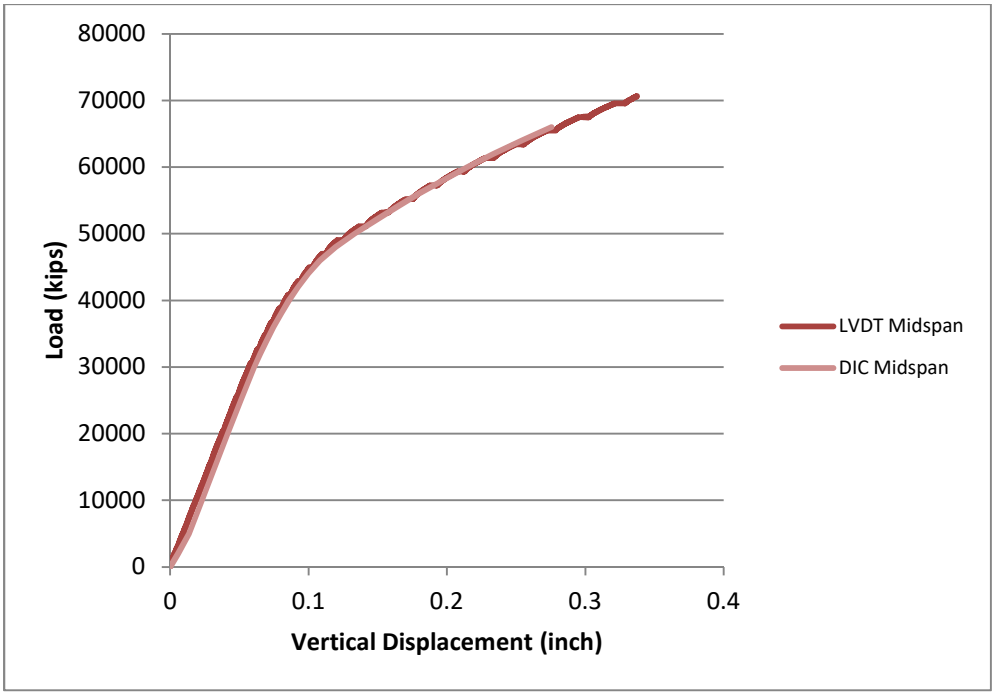

Figure 4.12 Validate the LVDT with the DIC

Rubber pads testing

In order to get the stiffness for the rubber pads that we were using in the qualification tests following AREMA guidelines as discuss in chapter 5 about the design qualification test per AREMA. As shown in figures 4.13 and 4.14.

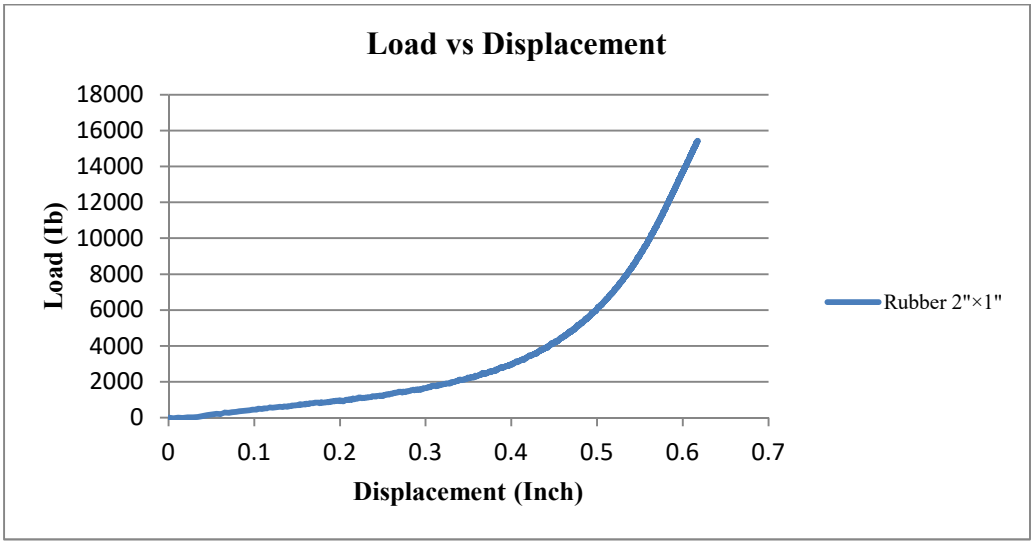

Figure 4.13 Rubber 2×1 inches Load vs. Displacement Curve

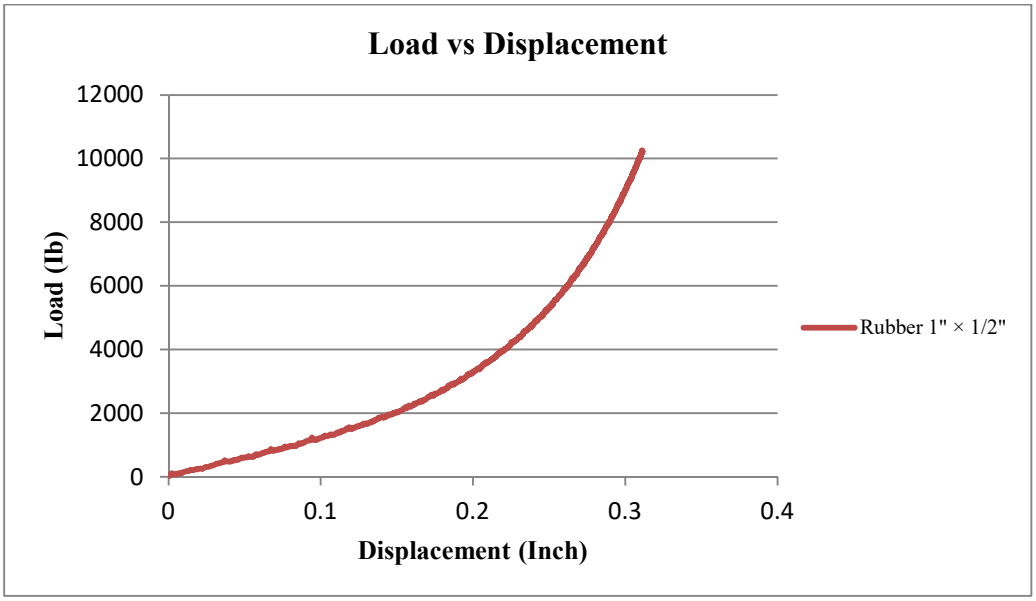

Figure 4.14 Rubber 1×1/2 inches Load vs. Displacement Curve

CHAPTER 5

DESIGN QUALIFICATION TESTS PER AREMA

In order to qualify the final product, the Standard and Prototype ties must be in compliance with AREMA guidelines as set forth in Chapter 30 section 4.9 Testing of Monoblock Ties of the AREMA Manual of Railway Engineering [4]. In particular, the sequence of design tests specified in sections 5.1 are conducted at the testing facilities at the University of South Carolina, and the tests specified in sections 4.9.1.9 and 4.9.1.10 are conducted at the RailTEC laboratories at the University of Illinois in Urbana-Champaign. Five HSRM and six Standard ties were selected randomly for testing at USC, and two HSRM and two Standard ties were shipped to the RailTEC facilities. Failure of the prestressed concrete ties to pass the following tests is a cause for rejection of the design.

5.1 The Sequence of Design Tests (Tie 1)

The sequence of design tests according to AREMA loading procedure are:

1- Rail Seat Vertical Load Test performed on one rail seat hereinafter designated rail seat A.

2- Center Negative Bending Moment Test.

3- Center Positive Bending Moment Test.

4- Rail Seat Vertical Load Test performed on the other rail seat hereinafter designated rail seat B.

5- Rail Seat Repeated Load Test performed on rail seat B.

6- Bond Development, Tendon Anchorage, and Ultimate Load Test performed on rail seat A.

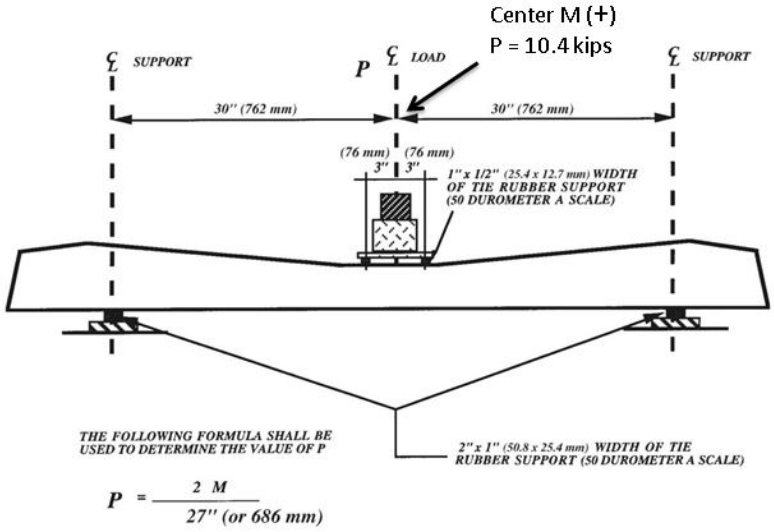

Figure 5.1 Tie Center Positive Moment Test (AREMA)

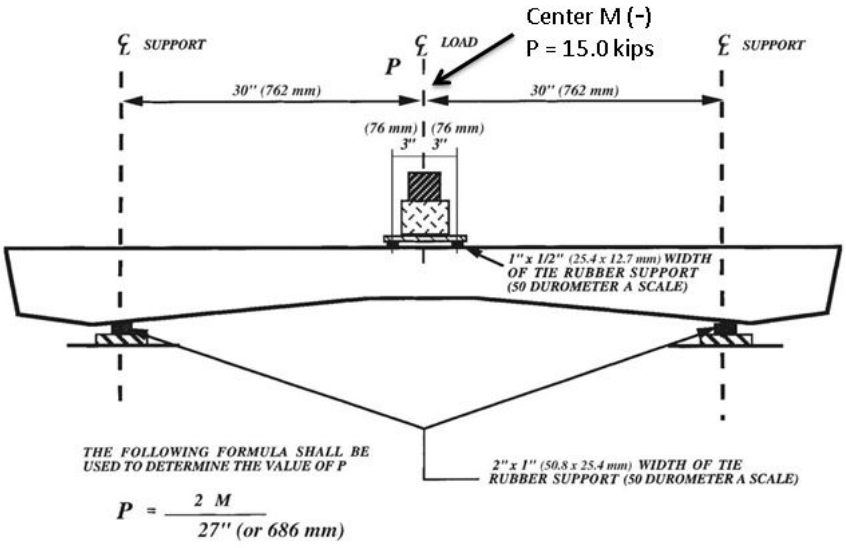

Figure 5.2 Tie Center Negative Moment Test (AREMA)

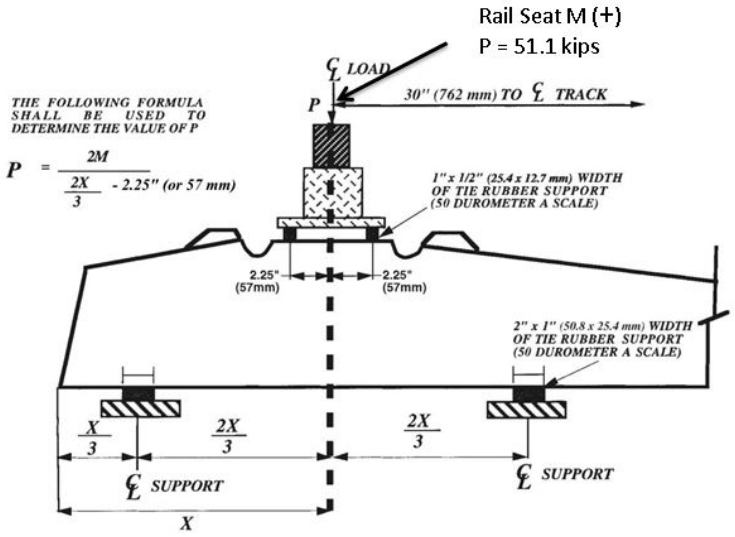

Figure 5.3 Rail Seat Positive Moment Test (AREMA)

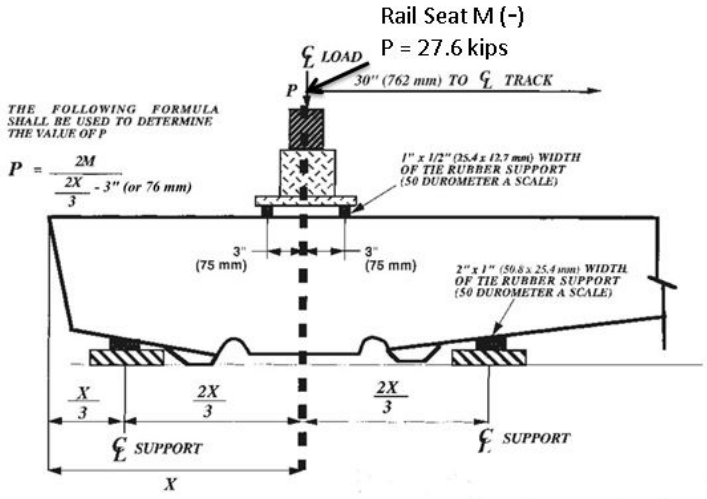

Figure 5.4 Rail Seat Negative Moment Test (AREMA)

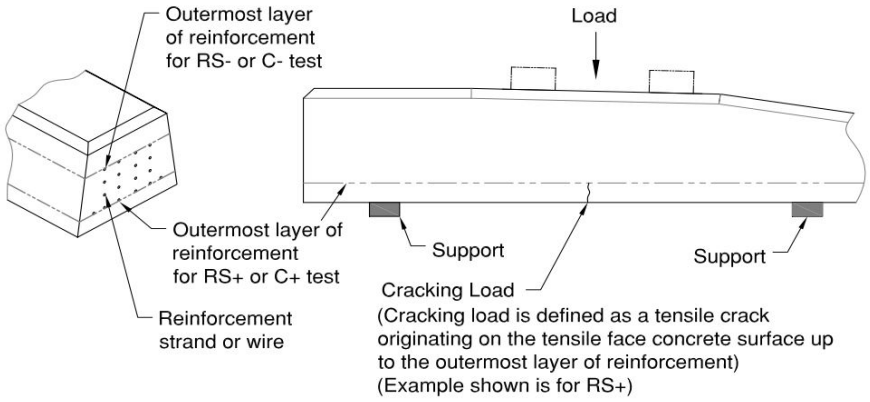

Figure 5.5 Cracking Load (AREMA)

All loading tests are load-controlled. The support arrangements for static and dynamic loading tests on rail seat and center sections are shown in figures 5.1, 5.2, 5.3, 5.4 and 5.5. Resilient pads (with dimensions of 1×2 inches on the bottom and 1/2×1 inch on top with a durometer of A50) required by the AREMA Standard are placed between the supports under the ties and the undersides of ties.

5.1.1 Rail Seat Positive Moment Test, AREMA Chapter -30- Section 4.9.1.4.

The prestressed concrete ties were supported and loaded as shown in figure 5.6 with the distance between bottom supports of 28 in. and top supports of 5 in. The load is applied continuously at a rate of 3 kips per minute without any shock until the required design load, P=51.1 kips is achieved. Once the design load is reached, the load is held not less than 3 minutes, and an inspection is made to check the tie for structural cracks using an illuminated 5-power magnifying lens. The StereoDIC measurements were also evaluated for identifying potential initiation of cracking at or before the design load is reached. The longitudinal strain field on the side of the tie as acquired by the DIC measurements is shown in figures 5.8 and 5.9, which indicates that the HSRM tie

distributes the load and has more longitudinal strain than the Standard tie. Figure 5.7 shows the load vs displacement curve that illustrates the flexibility of the HSRM tie through the higher deflection.

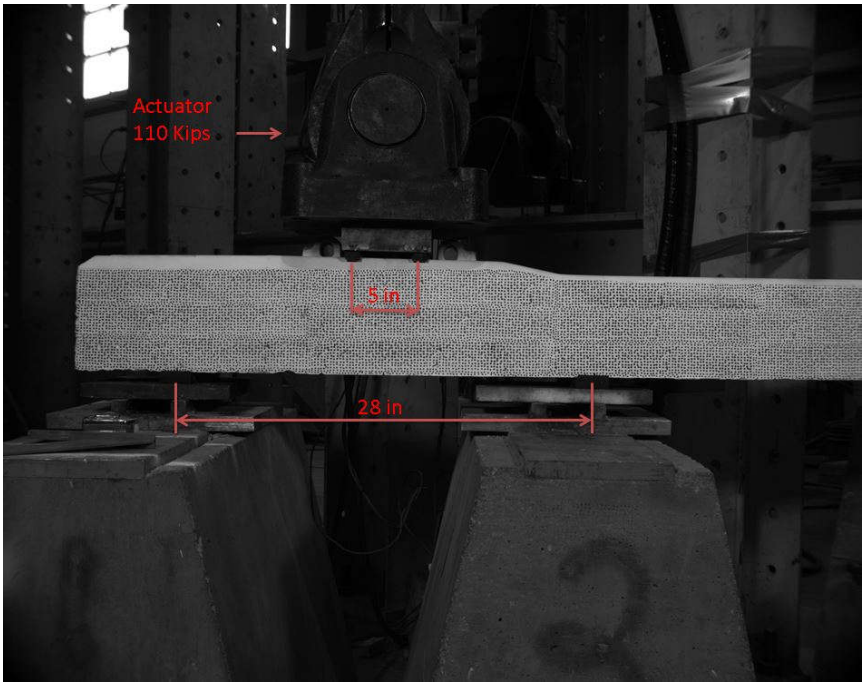

Figure 5.6 Rail Seat Positive Moment Test

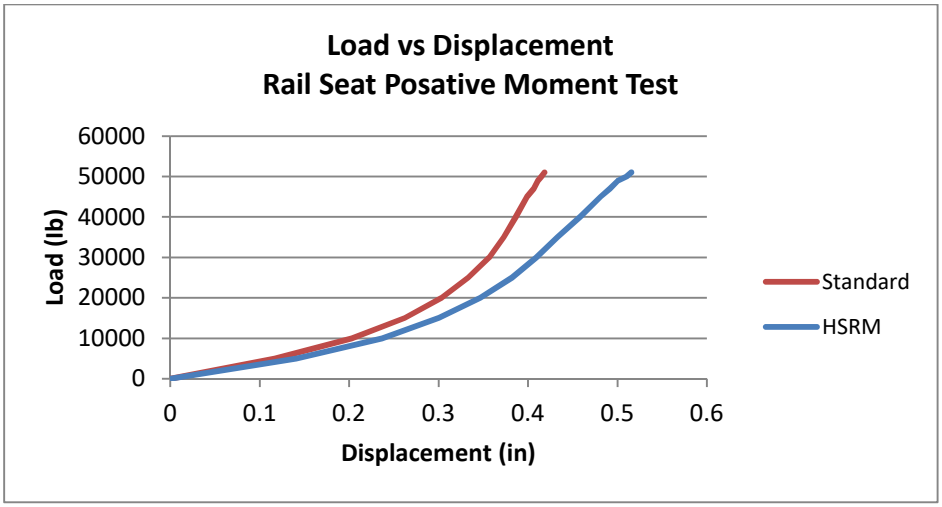

Figure 5.7 Rail Seat Positive Moment Test Load vs Deflection Curve

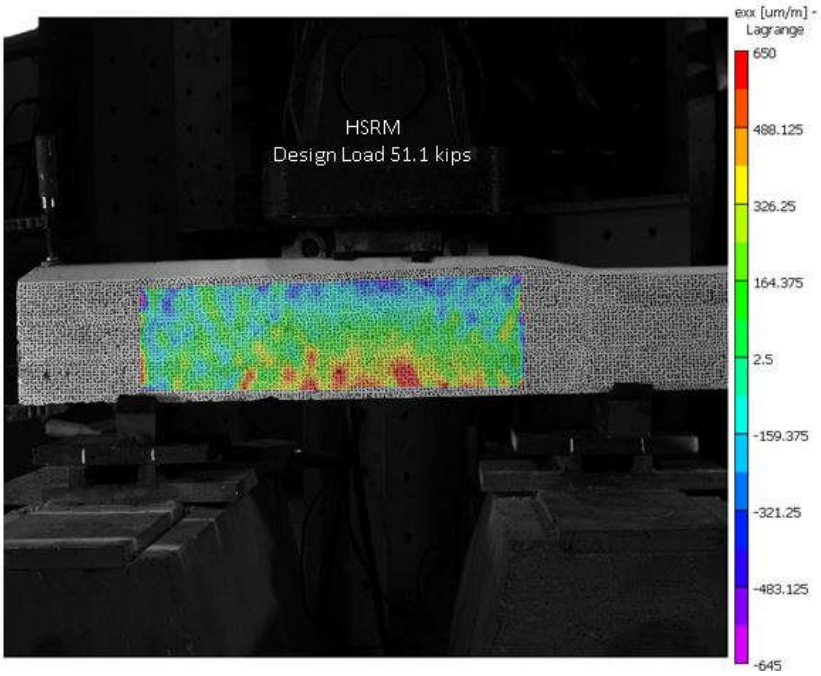

Figure 5.8 HSRM Rail Seat Positive Moment Test DIC Image

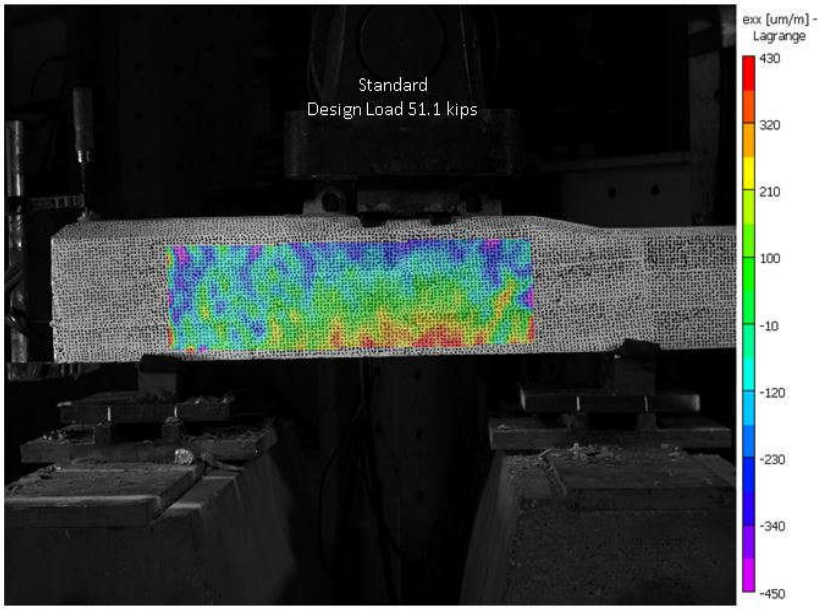

Figure 5.9 Standard Rail Seat Positive Moment Test DIC Image

5.1.2 Rail Seat Negative Moment Test, AREMA Chapter -30- Section 4.9.1.4.

The prestressed concrete ties were supported and loaded as shown in figure 5.10 with the distance between the bottom supports of 28 in. and the top support of 5 in. The

load is applied continuously at a rate of 3 kips per minute without any shock until the required design load, P=27.6 kips is achieved. Once the design load is reached, the load is held not less than 3 minutes, and an inspection is made to check the tie for structural cracks using an illuminated 5-power magnifying lens. The StereoDIC measurement was also evaluated for identifying potential initiation of cracking at or before the design load is reached. The longitudinal strain field on the side of the tie as acquired by the DIC measurements is shown in figures 5.13 and 5.14, which indicates that the HSRM tie distributes the load and has more longitudinal strain than the Standard tie. Figure 5.11 shows the load vs displacement curve that illustrates the flexibility of the HSRM tie through the higher deflection.

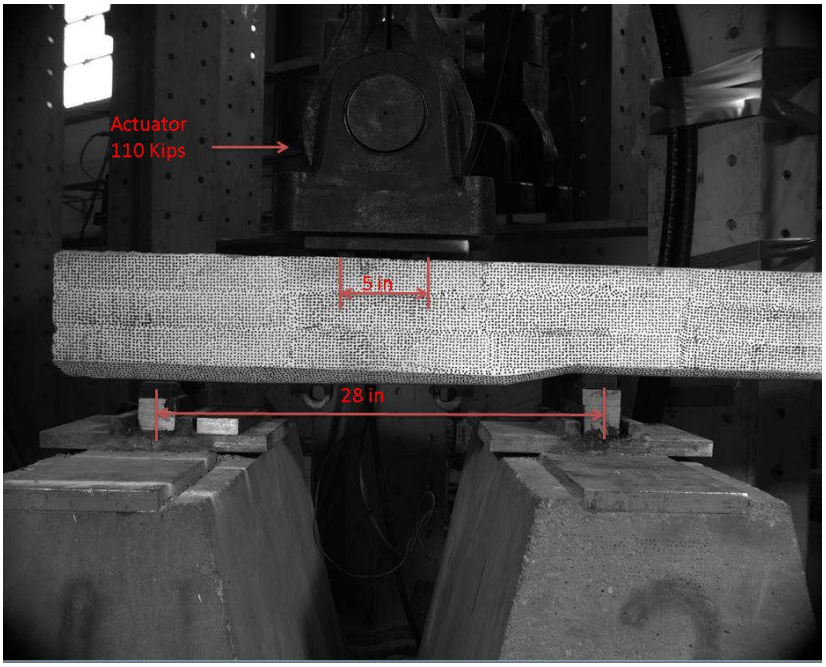

Figure 5.10 Rail Seat Negative Moment Test

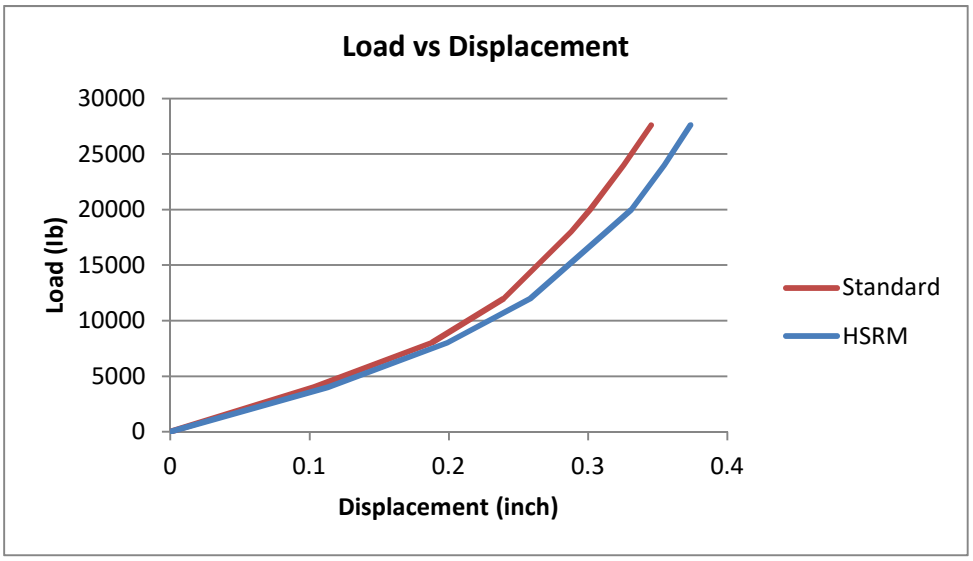

Figure 5.11 Rail Seat Negative Moment Test Load vs Displacement Curve

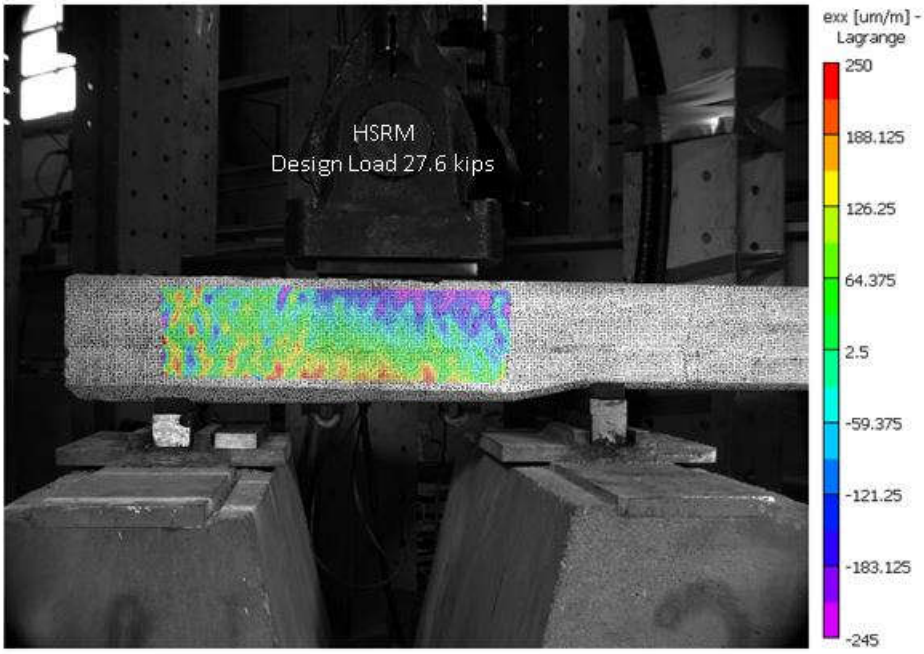

Figure 5.12 HSRM Rail Seat Negative Moment Test DIC Image

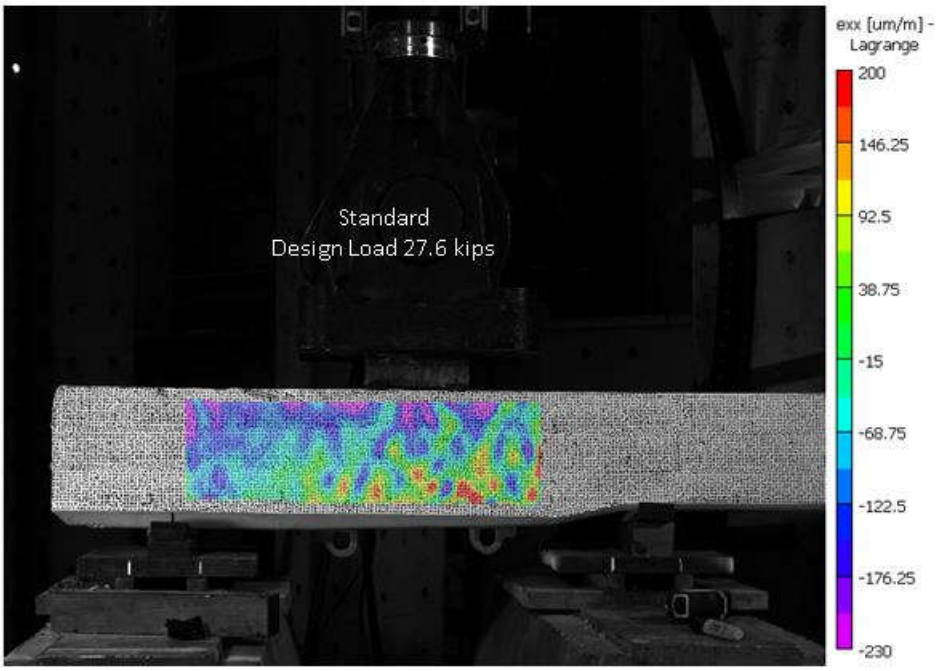

Figure 5.13 Standard Rail Seat Negative Moment Test DIC Image

5.1.3 Center Positive Moment Test, AREMA Chapter -30- Section 4.9.1.7.

The prestressed concrete ties were supported and loaded as shown in figure 5.14 with the distance between the bottom supports of 60 in. and the top supports of 6 in. The load is applied continuously at a rate of 3 kips per minute without any shock until the required design load, P=10.4 kips, is achieved. Once the design load is reached, the load is held not less than 3 minutes, and an inspection is made to check the tie for structural cracks using an illuminated 5-power magnifying lens. The StereoDIC measurement was also evaluated for identifying potential initiation of cracking at or before the design load is reached. The longitudinal strain field on the side of the tie as acquired by the DIC measurements is shown in figures 5.16 and 5.17, which indicates that the HSRM tie distributes the load and has more longitudinal strain than the Standard tie. Figure 5.15

shows the load vs displacement curve that illustrates the flexibility of the HSRM tie through the higher deflection.

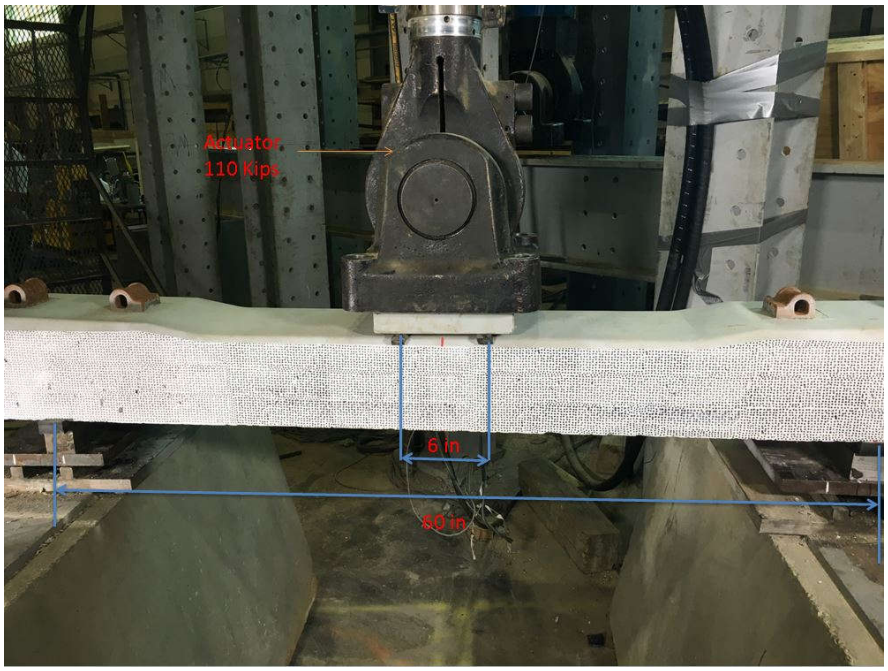

Figure 5.14 Center Positive Moment Test

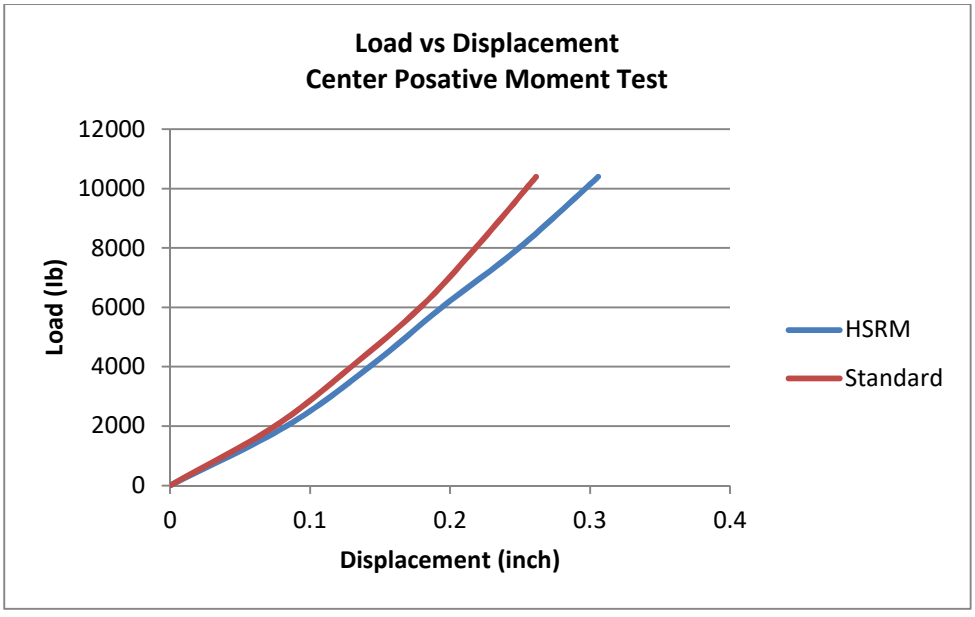

Figure 5.15 Center Positive Moment Test Load vs Displacement Curve

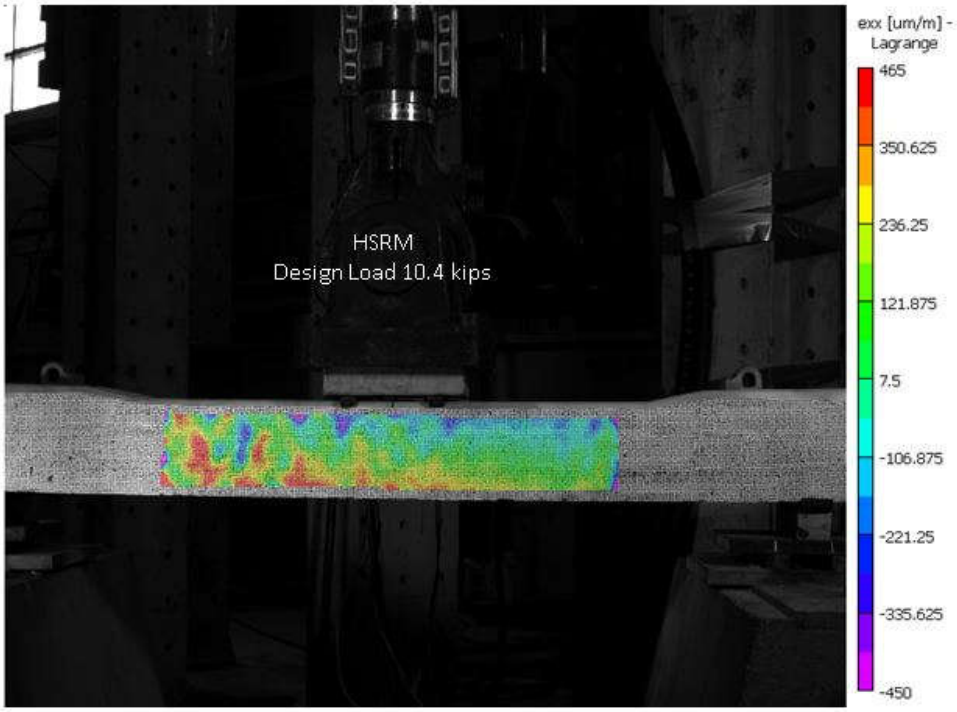

Figure 5.16 HSRM Center Positive Moment Test DIC Image

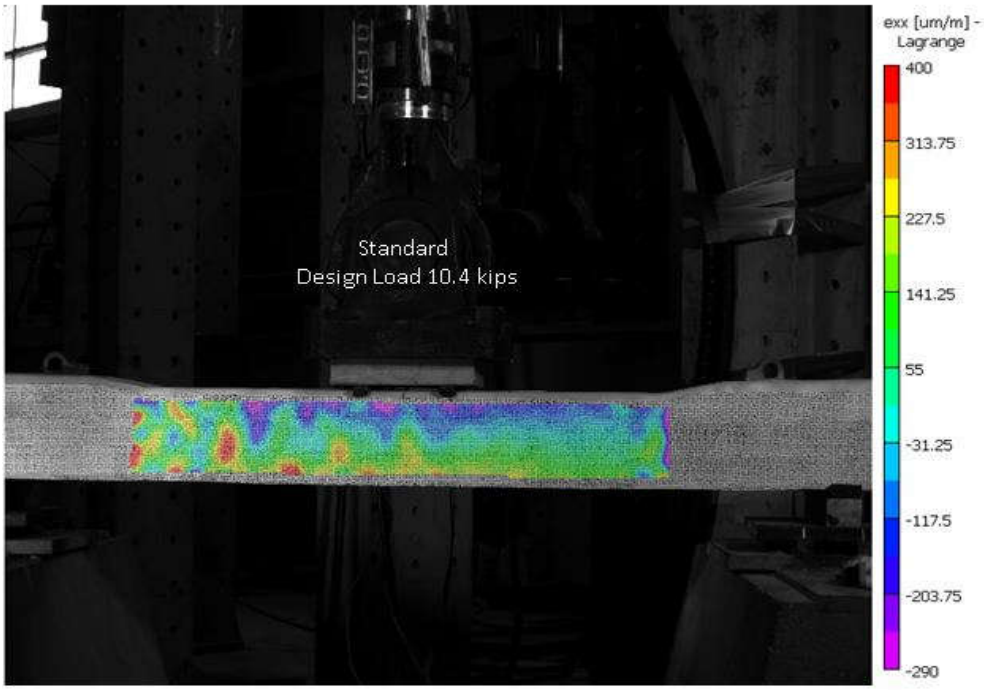

Figure 5.17 Standard Center Positive Moment Test DIC Image

5.1.4 Center Negative Moment Test, AREMA Chapter -30- Section 4.9.1.6.

The prestressed concrete ties were supported and loaded as shown in figure 5.18 with the distance between the bottom supports of 60 in. and the top supports of 6 in. The load is applied continuously at a rate of 3 kips per minute without any shock until the required design load, P=15 kips is achieved. Once the design load is reached an inspection is made to check the tie for structural cracks using an illuminated 5-power magnifying lens. The StereoDIC measurement was also evaluated for identifying potential initiation of cracking at or before the design load is reached. The longitudinal strain field on the side of the tie as acquired by the DIC measurements is shown in figures 5.20 and 5.21, which indicates that the HSRM tie distributes the load and has more longitudinal strain than the Standard tie. Figure 5.19 shows the load vs. displacement curve that illustrates the flexibility of the HSRM tie through the higher deflection.

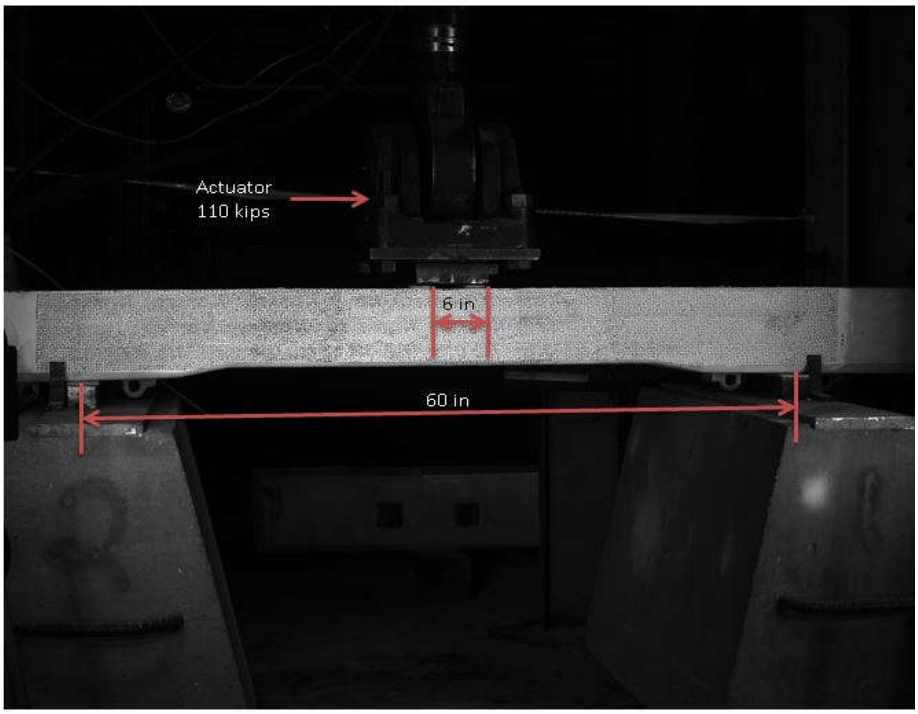

Figure 5.18 Center Negative Moment Test

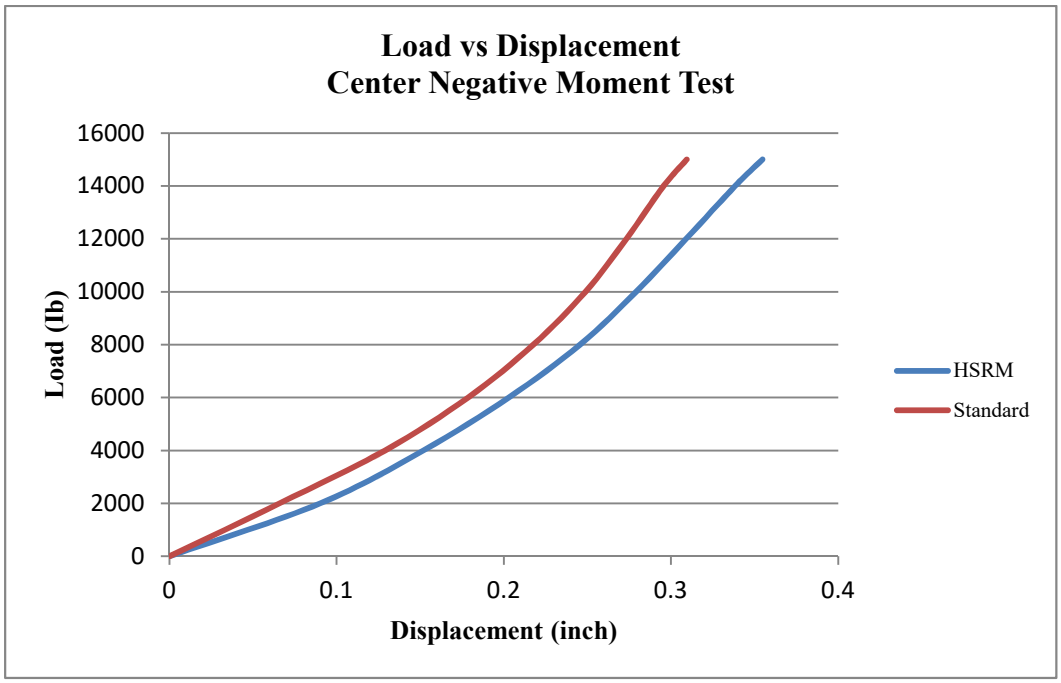

Figure 5.19 Center Negative Moment Test Load vs Displacement Curve

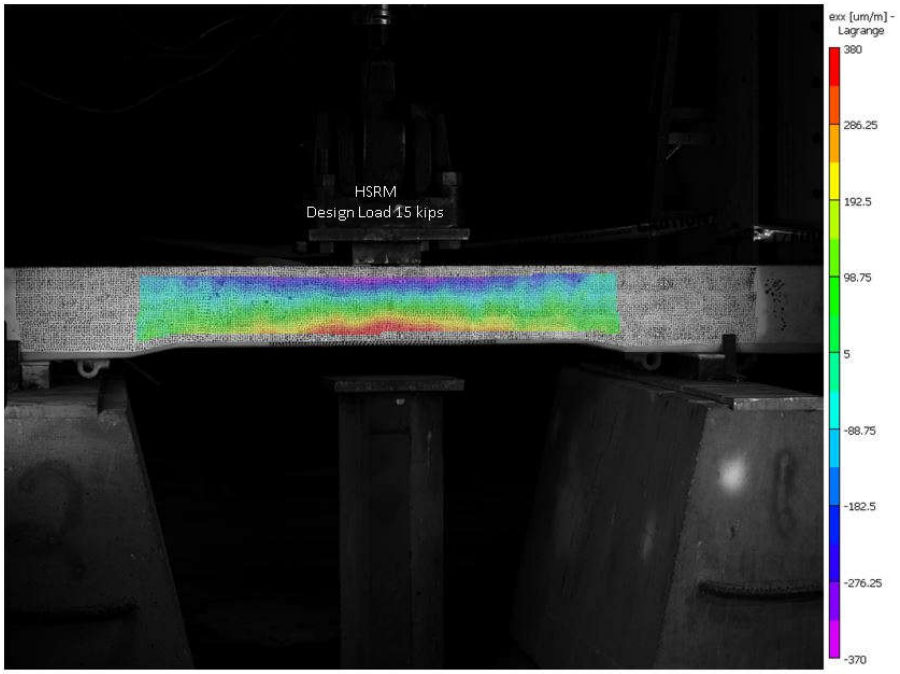

Figure 5.20 HSRM Center Negative Moment Test DIC Image

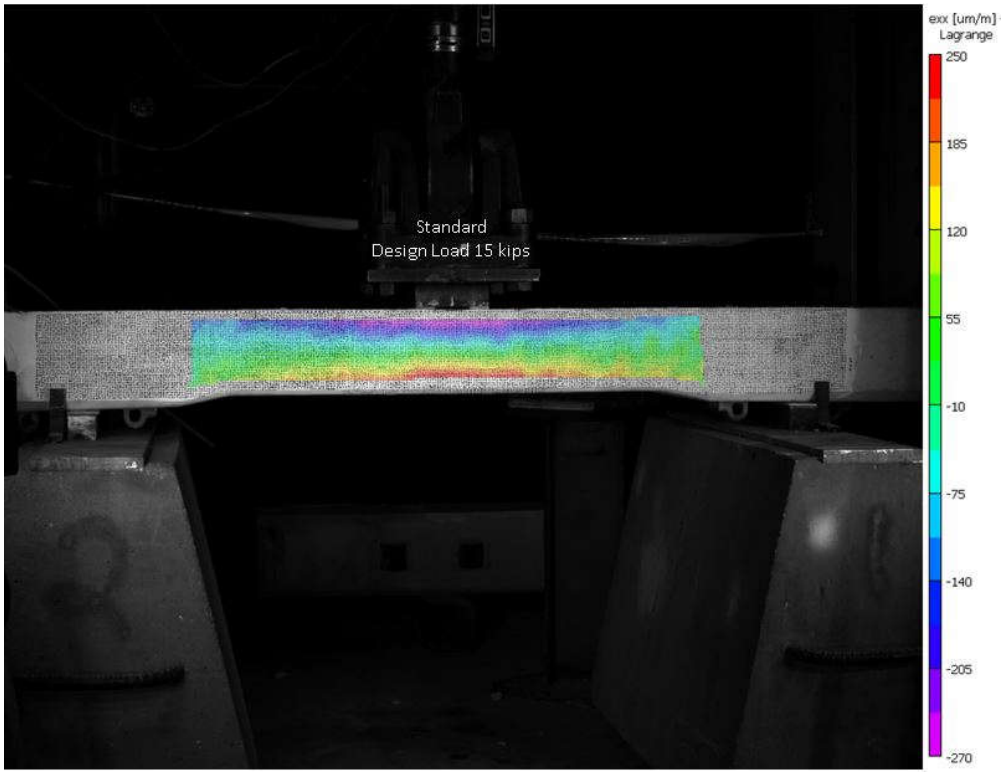

Figure 5.21 Standard Center Negative Moment Test DIC Image

5.1.5 Rail Seat Repeated load test and Ultimate test, AREMA Chapter -30- Section 4.9.1.6.

The railroad prestressed concrete tie was subjected to a static load on the rail seat with a load rate of 4 kips per minute until the tie cracked and the crack reached the first layer of the lower strands following the testing criteria that AREMA suggested in chapter 30 [4]. After the tie cracked and the crack arrived to the first layer of the strand, all the necessary pads that were used for the static load were removed and substituted with ¼ inch (6.35 mm) thick plywood strips as shown figure 5.23. In this test, the ties were also provided with lateral and longitudinal supports that prevented lateral and longitudinal sleeper movement during the cycling.

The railroad concrete ties (HSRM and Standard) were subjected to 3 million cycles of repeated loading with cycles varying uniformly from 4 kips (17.8 N) to the value of 1.1 from the design load, which is 51.1 kips; therefore, the load varied from 4 kips to 56.21 kips. Two cycles per second were applied, and the test was paused every 250,000 cycles in order to take images by DIC, then the test resumed until the next 250,000 cycles finished. The specimen was loaded statically to 1.1 of the design load in order to capture the strain field. The strain field was captured of 4, 10, 20, 30, 40, 51.1, and 56.21 kips. So the reference images were 0 kip load 0 cycles and used the average for the entire test to check the strain field of the ties for any changes.

After the tie was subjected to 3 million cycles, the railroad ties were subjected to a static load starting from 0 kips to 1.5 from the design load in order to check the ties from tendon slippage; then the specimens were loaded until failure. The tendon slippage has to be no more than 0.001 inches (0.025mm), and the tie had to pass this test with that load without concrete compressive failure, concrete shear cracks, or tendon failure [4].

The ties passed the test without any tendons failing, concrete compressive failure, and concrete shear cracks. The tendon slippage was checked by using LVDT on the left strand from the bottom layer of strands as shown in figure 5.22.

Tables 5.1 and 5.2 show the results of the qualification tests that have been done on the HSRM's ties and the Standard's ties. The results show that the HSRM ties passed all the qualification tests without any cracks at the design load. Two of the Standard ties failed in the rail seat positive moment test because of the high concentration of stress in the tension area, which caused the ties to start cracking before they reached the design load.

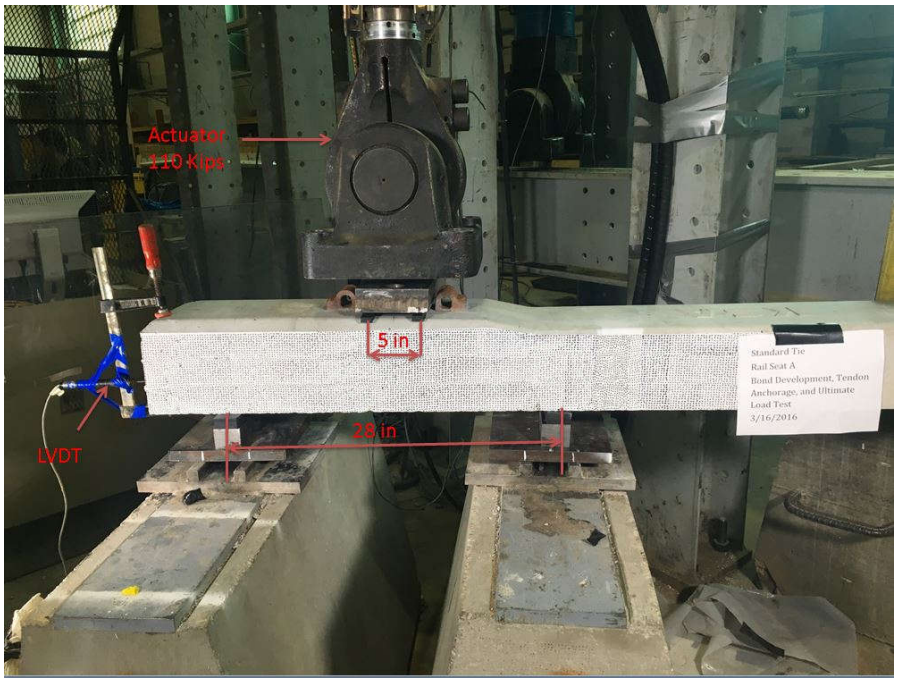

Figure 5.22 Bond Development, Tendon Anchorage, and Ultimate Load Test

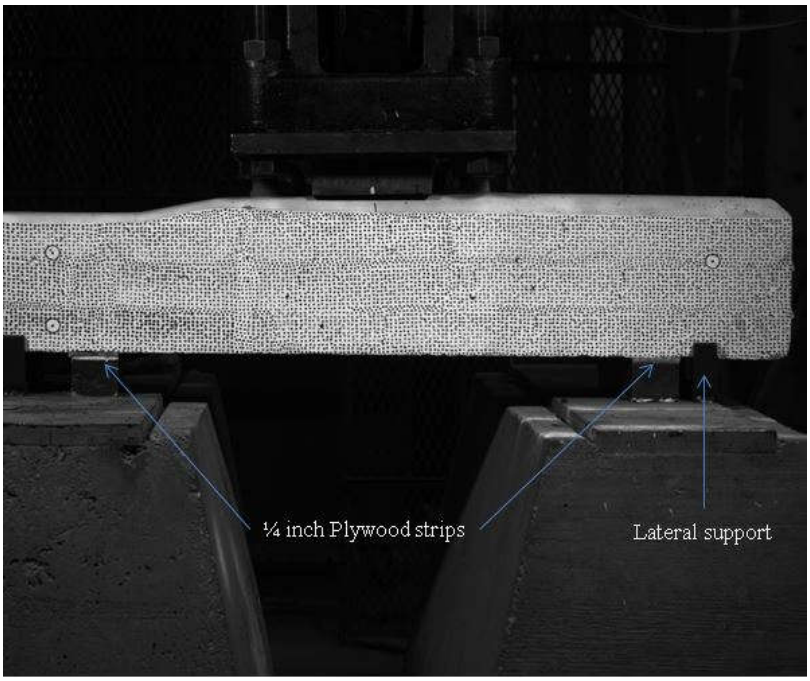

Figure 5.23 Repeated Load Test

Table 5.1 Qualification Tests Results

Tie ID		Rail Seat A		Rail Seat B		Center	
		M+	M-	M+	M-	M+	M-
Prototype	HSRM-1	Pass	Pass	Pass	Pass	Pass	Pass
	HSRM-2	Pass	Pass	Pass	Pass	Pass	Pass
	HSRM-3	Pass	Pass	Pass	Pass	Pass	Pass
	HSRM-4	Pass	Pass	Pass	Pass	Pass	Pass
	HSRM-5	Pass	Pass	Pass	Pass	Pass	Pass
Standard	Standard-1	Pass	Pass	Pass	Pass	Pass	Pass
	Standard-2	Pass	Pass	Pass	Pass	Pass	Pass
	Standard-3	Pass	Pass	Pass	Pass	Pass	Pass
	Standard-4	Fail	Pass	Pass	Pass	Pass	Pass
	Standard-5	Pass	Pass	Pass	Pass	Pass	Pass
	Standard-6	Fail	Pass	Pass	Pass	Pass	Pass

Table 5.2 Rail Seat A Ultimate Load Test Result

Tie ID		Rail Seat A				
		$\epsilon_{prestress}$ (+/- 10%) ϵ_{crack}	P_{crack}	1.5 P	Pu	Strand Slippage
Prototype	HSRM-1	~ 800με ~ 320με	56	Pass	104	No
	HSRM-2		58	Pass	103	No
	HSRM-3		57	Pass	100	No
	HSRM-4		52	Pass	96	No
	HSRM-5		54	Pass	98	No
Standard	Standard-1	~ 500με ~ 220με	52	Pass	97	No
	Standard-2		54	Pass	105	No
	Standard-3		51.2	Pass	98	No
	Standard-4		49	Pass	97	No
	Standard-5		52	Pass	95	No
	Standard-6		48	Pass	88.9	No

5.2 The Sequence of Design Tests (Tie 2).

The tests were executed by the Rail Transportation and Engineering Center (RailTEC) at the University of Illinois at Urbana-Champaign (UIUC) in accordance with the AREMA Manual for Railway Engineering, chapter 30 Ties, section 4.9.1.9 and section 4.9.1.10 by using a customized tie testing frame that was specifically designed for evaluating the fastening insert capacity. Figure 5.24 shows (a) The fastening insert test setup and (b) The Uplift Test setup. The experimentation plan and method are:

- The Standard tie, identified as (T1)
- The HSRM tie, identified as (T2)
- Each tie was marked with an (A) on one rail seat and a (B) on the other.
- The inserts in the ties were marked with an (F) and a (G) to indicate the field and gauge sides, as shown respectively in figure 5.25.
- Example: the insert on the field side of rail seat A for the prototype tie was labeled (T2A-F).

5.2.1 Fastening Insert Test performed on all inserts.

A 12 kips (53.4 KN) axial load was independently applied to each insert and held for 3 minutes. An inspection was made during loading to determine if there was any insert slippage or concrete cracking. A potentiometer was used to quantify any permanent deformation that may occur during loading.

(a) Fastening insert test setup

(b) Uplift test setup

Figure 5.24 (a) The fastening insert test setup and (b) The Uplift Test setup

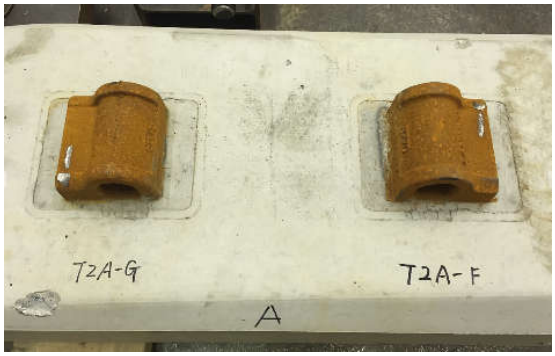

Figure 5.25 Example of the Prototype tie with marked rail seats and inserts on one rail seat

If no failure occurs, then the tie met the requirements and passed the test. The inability of the insert itself to resist the 12 kip (53.4 KN) load with no permanent deformation also signifies a failure of the test, while a mortar cracking in the proximity of the insert area is not a cause for failure.

Following the successful completion of the insert pull-out test, a torque of 250 ft-lb (339 N•m) was applied to the vertical axis of the insert using a calibrated torque wrench. The torque was held for 3 minutes by a ratchet strap and a steel bar fixed to the ground. During loading, an inspection was made to determine if the insert rotated, concrete cracked, or any permanent deformation occurred. Table 5.2 shows the results of the fastening insert test.

Table 5.3 Results from Fastening Insert Test Performed

Crosstie	Rail Seat	Insert	Pull-out (12kips)	Torque (250lb-ft)
Standard	Rail Seat A	Field	PASS	PASS
		Gauge	PASS	PASS
	Rail Seat B	Field	PASS	PASS
		Gauge	PASS	PASS
HSRM	Rail Seat A	Field	PASS	PASS
		Gauge	PASS	PASS
	Rail Seat B	Field	PASS	PASS
		Gauge	PASS	PASS

Table 1 indicates both the Standard tie and HSRM tie passed the Fastening Insert Test. The tie passed the test, because there was no permanent deformation observed when a vertical load of 12 kips (53.4 KN) was applied and held for 3 minutes, and there was no rotation, concrete cracking, or permanent deformation observed when a torque of 250 ft-lb (339 N•m) was applied and held for 3 minutes.

After the ties passed the Fastening Insert Test, an axial load was applied to the insert with the same test setup and conditions; the load was increased until failure occurred. During loading, an inspection was made to determine if the insert slipped or the concrete cracked. A potentiometer was used to determine if there was any permanent deformation during loading.

Table 5.4 Results from Fastening Insert Failure Test

Crosstie	Level of Distress	Load (kips)
Standard	Crack Initiation at	31.6
	Insert Pulled out	34.6
HSRM	Crack Initiation	33.2
	Insert Pulled out	35.1

According to the results of the additional Fastening Insert Test in table 5.3, the Standard tie exhibited cracking and insert pull out at a lower uplift force when compared to the HSRM tie.

5.2.2 Fastening Uplift Test performed on one rail seat.

An 18-inch section of rail was secured to one rail seat using a complete e-clip fastening assembly with four, 6-inch long, 1-inch wide, copper shims installed between the rail seat and abrasion frame. A vertical axial load at a rate of 1 kip/min was applied to lift the rail. During loading, the shims were pulled out to determine the load P at which separation of the pad from the rail seat occurred.

After releasing the load P, a load of 1.5P (not to exceed 10 kips) was applied, and the separation gap was measured. After releasing the load of 1.5P, the load was reapplied to create the same separation gap and the corresponding load, P2, was recorded. During the test, an inspection was made to determine if there were any failures, such as: pull out or loosening of the inserts in the concrete, fracturing of any component of the fastening system, or a complete release of the rail section.

For all ties using elastic fasteners, the inserts shall not pull out or loosen in the concrete, and no component of the fastening system shall fracture nor shall the rail be released. The results in table 5.4 indicate that both the Standard tie and the HRSM tie

passed the Uplift Test. The ties passed because the inserts were not pulled out or loosened and no component of the fastening system fractured [32].

Table 5.5 Results from Fastener Uplift Test Performed

Crosstie	Rail Seat	Result
Standard	Rail Seat A	PASS
	Rail Seat B	PASS
HSRM	Rail Seat A	PASS
	Rail Seat B	PASS

CHAPTER 6

ASSESSMENT STUDIES UNDER ULTIMATE LOAD

The advantages of the prototype tie as compared to the Standard are investigated through a series of tests that were conducted in the structures laboratory at USC. In particular, the performance of the ties under center binding conditions is considered for cyclic loading and monotonic loading until failure.

One prototype and one Standard tie have been tested under cyclic loading and two prototypes, and two Standard ties have been tested under monotonic loading until failure. These tests are not part of the AREMA qualification tests, and the following sections provide the testing protocol and results.

6.1 Center Positive Ultimate Moment test.

The prestressed concrete ties were supported and loaded as shown in figure 6.1 with the distance between the bottom supports of 60 in. and the top supports of 6 in. The load is applied continuously at a rate of 5 kips per minute without any shock until failure. The StereoDIC measurement was evaluated for identifying potential initiation of cracking. The load vs. deflection curve, as shown in figure 6.2, indicates that the HSRM is more flexible than the Standard.

The first crack in the HSRM appeared at 16 kips and for the Standard at 14 kips as shown in figures 6.3 and 6.4. An illuminated 5-power magnifying lens was used to detect the when the crack reaches the first layer of the bottom strands. The findings of the visual inspection were verified by DIC analysis. To this end, the longitudinal strain is

plotted along the length of the tie at the level of the first layer of strands and is shown in figures 6.7 and 6.8, for the HSRM and the Standard ties, respectively. The crack reached the first layer of the strand at 21 kips for the HSRM and at 19 kips for the Standard as shown in figures 6.5 and 6.6. The ultimate load was 34 kips for the HSRM and 30 kips for the Standard. So the HSRM shows higher resiliency compare to the Standard tie under the loading conditions considered in this test.

6.2 Rail Seat Ultimate Negative Moment test.

The prestressed concrete ties were supported and loaded as shown in figure 6.11 with the distance between the bottom supports of 28 in. and the top supports of 5 in. The load is applied continuously at a rate of 5 kips per minute without any shock until failure. The StereoDIC measurement was evaluated for identifying potential initiation of cracking. The load vs. deflection curve as shown in figure 6.12 shows that the HSRM has more flexibility than the Standard. The first crack in the HSRM appeared at 37 kips and for the Standard at 35 kips as shown in figure 6.13 and 6.14. A DIC and an illuminated 5-power magnifying lens were used to detect when the crack reaches the first layer of the bottom strands by drawing a line at the same position of the strand and plotting the longitudinal strain data vs. the width as shown in figures 6.17 and 6.18. The crack reached the first layer of the strand at 52 kips for the HSRM and at 50 kips for the Standard as shown in figures 6.13 and 6.14. The Ultimate load was 80 kips for the HSRM and 77 kips for the Standard tie; figures 6.19 and 6.20 show the ties close to failure. So the HSRM shows very good behavior on distributing the load, flexibility, and the compressive strength.

6.3 Center Negative repeated load test

The load carrying capacity and fatigue behavior of prestressed concrete ties under cyclic loads have been experimentally investigated by means of a four-point mid-span negative bending test. The fatigue behavior of the prestressed concrete ties has become a continual subject of interest. However, only limited research has been conducted on the fatigue behavior of ties. The railroad ties were subjected to the center negative repeated load test to investigate the flexural behavior under repeated or cycling load. The ties were also provided with lateral and longitudinal supports that prevented lateral and longitudinal sleeper movement during the cycles. Figure 6.21 shows the setup of the center negative fatigue test.

The AREMA manual does not provide any guidelines for such a test. The following testing protocol is developed and followed in this work. Testing is performed in three stages. In the first stage, 3,000,000 cycles of the load are applied at the center in the range 2 kips to 13.5 kips that correspond to 90% of the load that will develop the design moment at the mid-span. The load is applied at a frequency two cycles per second. The loading cycling is paused every 48 hours (approximately 350,000 cycles), and a monotonic static test is performed from 2 kips to 13.5 kips. During the static test, the side surface of the ties was imaged at loads 2, 6, 8, 10, 12, and 13.3 kips for full-field deformation measurements through DIC. After the image acquisition, the cyclic testing resumed. Once the 3 million load cycles were reached, the tie was loaded until a crack formed that reached the first level of strands and the load was recorded. Figures 6.24 and 6.25 show the longitudinal strain field acquired by DIC when the crack reached the first level of the strand. The load was 19 kips for the HSRM and 18 kips for the Standard. The

HSRM tie's first crack appeared at 19 kips and the Standard at 18 kips as shown in figures 6.22 and 6.23. Cyclic loading was then restarted as in stage 1 but in the range of 2 kips to 16.5 kips that correspond to 110% of the load associated to the design moment. As in stage 1, the cyclic loading was paused every 48 hours, the tie was loaded monotonically to 16.5 kips, and images were acquired at load levels 2, 4, 6, 8, 10, 12, 13.5, 15, and 16.5 kips for DIC full field deformation measurements. The cyclic loading continued until an additional 3 million cycles to stage 1 were applied, for a total of 6 million cycles. In stage 3, the tie was loaded monotonically until failure, and the full field deformation measurements were captured at loads levels 0, 2, 6, 8, 10, 12, 13.5, 15, 16.5, 18, 20, 22.5, 27, 29, 31, and 33. If the tie did not fail, the steps would continue manually until the failure occurred; however, in this case, the HSRM tie failed at 34 kips, and the Standard failed at 33 kips as shown in figures 6.26 and 6.27.

Figure 6.28 shows the load-deflection of the two ties for ultimate load after they were subjected to 6 million cycles. The HSRM tie is also more flexible than the Standard as indicated in figure 6.28.

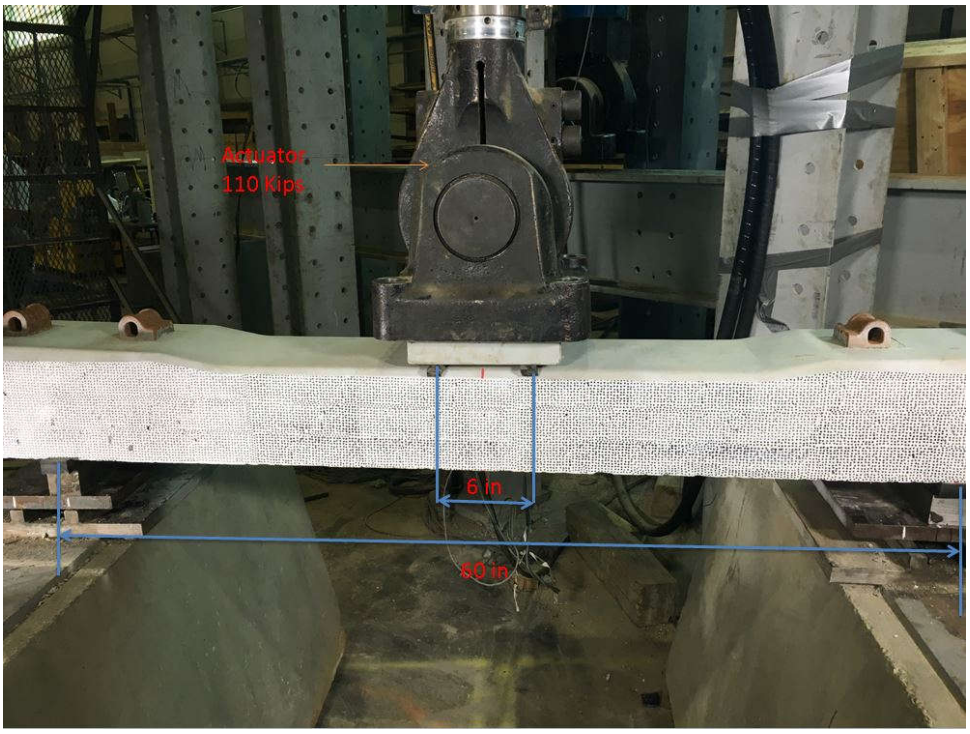

Figure 6.1 Center Positive Ultimate Moment Test

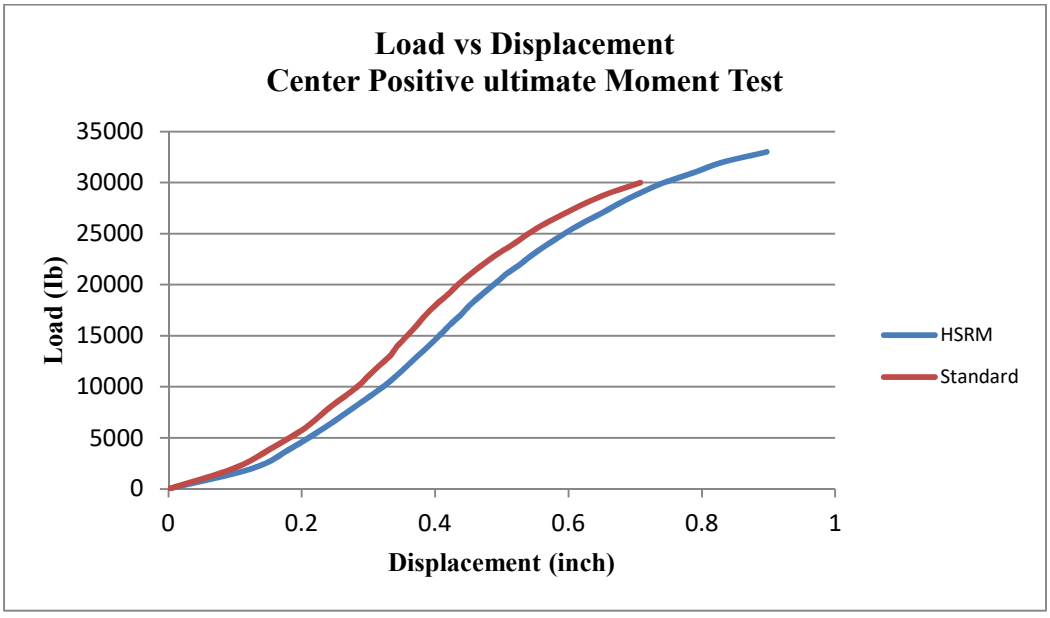

Figure 6.2 Center Positive Ultimate Moment Test Load vs. Deflection Curve

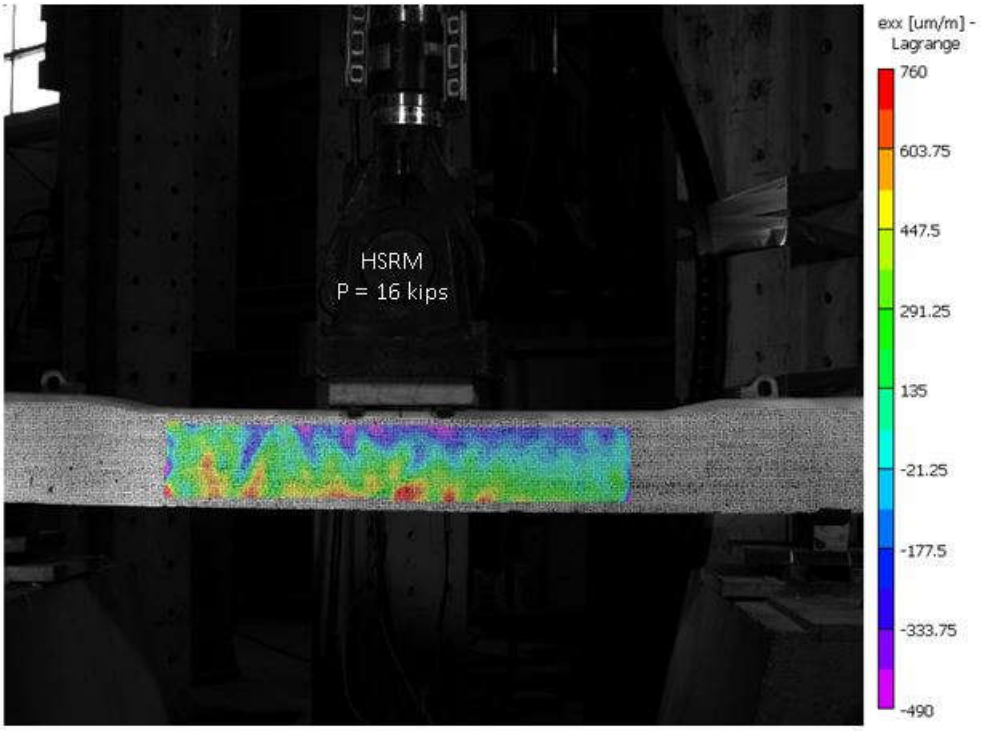

Figure 6.3 HSRM First Cracking

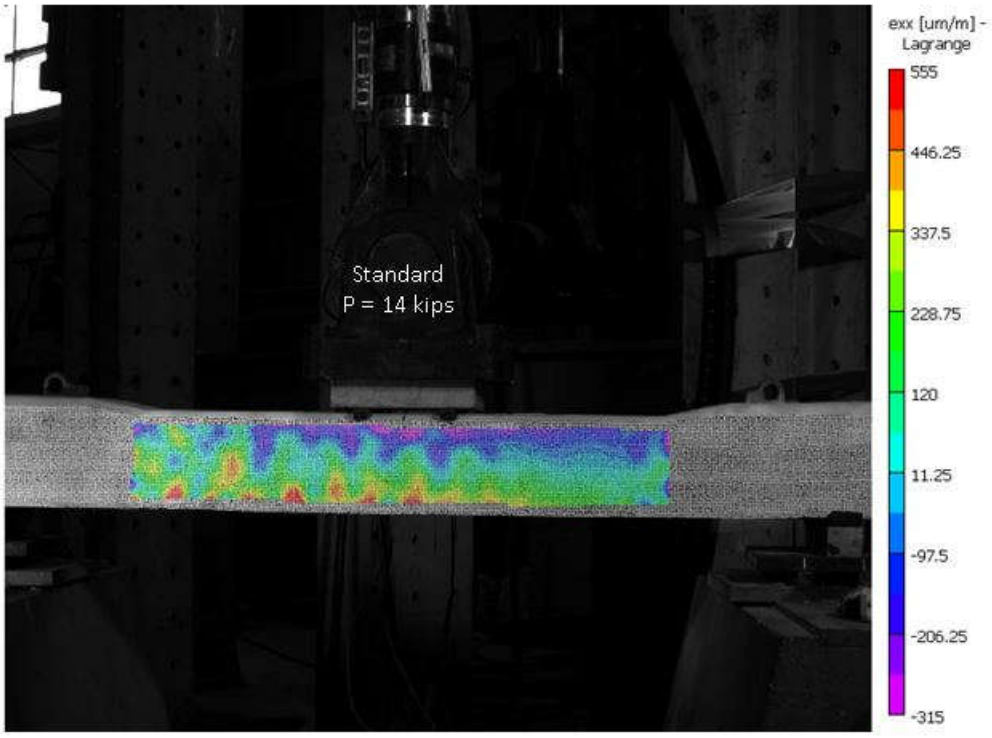

Figure 6.4 Standard First Cracking

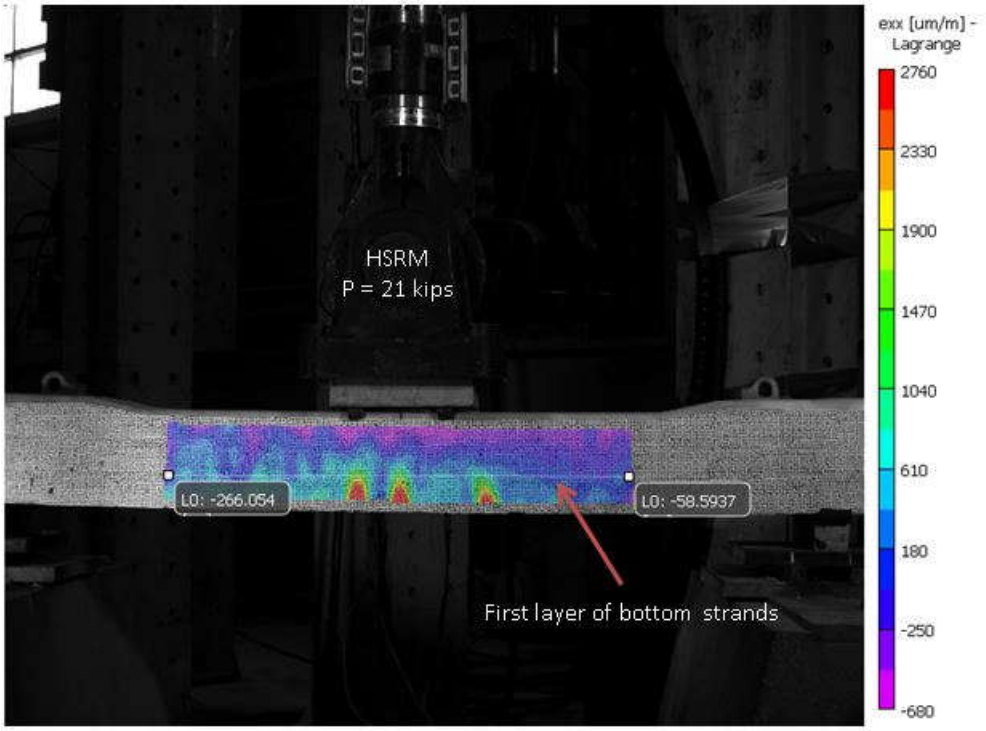

Figure 6.5 HSRM the Crack Reached the First Layer of Bottom Strands

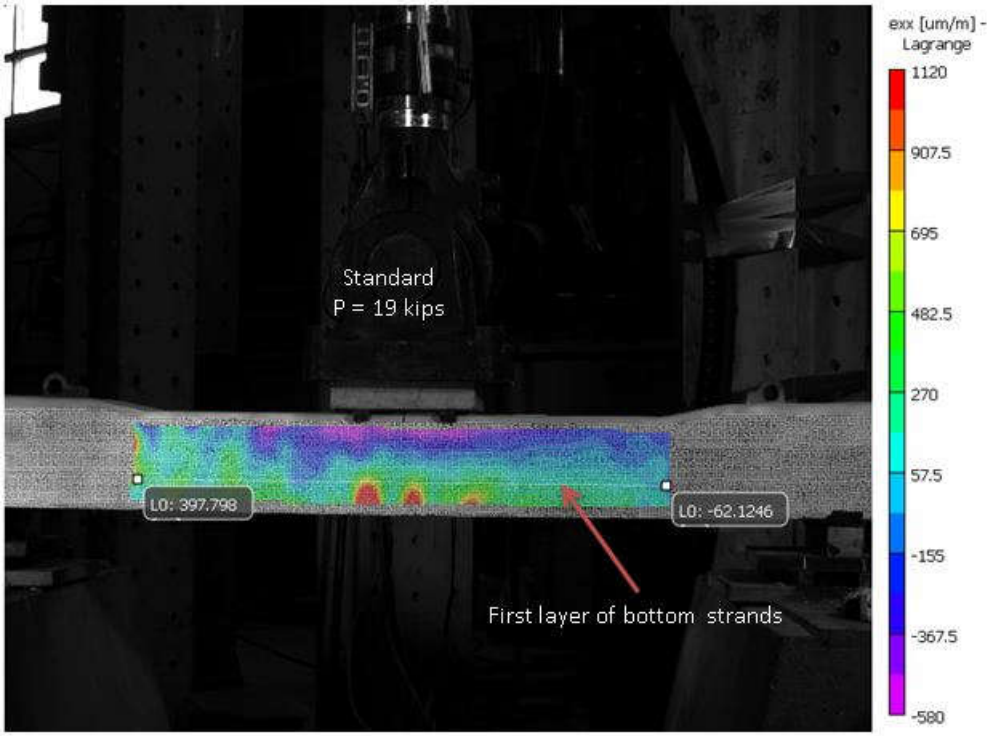

Figure 6.6 Standard the Crack Reached the First Layer of Bottom Strands

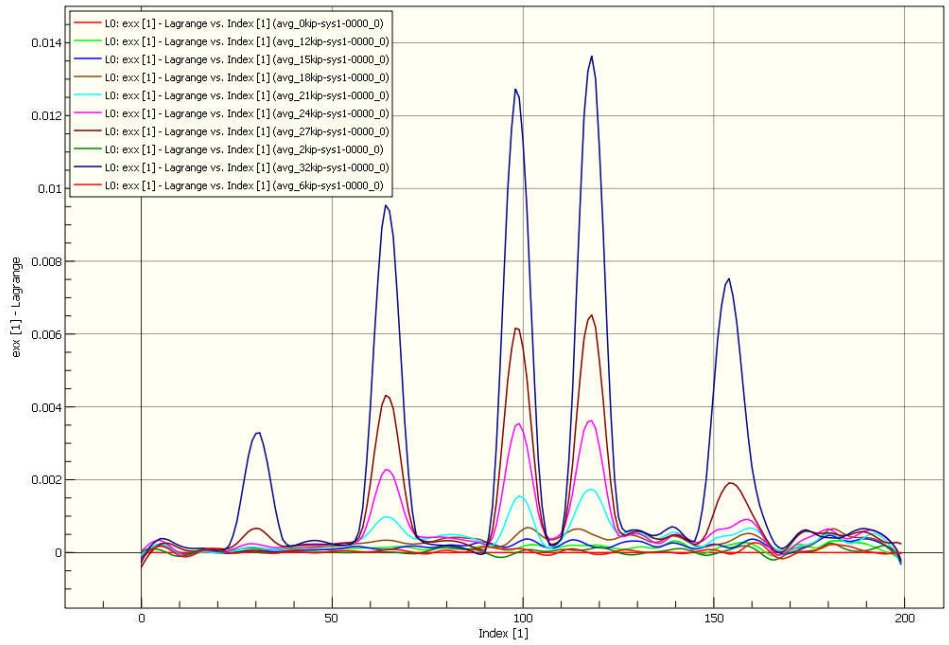

Figure 6.7 Longitudinal strain occurring at the HSRM tie's first bottom layer of the strand in Center Positive Moment Test

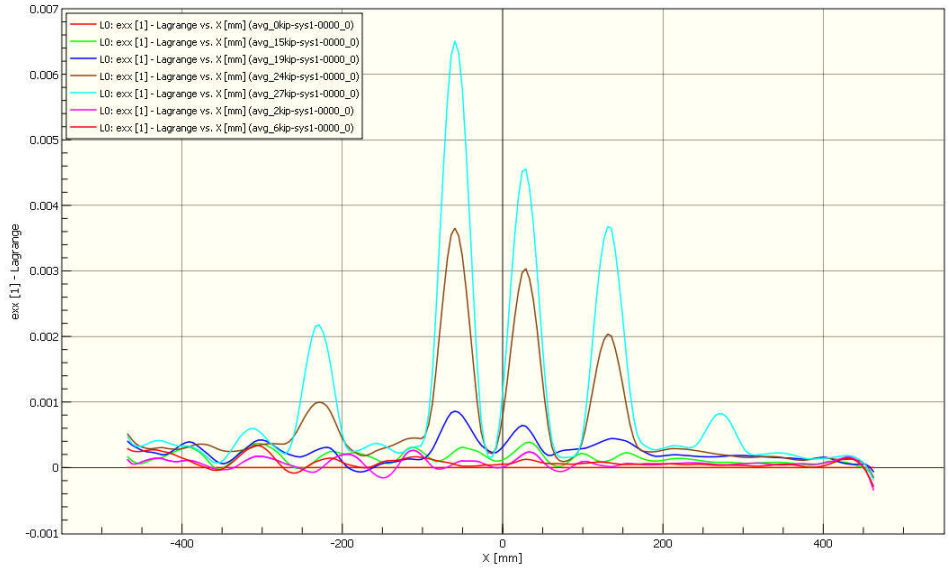

Figure 6.8 Longitudinal strain occurring at the Standard tie's first bottom layer of the strand in Center Positive Moment Test

Figure 6.9 HSRM close to failure

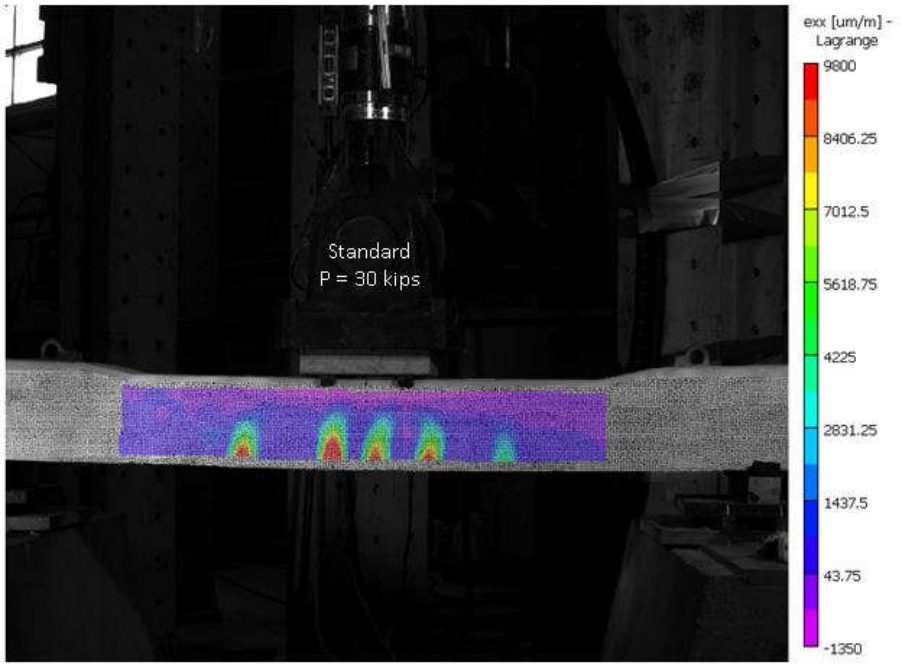

Figure 6.10 Standard close to failure

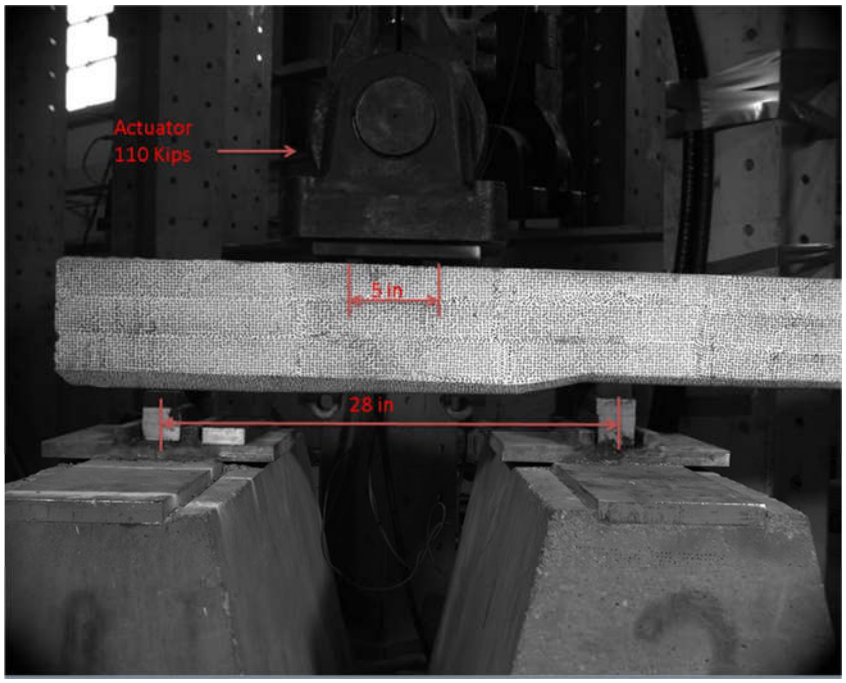

Figure 6.11 Rail Seat Ultimate Moment Test

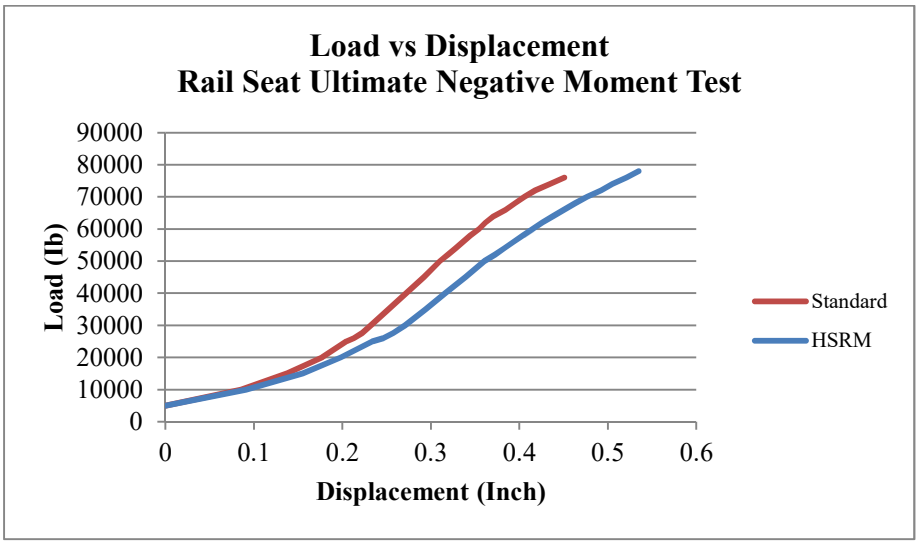

Figure 6.12 Rail Seat Ultimate Negative Moment Test Load vs. Deflection Curve

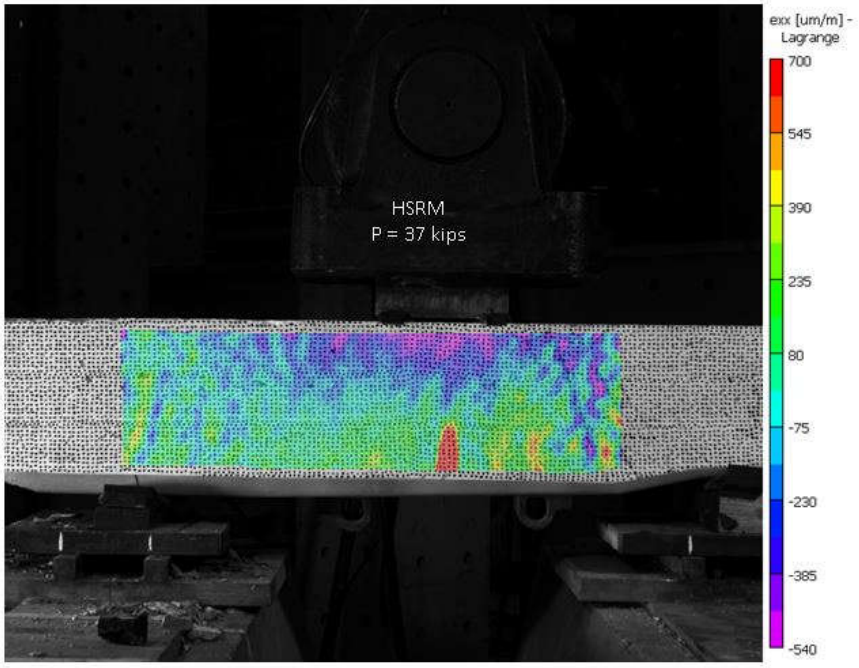

Figure 6.13 HSRM First Cracking

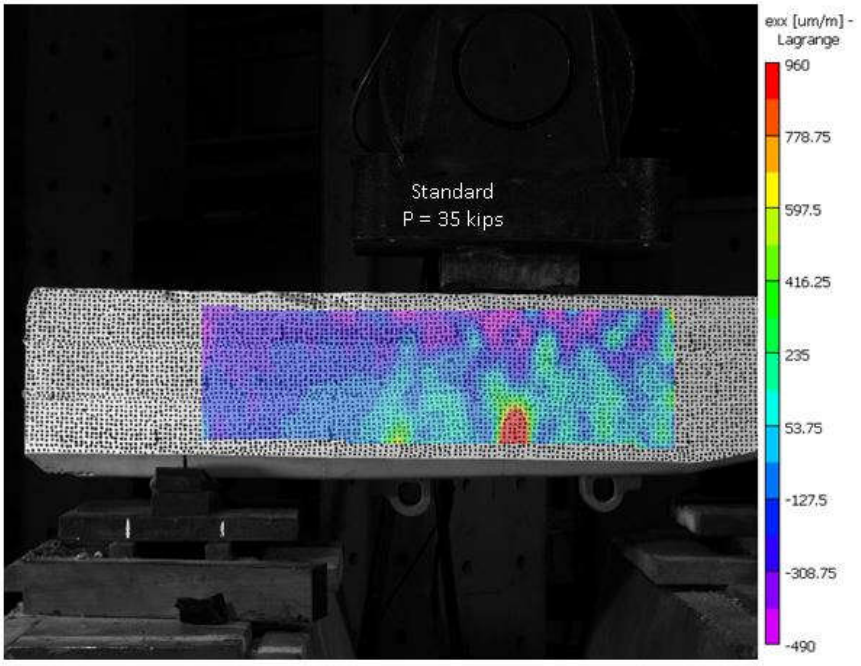

Figure 6.14 Standard First Cracking

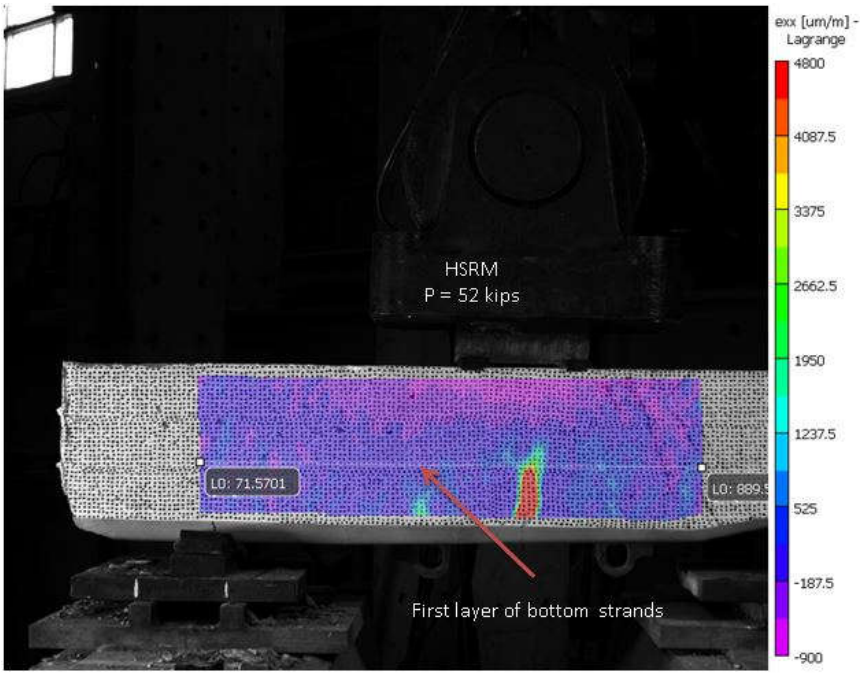

Figure 6.15 HSRM the Crack Reached the First Layer of Bottom Strands

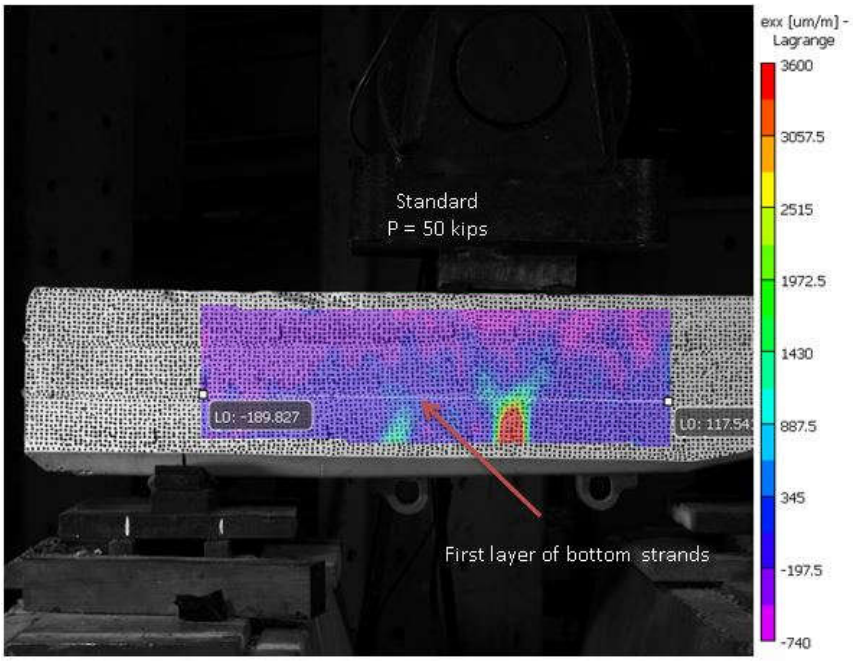

Figure 6.16 Standard the Crack Reached the First Layer of Bottom Strands

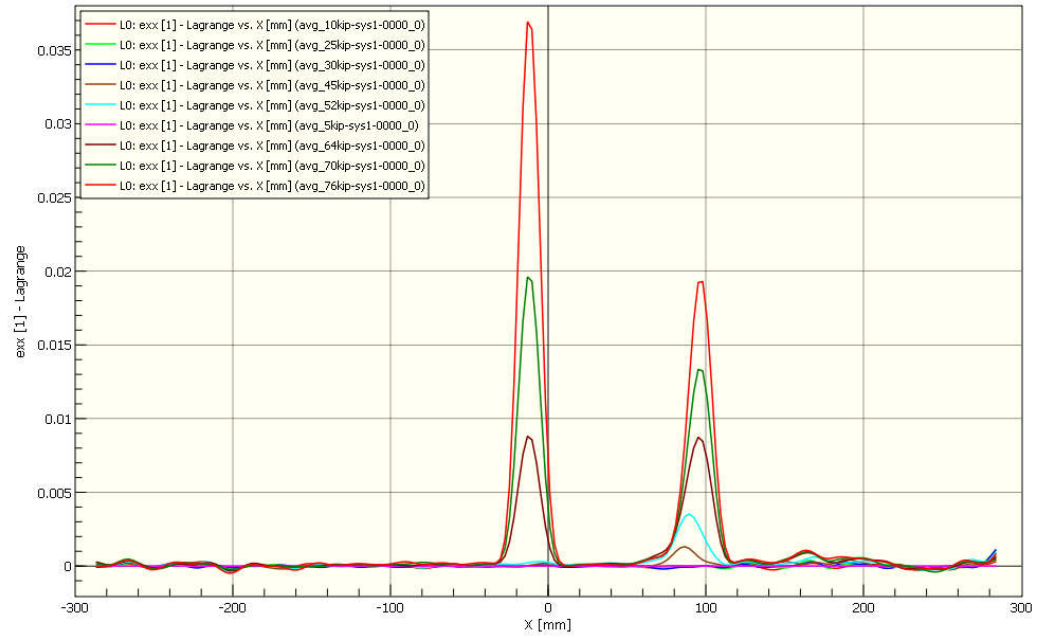

Figure 6.17 Longitudinal strain occurring at the HSRM tie's first bottom layer of the strand in Rail Seat Negative Moment Test

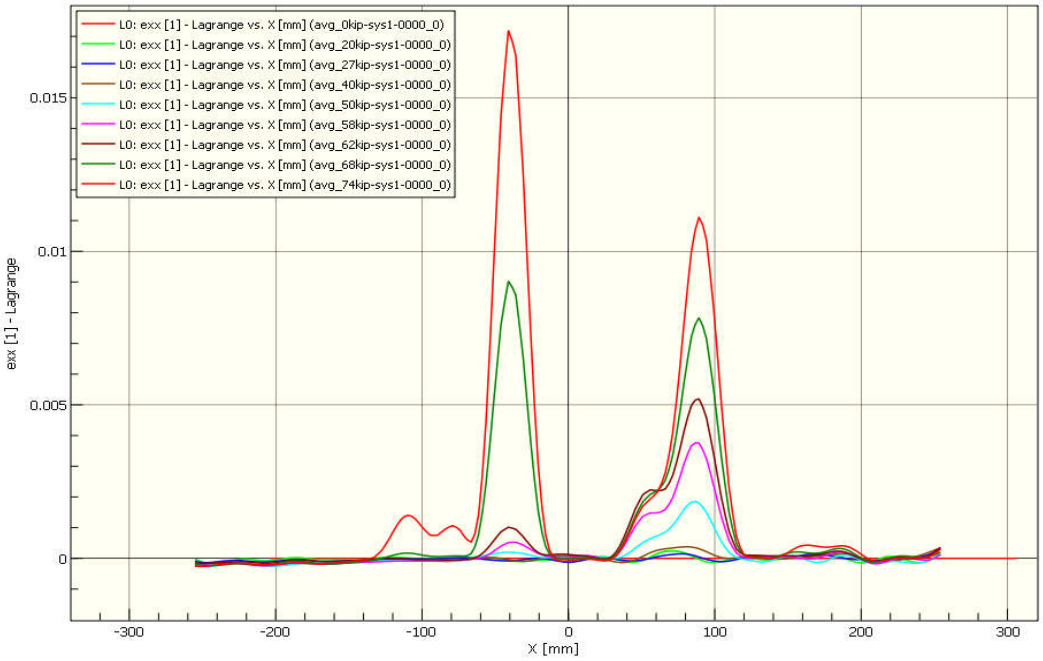

Figure 6.18 Longitudinal strain occurring at the Standard tie's first bottom layer of the strand in Rail Seat Negative Moment Test

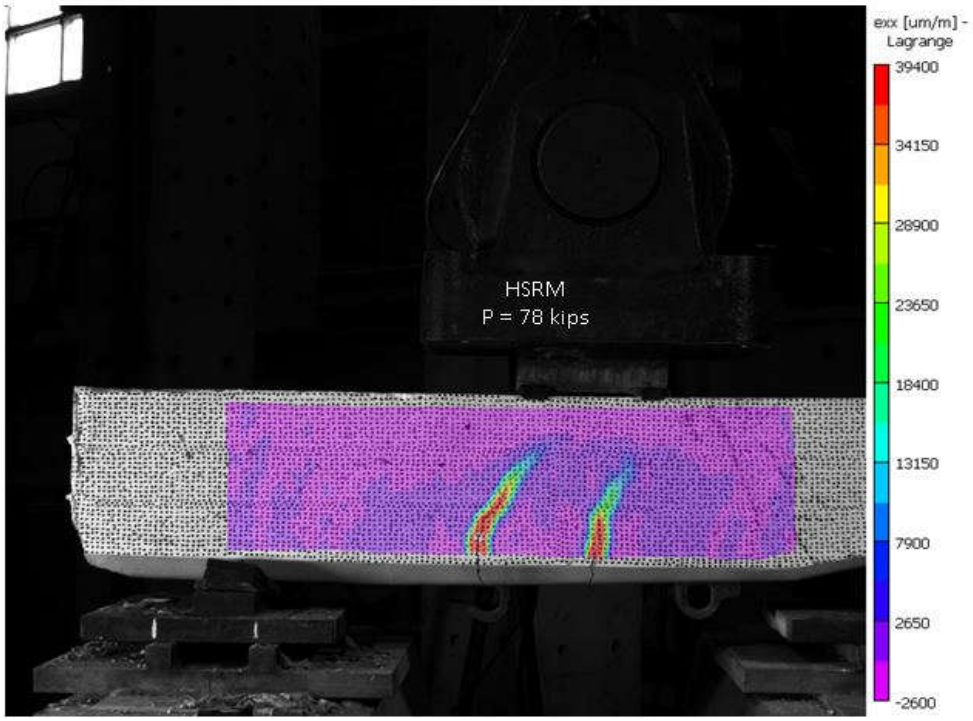

Figure 6.19 HSRM close to failure

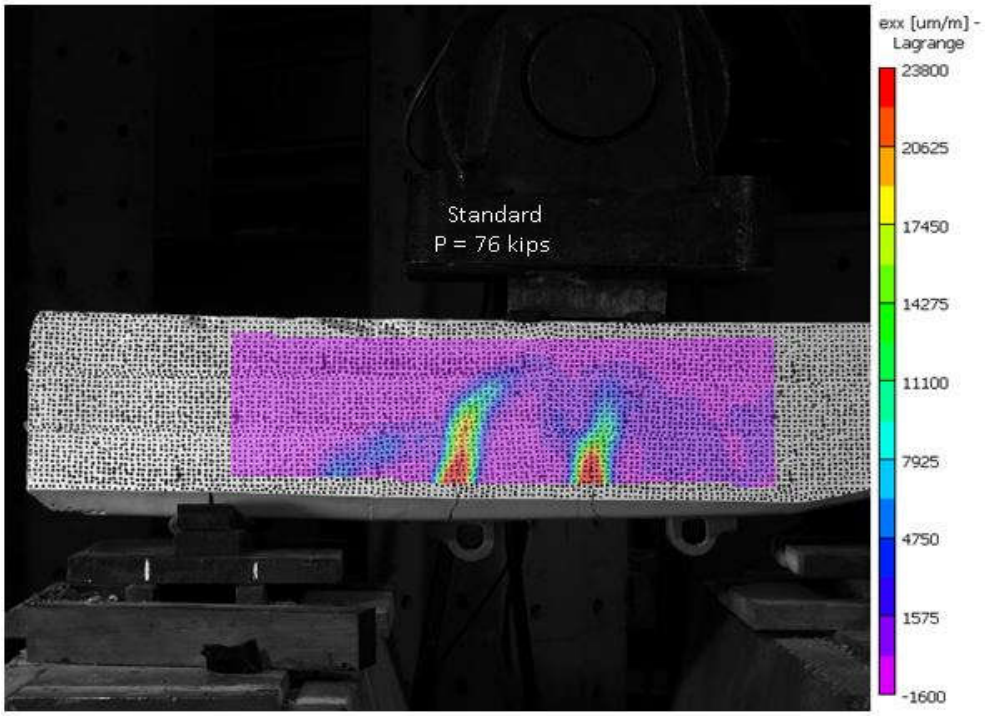

Figure 6.20 Standard close to failure

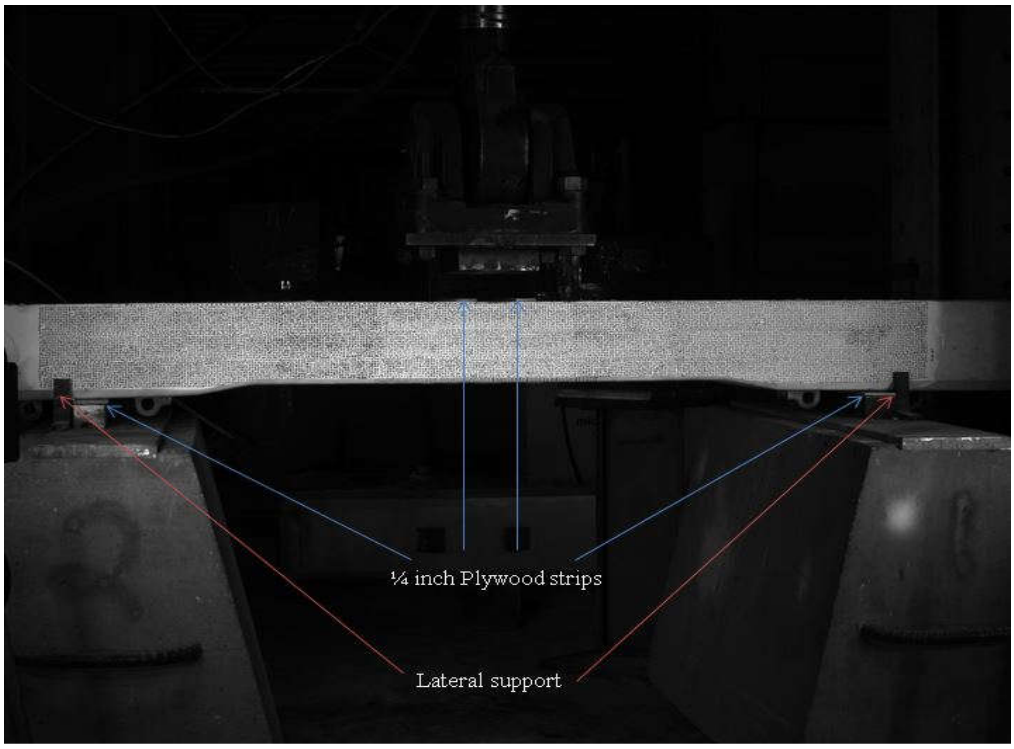

Figure 6.21 Center negative fatigue test

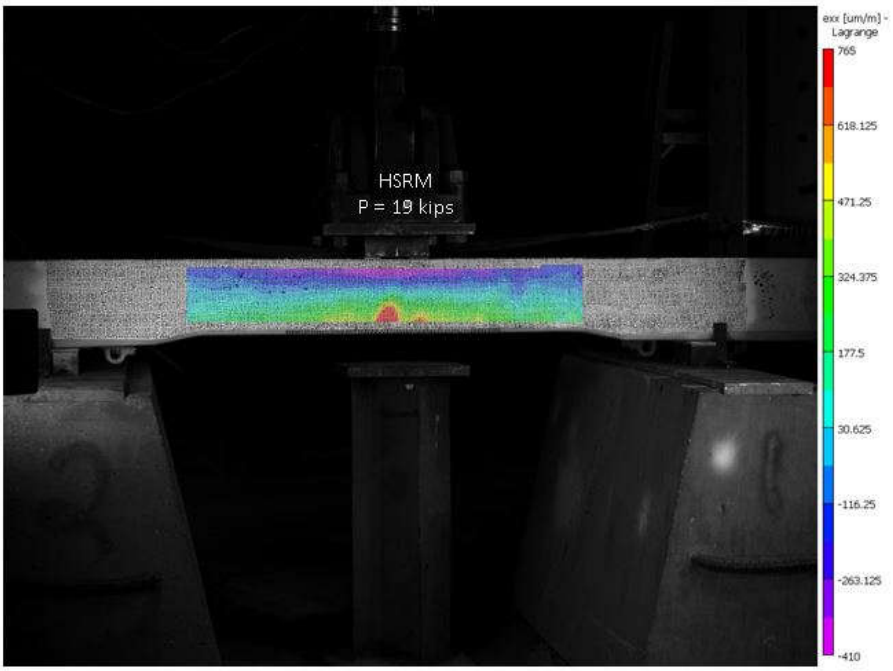

Figure 6.22 HSRM cracking load

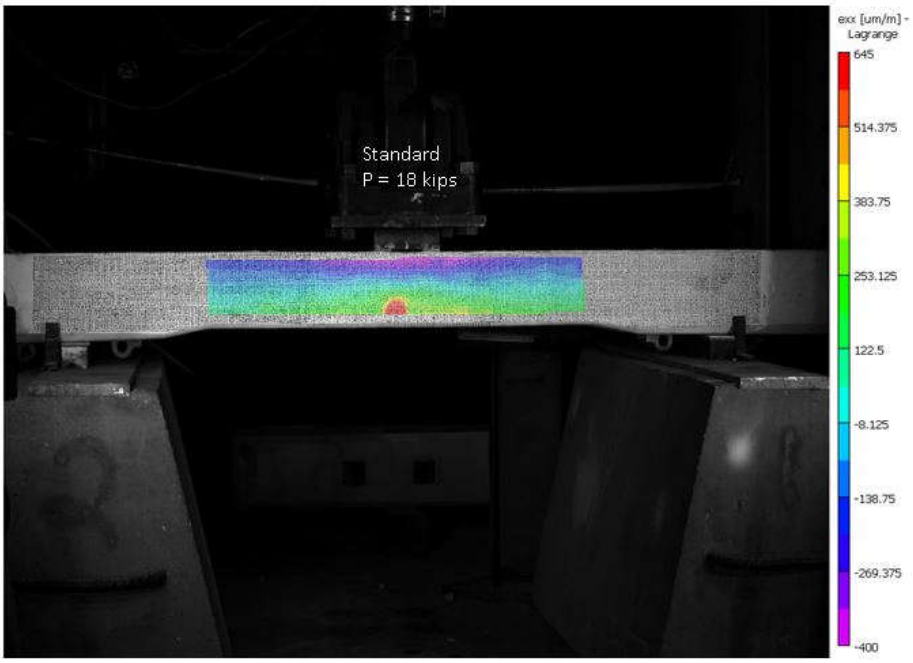

Figure 6.23 Standard Cracking Load

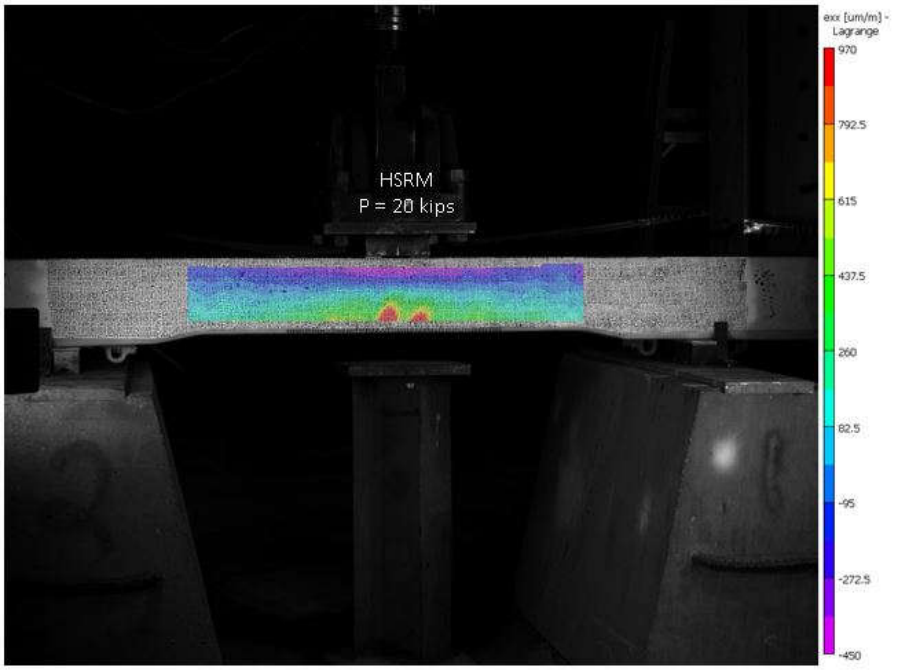

Figure 6.24 HSRM the crack reached the first layer of the bottom Strands

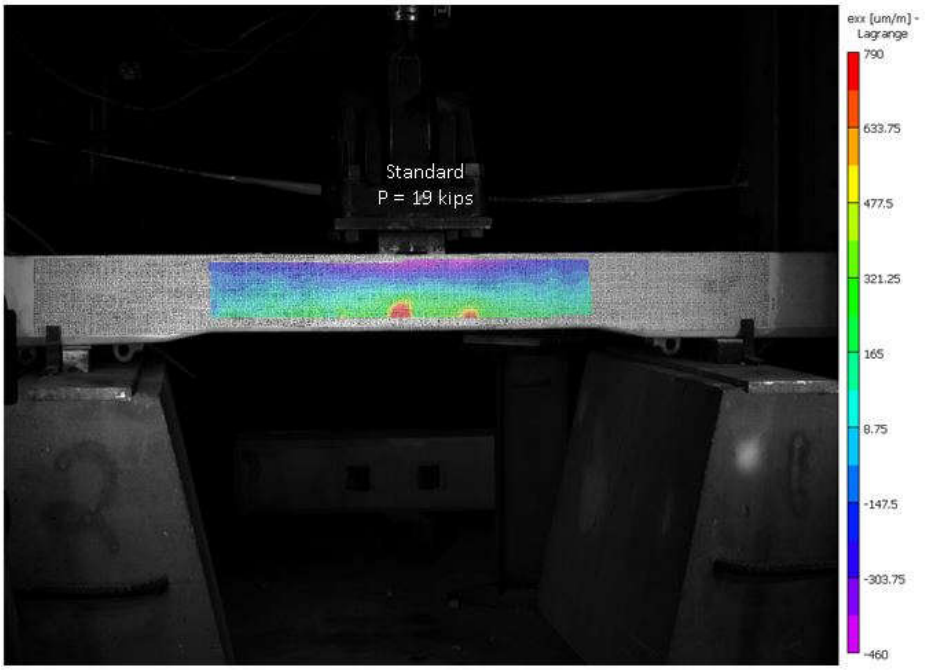

Figure 6.25 Standard the Crack Reached the First Layer of the Bottom Strands

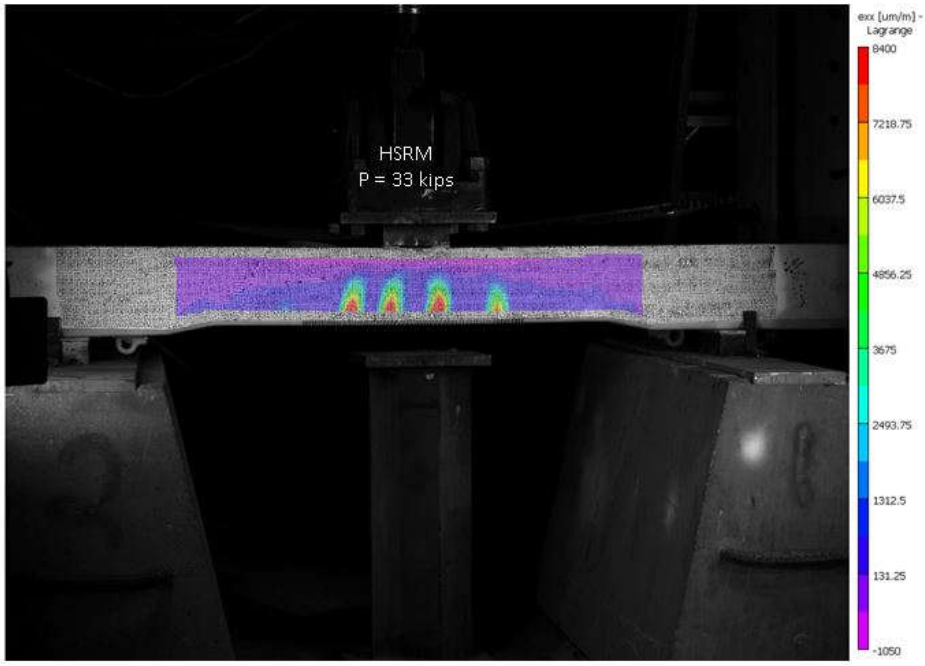

Figure 6.26 HSRM close to failure

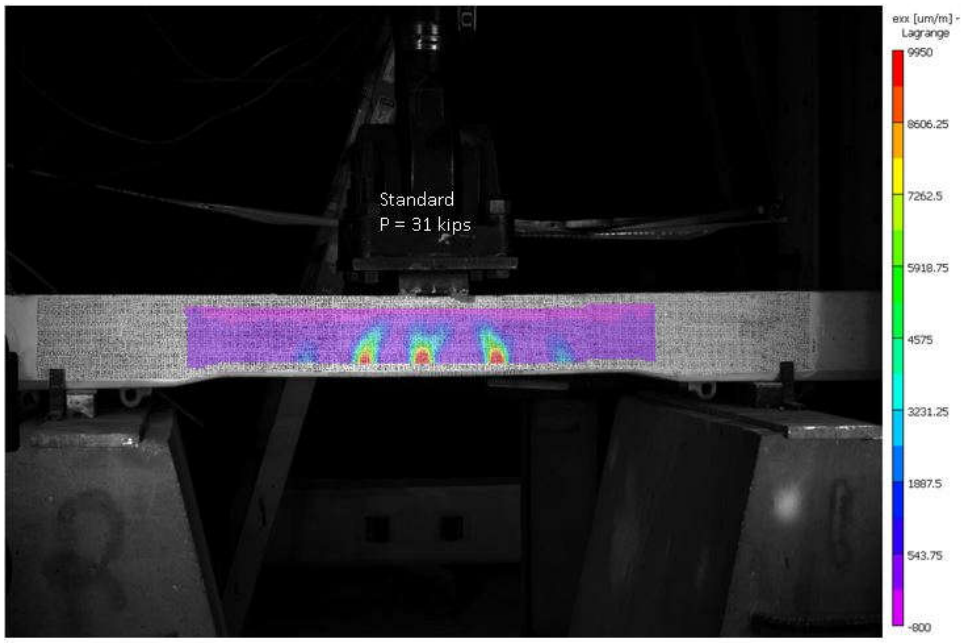

Figure 6.27 Standard close to failure

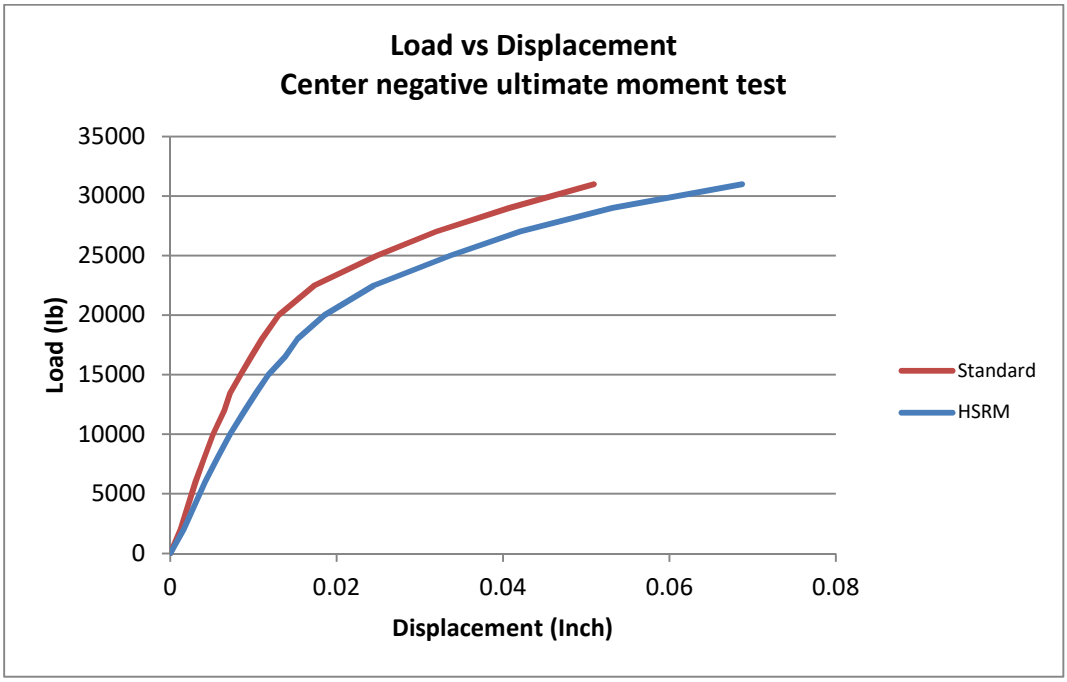

Figure 6.28 Center Negative Ultimate Moment Test after 6 million cycles

CHAPTER 7

ASSESSMENT STUDIES UNDER CENTER BINDING CONDITIONS

While unsuitable tie flexural capacity is a concern, problems of ties cracking at the top center location due to a negative moment have also been detected on mainline tracks [33]. The extent of ballast deterioration is unique to concrete ties when compared to that observed with wood ties resulting from the difference in the tie material strength and hardness. Surveys have shown that this failure type results from ballast conditions that are beyond the range of tie design [22][34].

The present AREMA method for concrete tie flexural analysis is a factored approach that is dependent on tie length, tie spacing, annual tonnage, and train speed [19]. The 4-point bending test for negative moment at the center of the tie listed in the AREMA recommendations is not representative of the center binding support condition because: (1) the failure mode of the AREMA test is normal at the center and a coupled normal-shear in the vicinity of the center, as observed in section 6.1. This mode is different than the one observed in the field. (2) The load required in the test to cause cracking is much lower than the axle load and, therefore, although the AREMA test shows an acceptable performance, the ties suffer cracking from center binding in the field.

We propose a modified 4-point bending test where the loading points are spaced at 34 inches symmetrically about the tie center. This allows for pure normal failure in the center section of the tie under higher applied load.

7.1 Experimental setup

Four point bending test was performed on ties (HSRM) and (Standard) as shown in figure 7.1. The tests were executed in load control using a hydraulic actuator with a maximum capacity of 110 kips. The load from the actuator was converted to two point loads using a spreader steel beam; the load was increased with no more than 5 kips per minute starting from 0 kips to the ultimate capacity of the ties. The distance between the support points was 60 inches; the shear span between the support points to the nearest point load is equal to 13 inches. The distance between the two point loads on the top of the beam is 34 inches.

Three linear variable differential transformers (LVDTs) were installed and attached to the bottom of the ties to calculate the deformation; five strain gauges with the length of 30 mm were installed in the critical areas as shown in figure 7.2. All these three LVDTs, strain gauges, and the load cell from the hydraulic actuator were connected to the data acquisition system (Vishay 7000). The hydraulic actuator was controlled by a separate computer to do a segment and apply a load control.

Apart from linear variable differential transformers (LVDT) and Strain gauges, full-field three-dimensional displacements were taken using two stereo-vision digital image correlation (DIC) systems for prestressed concrete ties.

A static load was applied on the prestressed concrete tie using a spreader beam through a hydraulic actuator to test the tie for flexural behavior under a center negative moment test. After the calibration was done, 100 images were taken as a first set without any load 0 kips loads to use those images as a baseline for the rest of images. The load rate was less than 5 kips per minute starting from 0 kips to the ultimate load that the load

can yield. The load steps were 0, 2, 5, 10, 15, 20, 25, 27, 28, 29, 30, 31, 32, 33, 34, 35, 40, 42, 44, 46, 48, 50, 52, 54, 56, 58, 60, 62, 64, 66, 68, 70, 71, 72, 73, 74, 75, 76, 77, 78, and until failure for each load step. To decrease image discrepancies caused by the environment, 100 images for DIC measurements were taken for each load step, and an average image was calculated using a Matlab code. This produced one average image for each camera.

7.2 Experimental results of four-point bending test.

Figures 7.3 and 7.4 show the load-displacement relationships for HSRM and Standard ties using DIC and LVDT measurements. The HSRM tie is more flexible than the Standard in the elastic range; however, the Standard tie shows softening compare to the HSRM tie in the inelastic region. The reason for the large deflection could be due to the desponding between the concrete and the Standard tie strand that happened at 68 kips, as shown in figure 7.3. They were subjected to the four-point bending test. The HSRM tie showed more displacement than the Standard tie, as evident in the linear part of the figure. Fine cracks appeared on the HSRM at 44 kips and on the Standard tie at 42 kips. The cracks were tracked using an illuminated 5-power magnifying glass and the DIC, as shown in figures 7.7 and 7.8. The crack reached the first layer of the bottom strands at 50 kips for the HSRM, while this occurred at 46 kips for the Standard tie as shown in figures 7.9 and 7.10. Figures 7.11 and 7.12 show the DIC image produced by VIC-3D that indicates when the crack reached the first level of the bottom strand. In the images, a line was drawn at the same position of the strand to compare against the longitudinal strain for changes. When changes occurred in the longitudinal strain, the crack had reached the

first level of the bottom strand. The maximum flexural load for the HSRM tie and Standard tie was 85 kips and 80 kips, respectively.

Figures 7.5 and 7.6 show how the HSRM tie distributed the load consistently between the compression and the tension areas. The Standard tie showed lower maximum flexural load capacity compared to the HSRM tie, which could have resulted due to the existing wide cracks on the bottom surface of the tie prior to testing.

Figure 7.1 Four-point bending test

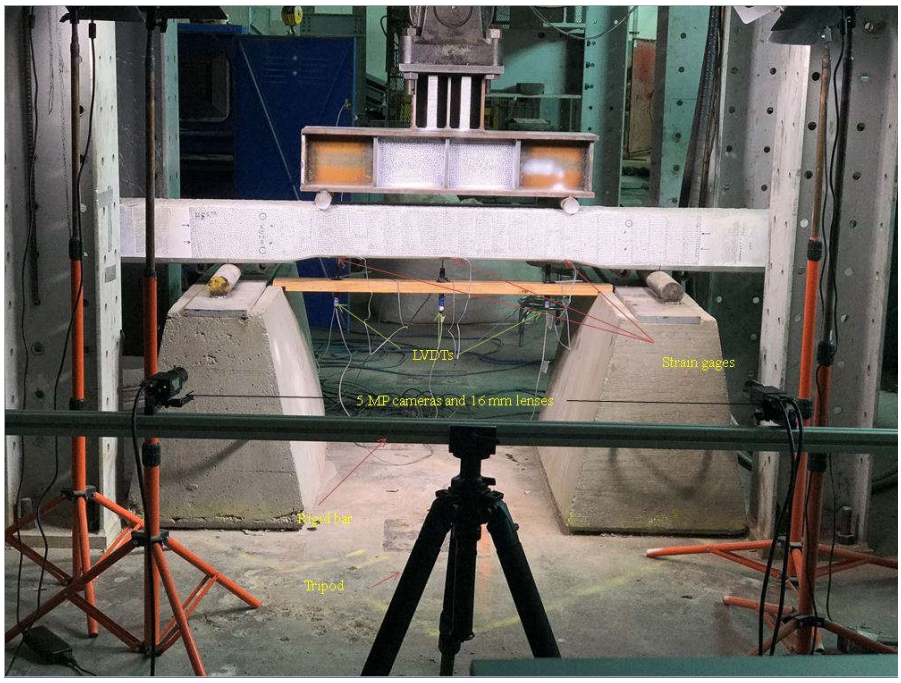

Figure 7.2 Four-point bending test instruments

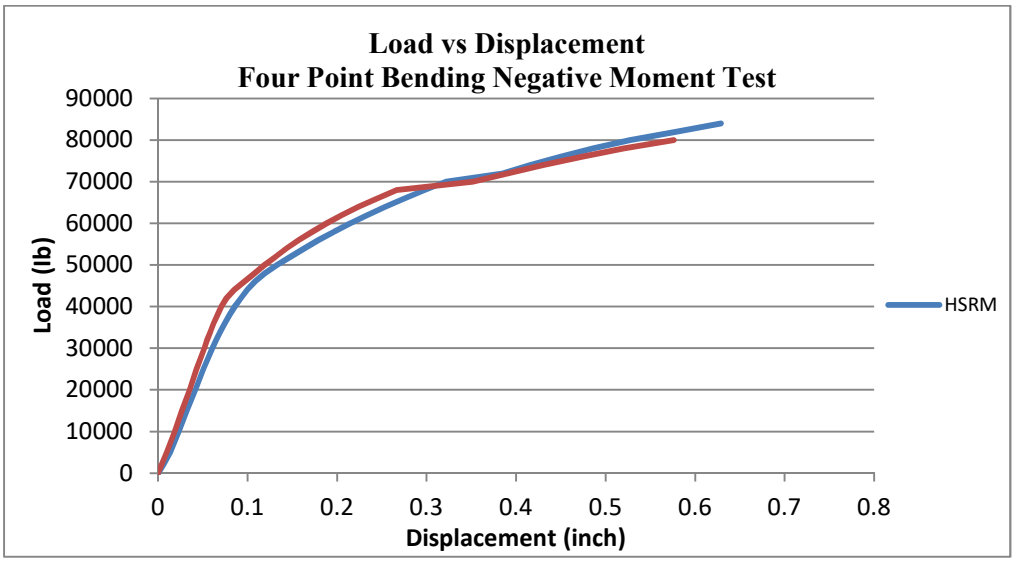

Figure 7.3 Load vs Displacement from DIC measurement

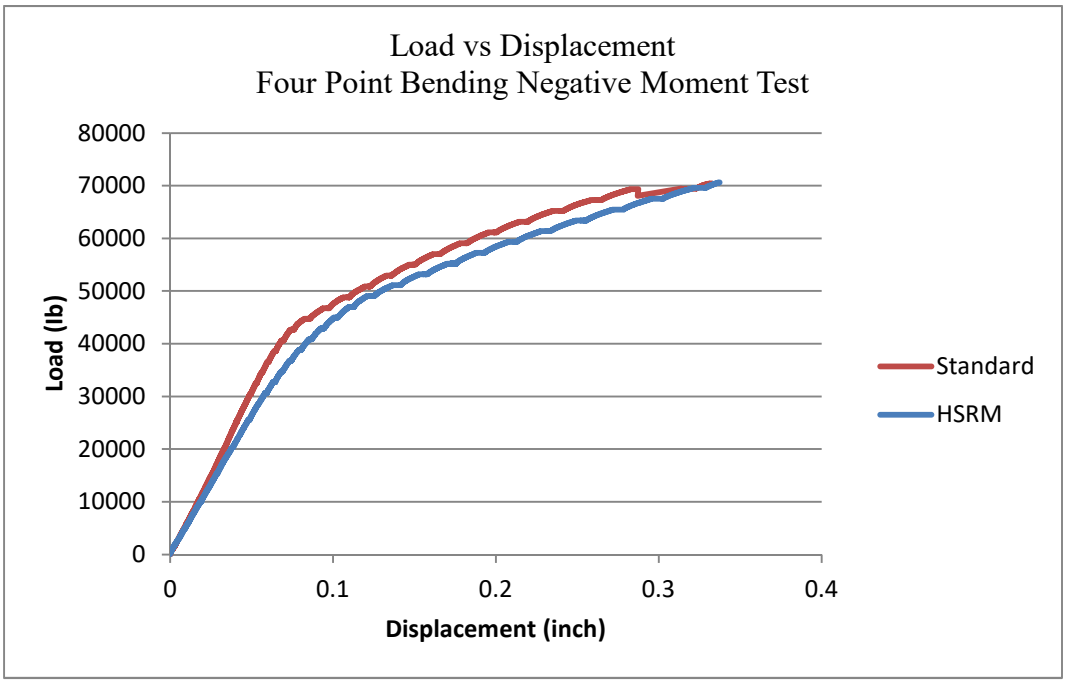

Figure 7.4 Load vs Displacement from LVDT's measurement

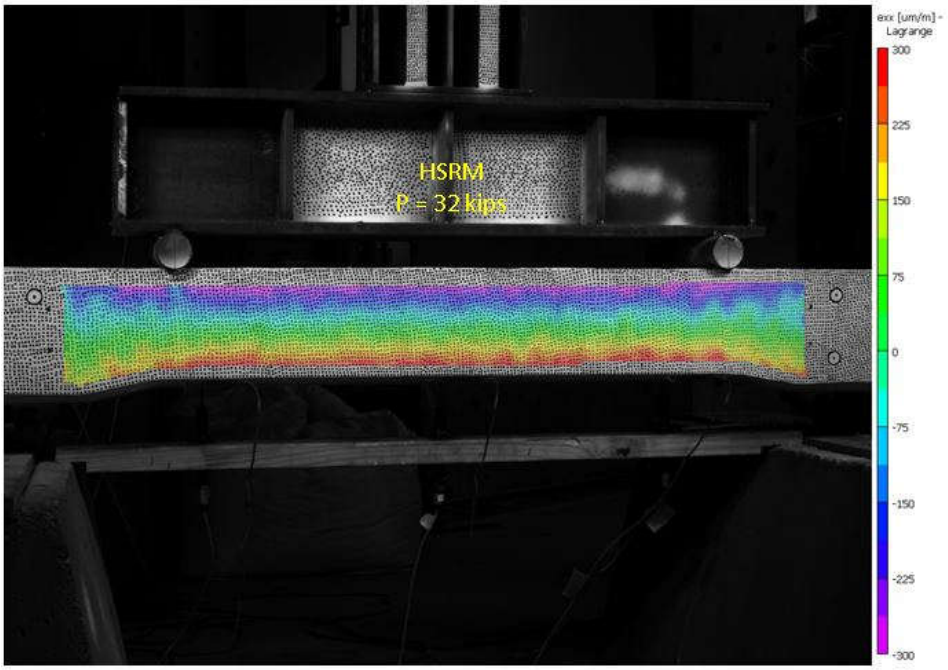

Figure 7.5 HSRM design load

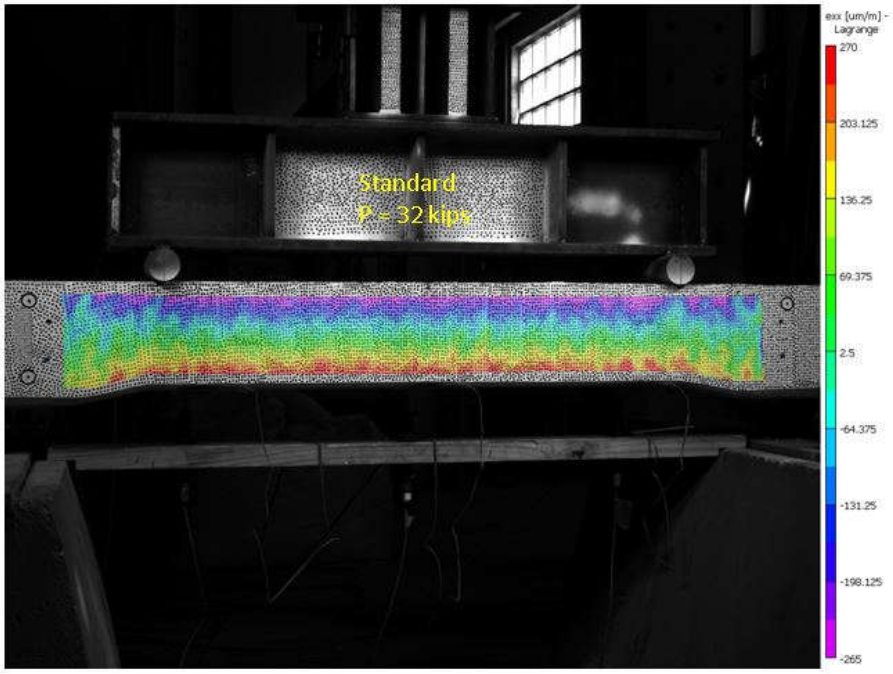

Figure 7.6 Standard design load

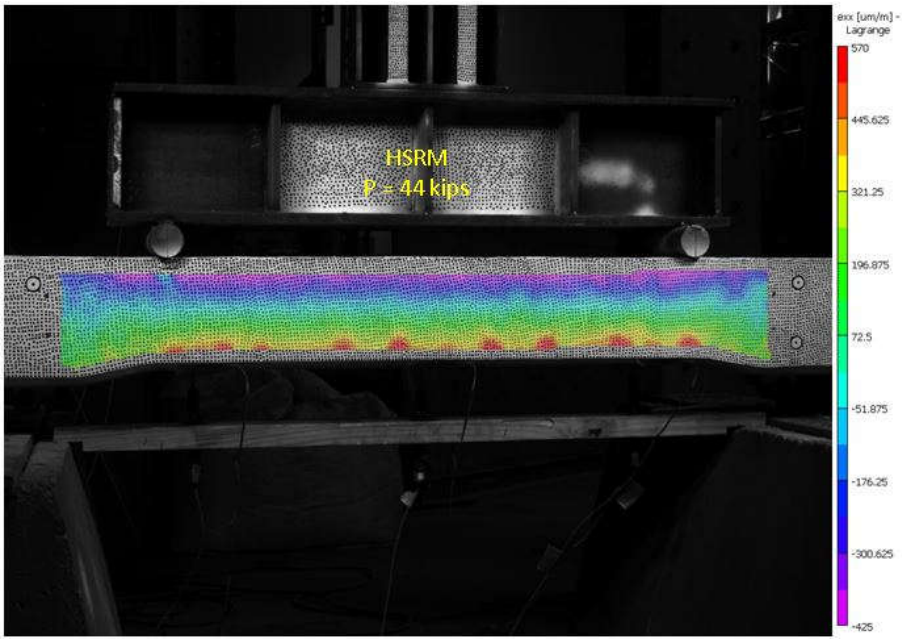

Figure 7.7 HSRM cracking load

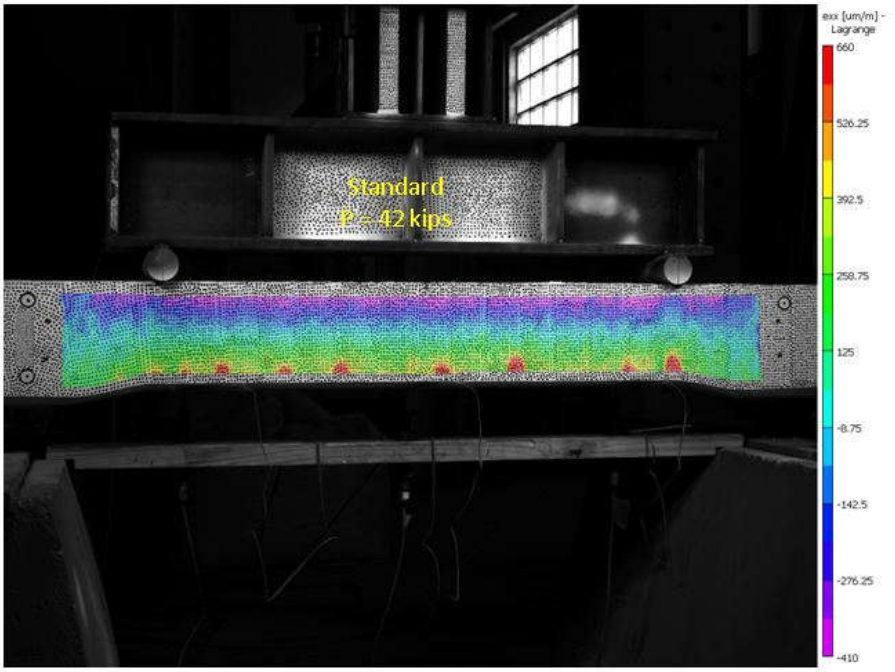

Figure 7.8 Standard cracking load

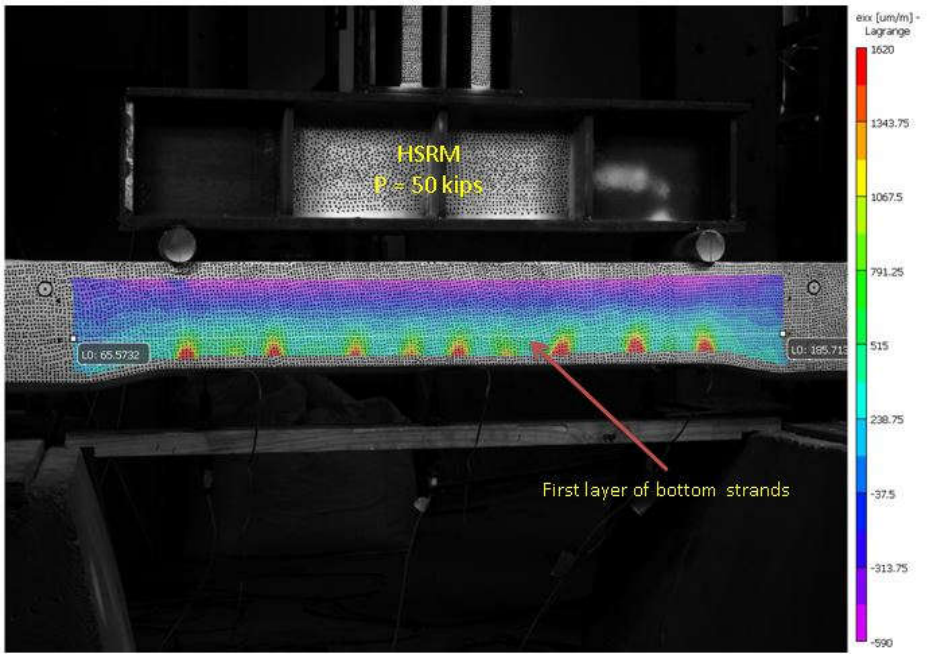

Figure 7.9 HSRM the crack reached the first layer of the bottom strands

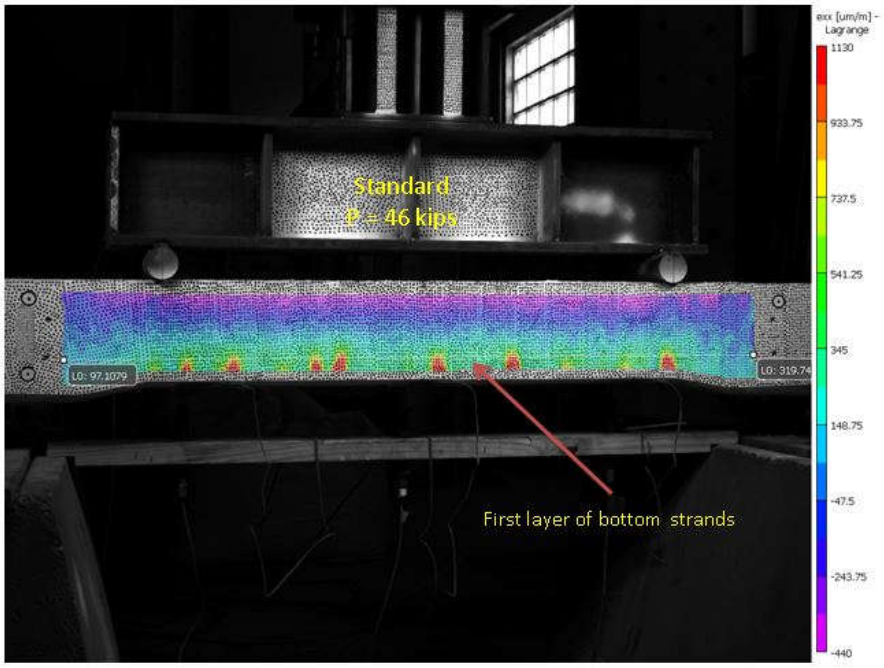

Figure 7.10 Standard the crack reached the first layer of the bottom strands

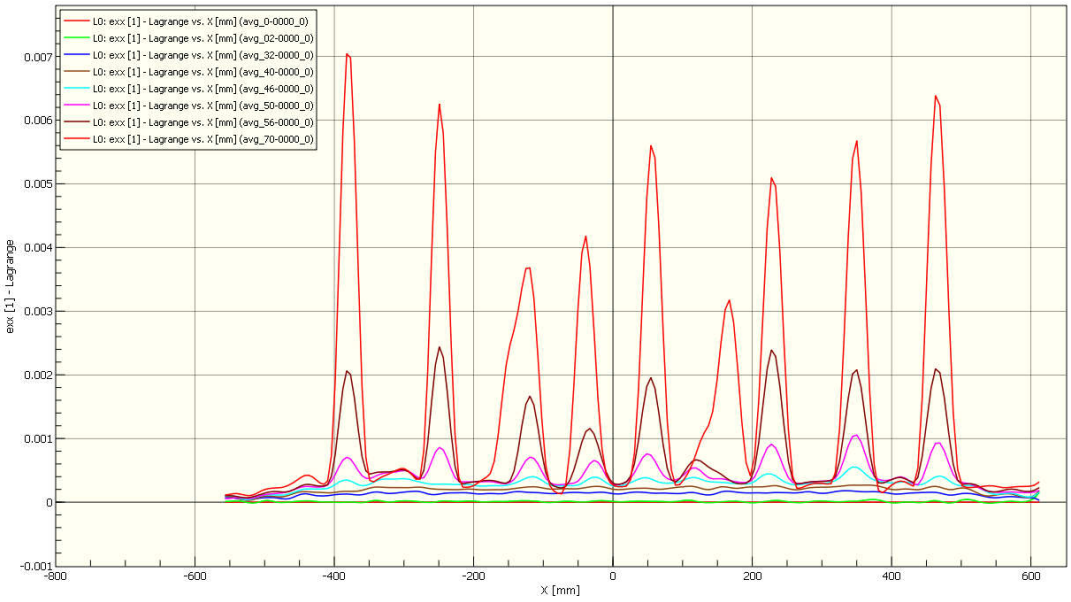

Figure 7.11 Longitudinal strain occurring at the HSRM tie's first bottom layer of the strand in Four Point Moment Test

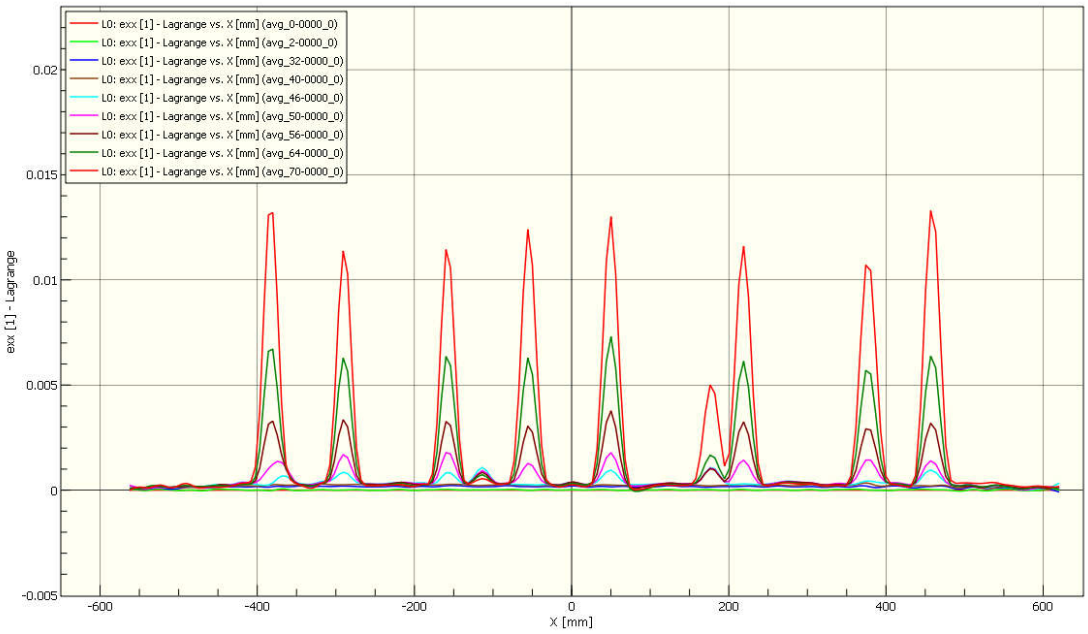

Figure 7.12 Longitudinal strain occurring at the Standard tie's first bottom layer of the strand in Four Point Moment Test

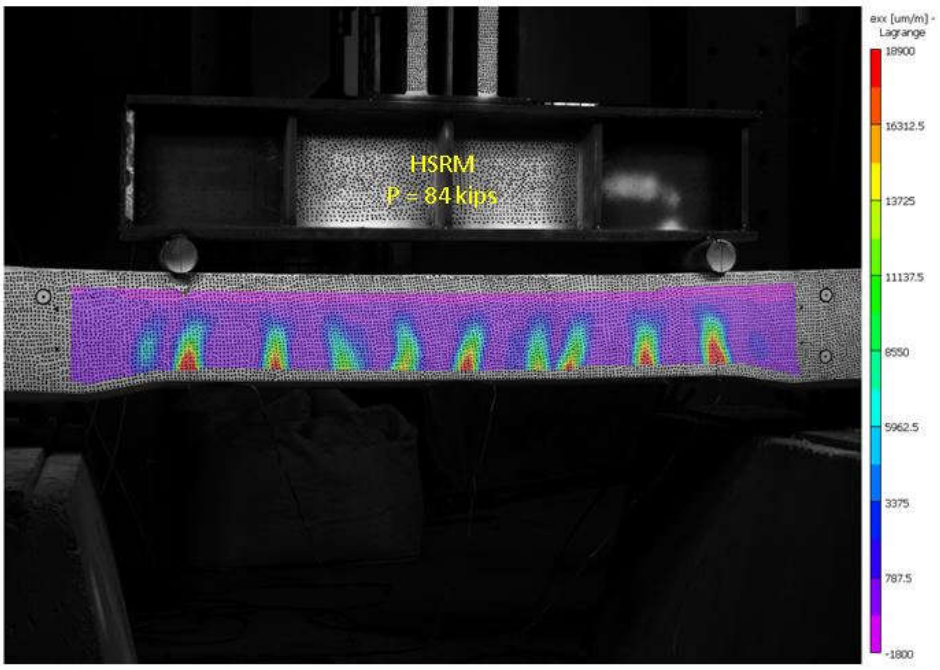

Figure 7.13 HSRM close to failure

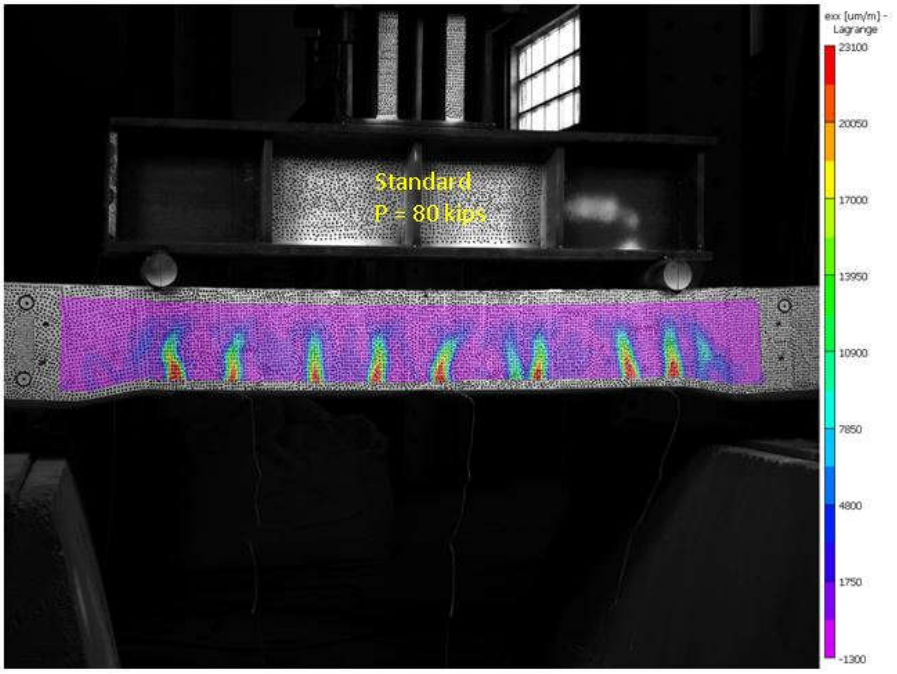

Figure 7.14 Standard close to failure

7.3 Material Properties

Four core samples were extracted from each tie and tested for a compressive strength and modulus of elasticity to see if there was any significant difference between ties. Figure 7.15 shows the ties with holes after the two ties failed in the four-point bending test. The dimensions of the samples were nominally 3.75 in. in diameter and 7 in. Long. The modulus of elasticity of the concrete core samples was tested in accordance with ASTM C469 (Standard Test Method for Static Modulus of Elasticity and Poisson Ratio of Concrete in Compression) [35] then the same cores were tested for compressive strength in accordance with ASTM C39 (Standard Test Method for Compressive Strength of Cylindrical Concrete Specimens) using a higher capacity universal testing machine [36]. LVDTs and DIC technique were used, as shown in figures 7.16 and 7.17, to obtain the modulus of elasticity as explained in table 7.1. The compressive strength was similar

for both ties; however, the HSRM cores cylinders show 20% lower modulus of elasticity compared to Standard cores cylinders.

Figure 7.15 Ties with holes

Table 7.1 Core Sample average result

Tie ID	Compressive Strength (psi)	Elastic Modulus (psi)
Standard	8620	4950000
HSRM	8622	3800000

Figure 7.16 Elastic Modulus Testing Using Machine

Figure 7.17 Elastic Modulus Testing Using DIC

CHAPTER 8

CONCLUSION

This study compared the prestressed concrete Standard tie with the High Strength Reduced Modulus (HSRM) prestressed concrete tie, the latter which uses crushed weathered granite aggregate instead of limestone. The concrete mix design for the Standard tie and the HSRM tie were optimally determined in accordance with the American Railway Engineering and Maintenance-of-Way Association (AREMA) mix design criteria for a PSC tie. The results of the first day, the seventh day, and 28^{th}-day compressive strength tests proved that the HSRM concrete was suitable to manufacture PSC ties and that the HSRM concrete satisfied the Standard requirements. The HSRM concrete showed higher compressive strength by 5% and lower modulus elasticity by almost 40% compared to Standard concrete. The HSRMs and the Standard ties typically used in North America were experimentally tested for their structural performance according to AREMA guidelines. They were compared using the following six tests:

- Rail Seat Vertical Load Test (Negative and Positive).
- Center Negative and positive Bending Moment Test.
- Rail Seat Repeated Load Test.
- Bond Development, Tendon Anchorage, and Ultimate Load Test.
- Four point bending test on the center negative.

Using HSRM concrete that has reduced elastic modulus and higher compressive strength results in the following beneficial effects on railroad ties: the initiation of cracks is delayed, stress is better distributed through the ties, and stronger bonding occurs between the concrete and the strands. The findings of this study also show that the type of aggregate has a strong effect on the performance of the railroad ties.

All the experimental results demonstrated that the newly developed HSRM ties not only satisfied the requirements of the design Standard but also showed superior structural performance to Standard prestressed concrete ties in terms of static and dynamic tests, in addition to superior bond strength between the strands and the concrete itself.

REFERENCES

[1] F. Rezaie, M. R. Shiri, and S. M. Farnam, “Experimental and numerical studies of longitudinal crack control for pre-stressed concrete sleepers,” Eng. Fail. Anal., vol. 26, pp. 21–30, 2012.

[2] H.-O. Shin, J.-M. Yang, Y.-S. Yoon, and D. Mitchell, “Mix design of concrete for prestressed concrete sleepers using blast furnace slag and steel fibers,” Cem. Concr. Compos., vol. 74, pp. 39–53, 2016.

[3] H. E. Wolf, “FLEXURAL BEHAVIOR OF PRESTRESSED CONCRETE MONOBLOCK CROSSTIES,” University of Illinois at Urbana-Champaign, 2015.

[4] A. R. E. and M.-W. Association, “Chapter 30,” no. September, 2006.

[5] J. C. Zeman, J. R. Edwards, C. P. L. Barkan, and D. A. Lange, “Failure Mode and Effect Analysis of Concrete Ties in North America,” 9th Int. Heavy Haul Conf., 2009.

[6] H. Donza, O. Cabrera, and E. F. Irassar, “High-strength concrete with different fine aggregate.”

[7] J. Hanson, “EFFECT OF COARSE AGGREGATE PROPERTIES ON THE MODULUS OF ELASTICITY OF HIGH PERFORMANCE CONCRETE,” University of South Carolina, 2013.

[8] S. Kaewunruen and A. M. Remennikov, “Effect of a large asymmetrical wheel burden on flexural response and failure of railway concrete sleepers in track systems,” Eng. Fail. Anal., vol. 15, no. 8, pp. 1065–1075, 2008.

[9] T. Koh, M. Shin, Y. Bae, and S. Hwang, “Structural performances of an eco-friendly prestressed concrete sleeper,” Constr. Build. Mater., vol. 102, pp. 445–454, 2016.

[10] H. Yu, D. Jeong, J. Choros, and T. Sussmann, “Finite Element Modeling of Prestressed Concrete Crossties with Ballast and Subgrade Support,” ASME 2011 Int. Des. Eng. Tech. Conf., pp. 1–10, 2011.

[11] R. H. Lutch, D. K. Harris, and T. M. Ahlborn, “Prestressed Concrete Ties in North America,” AREMA Annu. Conf., no. 906, pp. 1–39, 2009.

[12] J. Taherinezhad, M. Sofi, P. A. Mendis, and T. Ngo, “A review of behaviour of Prestressed concrete sleepers,” Electron. J. Struct. Eng., vol. 13, no. 1, pp. 1–16, 2013.

[13] AS-1085.14, “Railway Track Material Part 14: Prestressed Concrete Sleepers,” 2012.

[14] K. R. Manda, “Vertical Load Path Under Static and Dynamic Loads in Concrete Crosstie and,” 2014.

[15] J. Sýkorová, J. Bártová, and P. Štemberk, “Prestressed Concrete Sleeper Under Extreme Loading Conditions,” 18th Int. Conf. Eng. Mech., pp. 1281–1286, 2012.

[16] S. Kaewunruen and A. M. Remennikov, “Impact capacity of railway prestressed concrete sleepers,” Eng. Fail. Anal., vol. 16, no. 5, pp. 1520–1532, 2009.

[17] S. Kaewunruen and A. M. Remennikov, “Investigations of static and dynamic performance of railway prestressed concrete sleepers Ph.D. Candidate, 2 Senior Lecturer,” Annu. Conf. Expo. Exp. Appl. Mech., no. June, p. 11, 2007.

[18] S. Kaewunruen and A. M. Remennikov, “Experimental and Numerical Studies of

Railway Prestressed Concrete Sleepers Under Static and Impact Loads," Civ. Comput., pp. 25–28, 2007.

[19] A. Meeting, H. E. Wolf, S. Mattson, J. R. Edwards, M. S. Dersch, and C. P. L. Barkan, "Flexural Analysis of Prestressed Concrete Monoblock Crossties : Comparison of Current Methodologies and Sensitivity to Support Conditions," no. 217, 2015.

[20] G. Kumaran, D. Menon, and K. Nair, "Dynamic studies of railtrack sleepers in a track structure system," J. Sound Vib., 2003.

[21] H. E. Wolf, "Field Measurements and Proposed Analysis of Concrete Crosstie Bending Moments."

[22] R. H. Lutch, "Capacity Optimization of a Prestressed Concrete Railroad Tie," p. 230, 2009.

[23] D.C.Rizos,"High-Strength Reduced-Modulus High Performance Concrete (HSRM-HPC) for Prestressed Concrete Tie Applications," in 2016 Joint Rail Conference, 2016, p. V001T01A027.

[24] Tokyo 2017, "Tokyo Sokki Kenkyujo Co., Ltd." [Online]. Available: http://www.tml.jp/e/index.html. [Accessed: 12-Oct-2017].

[25] M. A. Sutton, J. H. Yan, V. Tiwari, H. W. Schreier, and J. J. Orteu, "The effect of out-of-plane motion on 2D and 3D digital image correlation measurements," Opt. Lasers Eng., vol. 46, no. 10, pp. 746–757, 2008.

[26] P. Synnergren and M. Sjok, "A stereoscopic digital speckle photography system for 3-D displacement "eld measurements," Opt. Lasers Eng., vol. 31, pp. 425–443, 1999.

[27] A. A. Mudassar and S. Butt, “Improved Digital Image Correlation method,” Opt. Lasers Eng., vol. 87, pp. 156–167, 2015.

[28] Schreier, H., Orteu, J. J., & Sutton, M. A. (2009). Image correlation for shape, motion and deformation measurements. Springer US.

[29] “Correlated Solutions.” [Online]. Available: http://correlatedsolutions.com/. [Accessed: 31-Jul-2017].

[30] B. Gencturk, K. Hossain, A. Kapadia, E. Labib, and Y.-L. Mo, “Use of digital image correlation technique in full-scale testing of prestressed concrete structures,” Measurement, vol. 47, pp. 505–515, 2014.

[31] S. Bartelmo,“JRC2016-5842 DIGITAL IMAGE CORRELATION TECHNIQUES FOR PRESTRESSED CONCRETE,” pp. 1–6, 2016.

[32] R. T. and E. Center and (RailTEC) at the University of Illinois at Urbana-Champaign, “High Strength , Reduced Modulus (HSRM) Concrete Crosstie Testing at University of Illinois at Urbana-Champaign (UIUC),” 2016.

[33] J. Cann, “CN Experience With Concrete Sleepers,” Railw. Gaz. Int., 1978.

[34] D. White, R. Arnlund, and R. Prause, “ECONOMICS OF CONCRETE-AND WOOD-TIE TRACK STRUCTURES,” 1978.

[35] ASTM C469, “Standard Test Method for Static Modulus of Elasticity and Poisson ’ s Ratio of Concrete,” vol. 4, pp. 1–5, 2002.

[36] ASTM C39, “Standard Test Method for Compressive Strength of Cylindrical Concrete Specimens,” ASTM Int., 2015.